CAC 2025 XXV Conference on Applied Crystallography



CAC 2025 XXV Conference on Applied Crystallography

ABSTRACT BOOK



XXV Conference on Applied Crystallography

organized by



held under the auspices of













CONFERENCE PARTNERS

Platinum partner

PIK Instruments sp. z o.o. ul. Źródlana 9 05-090 Laszczki, Poland https://pik-instruments.pl/



Gold partners

JEOL (EUROPE) - Poland Branch Al. Rzeczypospolitej 2/3 02-972 Warsaw https://www.jeol.com/

LABSOFT Sp. z o. o. ul. Puławska 469 02-844 Warszawa, Poland https://labsoft.pl/

Uni-Export Instruments Polska ul. Ludwika Kickiego 4a lok. 50 04-369 Warsaw, Poland https://www.uni-export.com.pl/

> Testchem Sp. z o.o. ul. Rybnicka 187 44-310 Radlin, Poland https://testchem.pl/









Bronze partners

3D Lab Sp. z o.o. Farbiarska 63B O2-862 Warsaw, Poland https://metalatomizer.com/

SCANMAT Sp. z o.o. ul. Zwoleńska 102D, 04-761 Warsaw, Poland https://scanmat.pl/

Helpi Optics Sp. z o.o. ul. Okulickiego 5F 05-500 Piaseczno, Poland https://helpi-optics.pl/







SCIENTIFIC COMMITTEE

***	prof. dr hab. Danuta Stróż	Poland
8	prof. dr Ute Kolb	Germany
	prof. dr Randi Holmestad	Norway
8	prof. dr hab. inż. Maria Sozańska	Poland
	prof. dr Manabu Ishimaru	Japan
8	dr hab. Katarzyna Jarzembska	Poland
***	dr hab. Marcin Nabiałek, prof. PCz	Poland
***	płk dr hab. inż. Marek Polański, prof. WAT	Poland
***	dr hab. Grzegorz Dercz, prof. UŚ	Poland
8	dr Maciej Zubko, prof. UŚ	Poland

ORGANIZING COMMITTEE



Chairman dr hab. Grzegorz Dercz, prof. UŚ



Co-chairman dr Maciej Zubko, prof. UŚ



Secretary dr inż.. Paweł Świec



Secretary dr inż. Izabela Matuła



mgr Patrycja Kierlik



dr Magdalena Szklarska



dr inż. Agnieszka Stróż



dr inż. Edyta Matyja



dr inż. Robert Albrecht



dr inż. Wojciech Gurdziel



Dr inż. Karsten Glowka



mgr inż. Khrystyna Khrushczyk

SCOPE

The Conference on Applied Crystallography is a prestigious scientific event organized since 1962 when Prof. Zbigniew Bojarski held a meeting dedicated exclusively to X-ray powder diffraction and its application to phase identification of various materials.

Today, the conference topics primarily focus on the use of crystallography to study different types of materials and the effect of their structure on their properties.

This includes discussions on the crystallographic characterization of metals, ceramics, polymers, and complex composites, as well as an in-depth exploration of how crystal structure directly impacts the physical, chemical, and mechanical properties of these materials. The conference aims to provide a comprehensive understanding of the relationship between structure and properties, fostering advancements in material science through the application of cutting-edge crystallographic techniques. The main topics of the conference are:

- Development of methods and techniques (X-ray, neutron and electron diffraction, PDF, EBSD)
- Crystal structure determination
- Texture analysis
- Crystallography of phase transformations
- Material structures (metals, ceramics, polymers, thin films, quasicrystals, amorphous material, nanomaterials, molecular crystals, structure of interfaces)

The conference will provide an opportunity to **present your innovative research in the form of both oral and poster presentations**.

VENUE

During early September, the region is adorned with the vibrant colours of late summer and early autumn, providing an ideal backdrop for academic engagement and leisurely exploration. Attendees can enjoy the rich cultural heritage, picturesque landscapes, and warm hospitality that southern Poland is renowned for.

The Conference will be organized at the Crystal Mountain ***** hotel in Wisła, where participants will have the opportunity to engage in fruitful scientific discussions and establish new academic connections in a luxurious setting surrounded by the nature of the Silesian Beskids.

Special cultural events will showcase the distinctive music, dance, and culinary delights of southern Poland, offering participants a taste of the region's rich heritage while fostering a warm and inviting atmosphere.

The conference will feature numerous events aimed at fostering new scientific connections and strengthening existing collaborations.



GENERAL INFORMATION

Badges

For security reasons and for catering purposes, please ensure that you wear your conference badge throughout the Conference and social events

Emergencies and insurance

The general emergency phone number in Poland is 112. This connects you to an operator who can alert the Police, Medical Aid, or the Fire Brigade.

The CAC25 Organising Committee will not be responsible for any medical expenses, losses, or accidents incurred during the Conference. Participants are strongly advised to arrange their own personal insurance to cover medical and other expenses, including accidents or loss. It is recommended that citizens from EU countries bring with them a valid EHIC card.

Registration desk

On Sunday, the registration desk will be located to the right of the main entrance to the building, next to the hotel reception, and will be open from 16:00 to 19:00.

On the following days, the registration desk will be moved close to the coffee break area and will open 15 minutes before the start of each session.

For any questions regarding the organisation of the conference, please contact a member of the Organising Committee. Committee members will wear badges that are distinct from those of other conference participants.

Conference will start at Sunday 7 September, with dinner and get-along party.

Welcome to XXV Conference on Applied Crystallography

Monday 8th September

- 9:00 Opening ceremony
- 9:30 **J. Georg Bednorz** High Temperature Superconductivity: 4 Decades of Development towards an Efficiency Technology
- 10:30 **Katarzyna N. Jarzembska** Photocrystallography in the study of photoactive materials at different time scales
- 11:00 Coffee break
- 11:30 Ute Kolb 3DED-Automated diffraction tomography in the case of agglomerated and intergrown nano crystals
- 12:20 **Zbigniew Mitura** Recognising inelastic scattering features in electron diffraction patterns
- 12:40 Magdalena Bieda Thermal Stability Of Biodegradable Zinc Alloys
 In Situ And Ex Situ Heating Experiments Combined With Orientation Microscopy in SEM and TEM
- 13:00 Lunch
- 14:00 **Gert Nolze** Bravais lattice type and lattice parameter determination from single EBSD patterns
- 14:50 **Jarosław Michalek -** Visual and chemical characterisation of solids using Laser-induced Breakdown Spectroscopy (LIBS)
- 15:10 **Tomasz Tokarski** Analysis of crystal defects by EBSD/TKD in a scanning electron microscope
- 15:30 Coffee break
- 16:00 **Jacek Podwórny** Formation and composition of magnesia– aluminate spinel in shaping the high-temperature properties of corundum refractory castables
- 16:30 **Muhammad Shabbir** The atomic structure of carbon materials from banana biomass and their catalytic graphitization
- 16:45 **Taoufik Lamrani** Modulation of smectic liquid-crystalline order in itraconazole via solvent evaporation
- 17:00 **Karolina Rogalewska** Oxidation of SiC-containing refractory concretes
- 17:15 **Julia Zając** Structure and Microstructure of Zr–Nb–Mo Alloys: Effect of Composition and Heat Treatment
- 17:30 **Khrystyna Khrushchyk** Influence of short-term annealing on the physical and chemical properties of amorphous metal alloys based on aluminium
- 17:45 **Iwona Wyrębska** The synthesis of binary transition-metal hydrides through self-shearing reactive milling
- 19:00 Regional dinner trip to the Biała Wisełka Valley with a guide

Photocrystallography in the study of photoactive materials at different time scales

K. N. Jarzembska^{1a}, R. Kamiński¹

a katarzyna.jarzembska@uw.edu.pl

¹ University of Warsaw, Faculty of Chemistry, Warsaw, Poland

Keywords: photocrystallography, photoswitches, luminescence, excited states, transition-metal coordination compounds

The term photocrystallography encompasses a set of experimental techniques combining crystallography and spectroscopy [1-3]. This approach is used to study structural changes and dynamics of light-induced processes that occur in solid samples (single crystals, nanocrystals, thin films) on different time-scales. We can distinguish static photocrystallography (study of long-lived excited states) and time-resolved photocrystallography (with time resolution of even sub-ps/fs). Static and possibly time-resolved experiments for slower processes (~ms) can be performed in a home laboratory, if it is properly equipped, while faster processes occurring under the influence of light are studied using synchrotron sources and X-ray free-electron lasers (XFELs).

communication, we will briefly present the In this range photocrystallographic and complementary methods and their applications. Static photocrystallography will be discussed using the example of studying metastable states generated by light in crystals of molecular switches [4]. Optically induced solid-state transitions, however, can last not only days or hours, but can also be completed in less than a few ps (especially the initial stages of the processes right after excitation). Therefore, to understand the full dynamics of solid-state transitions, we need to gain access to monitoring very short-lived metastable states. In this context, we will present the current measurement capabilities and challenges of photocrystallography in the case of studying short-lived excited states in crystals of small molecules of organic compounds, coordination compounds, molecules trapped in MOF (metalorganic framework) networks or proteins, including the Laue method and serial crystallography [1-8]. Such experiments and analyses significantly contribute to understanding of important electronic processes. changes/photochemical reactions induced by them or changes in material properties. This is important not only from a cognitive point of view, but also in the context of designing new functional materials.

Acknowledgement: K.N.J. acknowledges the National Science Centre (Poland) (2020/38/E/ST4/00400, SONATA BIS programme), and both K.N.J. and R.K. thank the Ministry of Science and Higher Education (Poland) for financial support (agreement No. 2022/WK/13, project title: "Support for Polish Users of EuXFEL – Supervision II (2022–26)", "Support for the Participation of Polish Scientific Teams in International Research Infrastructure Projects" programme).

- [1] P. Coppens, J. Phys. Chem. Lett. 2011, 2, 616.
- [2] L.E. Hatcher, M.R. Warren, P.R. Raithby, Acta Cryst. Sect C. 2024, 80, 585.
- [3] K.A. Deresz, P. Łaski, R. Kamiński, K.N. Jarzembska, Crystals 2021, 11, 1345.
- [4] K.A. Deresz, R. Kamiński et al., Chem. Commun. 2022, 58, 13439.
- [5] P. Łaski et al., J. Phys. Chem. Lett. 2024, 41, 10301.
- [6] D. Vinci et al., Nat. Commun. 2025, 16, 2043.
- [7] J. Kang et al., Nat. Chem., 2024, 16, 693.
- [8] E. Nango et al., Science 2016, 354, 1552.

3DED-Automated diffraction tomography in the case of agglomerated and intergrown nano crystals

<u>U. Kolb^{1a}, M. Appelmann1 and L. Gemmrich Hernandéz¹</u>

^a kolb@uni-mainz.de

¹ Department Chemistry, Johannes Gutenberg-University Mainz, Duesbergweg 10-14, 55128 Mainz, Germany

Keywords: electron diffraction, crystal structure analysis, twinning

Close to two decades after the development of automated diffraction tomography (ADT) [1, 2] allowing for the direct solution of crystal structures based on electron diffraction data taken from nano crystals a variety of data collection protocols exist3. The approaches have in common that they tilt a nonoriented crystal in the electron beam but use for integration of the reciprocal space either a defined tilt step combined with electron beam precession or a continuous tilt movement with a high speed camera. As an overarching term three dimensional electron diffraction (3DED) was chosen. Nowadays, dedicated electron diffractometers are on the market, but many groups use as well the possibility to upgrade existing transmission electron microscopes. This talk will cover advances in data acquisition and processing4 and will discuss important tricks and pitfalls for the method using a few showcases. It points out new approaches to enable a wide community to use 3DED as well as new tracking routines allowing to take datasets from nano crystals of around 20nm with a 25 nm probe from highly agglomerated crystals or the investigation of vacuum sensitive hydrated samples with a high water conten [3,4,5]. The potential of 3DED two fully characterize a material including structural specialities like twinning or disorder will be demonstrated.

- U. Kolb, T. Gorelik, C. Kübel, M. T. Otten, D. Hubert, *Ultramicroscopy*, 2007, 107(6-7), 507 and 2008, 108(8), 763.
- [2] M. Gemmi, E. Mugnaioli, T. E. Gorelik, U. Kolb, L. Palatinus, Ph. Boullay, S. Hovmöller, J. P. Abrahams, *ACS Cent. Sci.*, 2019, **5(8)**, 1315.
- [3] S. Plana-Ruiz, Y. Krysiak, J. Portillo, E. Alig, S. Estradé, F Peiró, U. Kolb, Ultramicroscopy, 2020, 211, 112951.
- [4] F. Steinke, L. Gemmrich Hernandéz, S. J. I. Shearan, M. Pohlmann, M. Taddei, U.
- [5] Kolb, N. Stock, *Inorganic Chemistry*, 2023 **62** (1), 35.
- [6] P. Gollé-Leidreiter, B. Durschang, U. Kolb, G. Sextl, Ceramics International, 2022, 48(3), 3790.

Recognising inelastic scattering features in electron diffraction patterns

Z. Mitura^{1a}, Ł. Kokosza¹, G. Szwachta^{2,3}, J. Pawlak², A. Naumov² and M. Przybylski^{2,4}

a mitura@agh.edu.pl

Keywords: Kikuchi patterns, digital images, perovskites

Electron diffraction patterns exhibit various geometrical features that arise due to elastic and inelastic scattering. The features, such as Kikuchi lines, bands, and envelopes, resulting from the interference of inelastically scattered waves, can provide important structural information about the atomic arrangement within the sample. In some cases, inelastic effects may be weak – this is particularly true during reflection high-energy electron diffraction (RHEED) experiments conducted in vacuum systems designed for thin film deposition [1]. This is usually a consequence of the use of small angle geometry. Additionally, the occurrence of a non-ideal termination of samples also disturb the regularity of inelastic scattering. Similar situations may also happen when diffraction patterns are collected using scanning or transmission electron microscopes. When the intensity of Kikuchi features is weak, their use in structural analysis becomes challenging. Recently, it has been shown that their recognising can be significantly enhanced by processing raw patterns using computer graphics software for image filtering [2].

In the current study, we examined various aspects of digital diffraction data processing in detail. Experimental RHEED patterns of perovskite materials were collected, including data from both SrTiO₃ substrates and deposited thin films. Two types of substrates were investigated: some with rough surfaces (terminated with mixed SrO and TiO₂ domains) and others with especially prepared uniform flat surfaces (terminated only with TiO₂ domains). The experiments were performed in a pulsed laser deposition chamber, with thin film growth carried out using a KrF (248 nm) excimer laser. Raw diffraction patterns were recorded and subsequently processed using a number of Python-based image processing

¹ Faculty of Metals Engineering and Industrial Computer Science, AGH University of Krakow, Poland

² Academic Centre for Materials and Nanotechnology, AGH University of Krakow, Poland

³ Faculty of Physics, University of Warsaw, Poland

⁴ Faculty of Physics and Applied Computer Science, AGH University of Krakow, Poland

tools. In general, many Kikuchi lines became visible – especially when the image background was first subtracted and adaptive histogram equalization was then applied.

We conclude that with the aid of digital image processing, significantly more structural information can be extracted from sample surfaces than is possible through basic analysis of elastic scattering features alone.

- [1] J. Pawlak, M. Przybylski and Z. Mitura, Materials 14 (2021) p. 7077:1-7077:14.
- [2] Z. Mitura, G. Szwachta, Ł. Kokosza and M. Przybylski, Acta Cryst. A80 (2024) 104–111.

Thermal stability of biodegradable zinc alloys - in situ and ex situ heating experiments combined with orientation microscopy in SEM and TEM

M. Bieda^{1a}, M. Gieleciak¹, J. Donaghue², A. Smith³, N. Iyappan⁴, A. Jarzębska¹, Ł. Maj¹, M. Kulczyk⁵

a m.bieda@imim.pl

Keywords: zinc alloys. SEM/EBSD, OM/TEM

Zinc is recognized as a promising candidate for biodegradable bone implants and cardiovascular stents due to its suitable corrosion rate [1]. However, one significant drawback of using pure zinc is its low recrystallization temperature, which is close to room temperature. Research has shown that adding alloying elements, such as magnesium or copper, can significantly enhance the thermal stability of zinc alloys [2].

Despite this, there is still a lack of comprehensive research quantifying how factors such as annealing temperature, alloying elements, and second-phase particles influence the recrystallization behaviour and mechanical properties of zinc-based alloys [3]. Additionally, it is essential to assess the thermal stability of low-alloyed zinc after undergoing plastic deformation, particularly considering body temperature and potential exposure to higher temperatures during the transportation and storage of the final products.

The main goal of this study was to investigate the thermal stability of pure zinc and zinc alloys (e.g., those with magnesium and copper) after plastic deformation using the hydrostatic extrusion method. Advanced microscopy methods were employed to observe changes in the microstructure of the materials following in-situ and ex-situ heating.

Ex-situ microstructural studies were conducted on samples heated in a Memmert UNE 400 drying oven at 50 °C, 100 °C, and 150 °C for 1 hour, followed by air cooling [4]. Additionally, the 4D-STEM TESCAN TENSOR was utilized to obtain orientation maps for samples before and after heating up to 200 °C for

¹Institute of Metallurgy and Materials Science of Polish Academy of Sciences, Reymonta 25, 30-059 Krakow, Poland

²Department of Materials, University of Manchester, Manchester M13 9PL, UK

³TESCAN-UK, Cambridge, UK

⁴ TESCAN GROUP, Libušina třída 1, 62300 Brno, Czech Republic

⁵Institute of High Pressure Physics, Polish Academy of Sciences, Sokolowska, 29/37 01-142. Warsaw, Poland

1 h through precession assistance, enabling the characterization of the intermetallic phase (Mg₂Zn₁₁), as well as the grain size and orientations of the eutectic mixture.

In-situ SEM/EBSD studies were conducted at 100°C using the TANIST TESCAN system to analyze microstructural changes in the studied materials. Samples were held at this temperature for 48 hours, with repeated electron backscatter diffraction (EBSD) analysis performed to track grain nucleation and growth. An alloy containing 0.6 wt.% magnesium was selected for 3D analysis using the L-PFIB Thermo Fisher system. This analysis was conducted both before and after the TANIST heat treatment to compare grain structures and determine whether the surface microstructure observed during the TANIST experiment was representative of the bulk material.

The results proved that zinc alloys exhibit higher thermal stability compared to pure zinc. The presence and distribution of second-phase particles during the recrystallization process have a significant impact on the behaviour of the material. Advanced microstructural characterization enabled both qualitative and quantitative characterization of the changes that occurred in the materials during heating at elevated temperatures.

Acknowledgement:

This work was co-financed by the National Science Centre Polish UMO-2020/39/O/ST5/02692 and supported by the Henry Royce Institute for Advanced Materials, funded through EPSRC grants EP/R00661X/1, EP/S019367/1, EP/P025021/1 and EP/P025498/1."

Cooperation with TESCAN DEMO-Lab in Brno for the use of TENSOR is acknowledged.

- [1] P.K. Bowen, J. Drelich, J. Goldman, Adv. Mater. 25 (2013) 2577–2582.
- [2] J.C.T. Farge, W.M. Williams, Canadian Metallurgical Quarterly, 5:4 (1966), 265-272.
- [3] G. Li, H. Yang, Y. Zheng, XH. Chen, JA. Yang, D. Zhu, L. Ruan, K. Takashima, Acta Biomater. Oct 1;97(2019), 23-45.
- [4] M. Gieleciak, A. Jarzębska, Ł. Maj, P. Petrzak, M. Kulczyk, Ł. Rogal, M. Bieda, Bioactive Materials 44, (2025), 1-14,

Bravais lattice type and lattice parameter determination from single EBSD patterns

G. Nolze^{1a}, T. Tokarski²

a gert.nolze@bam.de

¹ Federal Institute for Materials Research and Testing, Berlin, Germany ² ACMiN, AGH Krakow, Poland

Keywords: lattice metric, symmetry, Kikuchi patterns

For crystalline materials, EBSD offers a wide range of interpretations which now go far beyond local orientation, grain size, and phase distribution. Pattern matching, a digital image correlation (DIC) of often highly bound EBSD patterns with purely physics-based simulations, increases the achievable angular resolution by about an order of magnitude and even enables the differentiation of similarly diffracting phases, both of which seemed completely impossible just a few years ago [1]. One of the remaining limitations, however, concerns the knowledge of all phases involved, without which further interpretation of measurement data is only possible to a limited extent.

The essential fundamentals for a purely crystallographic analysis of an EBSD pattern were worked out in the past [2,3], the determination of the lattice metric was previously considered too error-prone ($\pm 10\%$) to be used meaningfully. Although most physically induced limitations are truly unavoidable, errors can be statistically reduced by considering certain principles derived from lattice projection when evaluating patterns. An EBSD pattern can be understood as a system of equations in which (up to 6) lattice parameters, the crystal orientation (3 unknowns) and the relative position of the signal source point to the detector (3 unknowns) are encoded in approximately one hundred easily evaluable Kikuchi bands, which change sensitively with respect to their position (2) numbers) and width (1 number) with the unknowns. The correlations between the lattice and the reciprocal lattice, e.g., $[uvw]_1 \times [uvw]_2 = [hkl]^*$ and $[hkl]_1^* \times$ $[hkl]_2^* = [uvw]$, severely restrict the freedom of the position of Kikuchi bands and their intersections. Similar restrictions apply to the widths of Kikuchi bands of a single zone [uvw], which must all correspond to the linear combination of two basis vectors hkl in the perpendicular reciprocal lattice plane (uvw)*. Since all hkl in $(uvw)^*$ in turn represent elements of other $(uvw)_i^*$, the deviations between theoretical and experimental band widths can be minimized, so that not only the alignment of (hkl) and [uvw] can be determined with astonishing accuracy, but also their band widths as distance to the respective reciprocal lattice points hkl. Although the band widths are in general less precise, the

standard deviation in the lattice parameter ratios and angles is commonly clearly below 1%. However, for physical reasons, the absolute size of the lattice parameters is less accurate. Furthermore, determining the Bragg angle position is not as easy as it is in X-ray diffraction, for example. The simplest approach, which is to use the inflection point [4] of the S-shaped band edge profile as the Bragg angle, underestimates the lengths of the basis vectors for weakly scattering phases, while overestimating them for strongly scattering phases. Simulated patterns show a comparable increase, but the deviations are negligible for weak scatterers and therefore greater for strong scatterers, i.e. the curve is shifted. Obviously, the position of the Bragg angle shifts within the S-shaped band edge profile with the mean atomic number Z of the scattering phase. On the other hand, compensating for this is the wavelength λ at which the electron energy of the incident beam is used for the calculation. However, the effective electron energy is known to change, not only with Z but also with the exit angle of the electrons, which means that although the position of the bands in an EBSD pattern does not change with λ , the width probably does [5].

Nevertheless, with the help of the software CALM [6] it is generally surprising how reliably the symmetry, type, and metric of a phase's lattice can be derived from a single EBSD pattern, which often shows only about 13% of the total signal in the visible sector. An extension to point group symmetry is currently limited by the omnipresent excess-deficit effects.

In summary, EBSD patterns are better suited to determining the Bravais lattice type and its metrics than has long been assumed [7]. Like other techniques, EBSD is influenced by pseudosymmetry, and so are the diffraction patterns, which is further exacerbated by the asymmetric acquisition geometry and Kikuchi band overlaps [8]. However, for many problems, knowledge of the sublattice, possibly symmetry, or an initial estimate of the lattice parameters is helpful [9]. The main advantage is that the crystal lattice metric can be determined locally with good accuracy and relatively little preparation effort.

- [1] G. Nolze, M. Jürgens, J. Olbricht and A. Winkelmann. Acta Mater. 159 (2018), 408-415
- [2] R.P. Goehner and J.R. Michael, J. Res. Natl. Inst. Stand. Technol. 101(3) (1996), 301-308.
- [3] L. Li and M. Han, J. Appl. Cryst. 48(1) (2015), 107-115
- [4] N. Saowadee, K. Agersted and J.R. Bowen, J. Microscopy. 266 (2017), 200–210.
- [5] A. Winkelmann, B. Britton and G. Nolze. Phys. Rev. B99(6) (2019), 064115
- [6] G. Nolze, T. Tokarski, Ł. Rychłowksi, G. Cios and A. Winkelmann. J. Appl. Cryst. 54(3) (2021), 1012-1022
- [7] G. Nolze, T. Tokarski and L. Rychłowski. J. Appl. Cryst. 56(2) (2023), 349-360
- [8] G. Nolze, T. Tokarski and L. Rychłowski. J. Appl. Cryst. 56(2) (2023), 367-380
- [9] S. Martin, A. Walnsch, G. Nolze, A. Leineweber, F. Lèaux and C. Scheuerlein. Intermetallics 80 (2017), 16-21

Analysis of crystal defects by EBSD/TKD in a scanning electron microscope

T. Tokarski^{1a}, K. Wojciak¹, G. Cios¹, A. Winkelmann¹, and G. Nolze²

a tokarski@agh.edu.pl

Keywords: EBSD, TKD, dislocations

Kikuchi diffraction patterns acquired in EBSD and TKD systems are routinely employed for crystallographic phase identification and orientation mapping of polycrystalline materials. Despite the inherent complexity of these patterns, conventional analysis primarily focuses on the positions of Kikuchi bands, often neglecting local intensity variations. Due to the limited angular resolution of standard EBSD, applications are largely confined to phase and orientation imaging. Advanced analytical methods such as template (pattern) matching and High-Resolution EBSD (HR-EBSD) have enabled improvements in angular resolution, allowing for the mapping of local lattice rotations and elastic strains near dislocation cores. These techniques have demonstrated the potential to identify the Burgers vector of individual dislocations by comparing experimental data with simulated dislocation strain fields. However, such methods require highly demanding computational and analytical procedures. both in pattern analysis and strain field modeling. Consequently, their adoption within the EBSD community remains limited, with applications primarily restricted to threading dislocations in GaN (EBSD mode) [1] and a single report on metallic systems using TKD [2].

In contrast, the transmission electron microscope (TEM) [3] or scanning TEM (STEM) [4] offers a well-established method for Burgers vector determination based on dislocation contrast extinction. Using the invisibility criterion **g·b=0**, dislocations can be identified by acquiring images under different two-beam diffraction conditions.

This work introduces a novel approach that draws inspiration from the TEM methodology and applies it to Kikuchi diffraction patterns. By decomposing complex Kikuchi images into individual bands, each corresponding to a distinct crystallographic reflector, the sharpness of each band is quantified as a measure of local lattice distortion. This method enables the detection of dislocations through variations in band quality between distorted and undistorted regions

¹ AGH - University of Krakow, Academic Centre for Materials and Nanotechnology, Krakow, Poland

² Federal Institute for Materials Research and Testing (BAM), Berlin, Germany

³ TU Bergakademie Freiberg, Institut für Mineralogie, Freiberg, Germany

(Fig. 1). Analogous to the TEM extinction rule, dislocations may become visible or invisible depending on the diffraction vector (Kikuchi band) employed during reconstruction. Details of the technique, including its implementation, sensitivity, and limitations, will be presented, with a focus on its application to the discrimination of Burgers vectors using TKD and standard EBSD hardware.

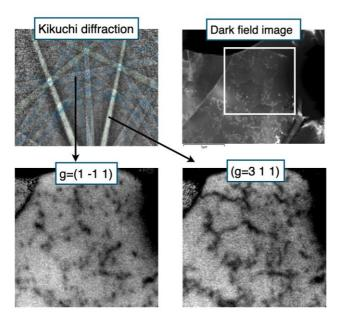


Fig. 1. An example of two dislocation images reconstructed from Kikuchi diffraction patterns recorded in the region marked by the white rectangle in the dark-field image.

- [1] F Y.N. Picard, M.E. Twigg, J.D. Caldwell, C.R. Eddy Jr., M.A. Mastro and R.T. Holm, Scripta Materialia 61 (2009), p. 773.
- [2] H. Yu, J. Liu, P. Karamched, A.J. Wilkinson, F, Hofmann, Scripta Materialia 164 (2019), p. 36.
- [3] D.J. Dingley, Phys. Stat. Sol. 38 (1970), p. 345.
- [4] C. Sun, E. Müller, M. Meffert and D. Gerthsen, Adv Struct Chem Imag 5 (2019), p. 2.

Formation and composition of magnesium—aluminate spinel in shaping the high-temperature properties of corundum refractory castables

J. Podwórny

jacek.podworny@icimb.lukasiewicz.gov.pl

Lukasiewicz Research Network – Institute of Ceramics and Building Materials, Center of Refractory Materials, Poland

Keywords: HT-X-ray diffraction, phase transformation, corundum refractory castables

Spinels constitute an important group of chemical compounds comprising a range of raw materials and materials used in many industries. They can be found in refractory materials, electro-ceramics (ferrites), the chemical industry (catalysts and ceramic supports for catalysts and components of refractory anticorrosion coatings), electronics (solid-state batteries), plastics and utility ceramics (as pigments), as well as in abrasives, nuclear power, jewelry, and many other industries.

Magnesium aluminate spinel MgAl₂O₄ is an important representative of this group of compounds, characterized by high refractoriness (melting point 2135°C) and therefore used in refractory materials technology. It is incorporated into refractory materials directly as MgAl₂O₄ or produced from substrates insitu during the firing process. In technologies based on in-situ synthesis, spinel formation in the material is accompanied by a significant volume change. The unit cell of spinel is about 60% larger by volume than the sum of the unit cells volume of the substrates required for its formation (MgO and α -Al₂O₃). During spinel synthesis, stresses arise, which can lead to the formation of microcracks. However, in practical applications, the synthesis of a reaction product with a volume larger than the substrates can be used to improve material properties, for example, to compensate for shrinkage during firing, or the resulting microcracks can be used to compensate for stresses induced by thermal shocks. This, however, requires the thoughtful use of spinel-forming additives to modify the properties of the refractory material for specific applications.

This paper presents the role of MgO as a spinel-forming additive in corundum castables, improving thermomechanical properties. Studying the in-situ synthesis of spinel, it was observed that the unit cell parameter of the formed spinel increases up to a temperature of 1250°C, while it decreases above 1250°C. This observed phenomenon was explained by the diffusion of the depleting substrate (Mg²⁺ ions) into the corundum grains.

After the initial formation of a stoichiometric $MgAl_2O_4$ spinel with a large unit cell, a sub-stoichiometric $Mg_xAl_2O_{4-x}$ spinel begins to form, and the unit cell parameter begins to decrease with increasing temperature. Spinel depleted in Mg^{2+} ions, with a larger ionic radius (1.95 Å) than $(Al^{3+}; 1.77 \text{ Å})$, causes contraction of the unit cell. It was shown that changes in the chemical composition of the spinel affect the unit cell volume more strongly than thermal expansion. Diffusion of Mg^{2+} ions into the corundum increases the total spinel fraction, but with a sub-stoichiometric composition.

The higher the in-situ synthesis temperature, the more intense this process is and the greater the impact on the stress state in the material. The observed phenomenon allowed us to understand the relationship between the volume of the unit cell of the forming spinel and the change in the stress state in the material, which is reflected in the results of tests of mechanical and thermomechanical properties.

Acknowledgement:

This project was implemented under the CORNET initiative. It was funded by the National Centre for Research and Development (NCBR) in Poland and the German Federation of Industrial Research Associations (AiF). This project was carried out under the auspices of AiF and financed from the budget of the Federal Ministry of Economics and Technology (BMWi) within the framework of the programme for promoting collective industrial research (IGF), project No.175 EN.

The atomic structure of carbon materials from banana biomass and their catalytic graphitization

M. J. Shabbir^{1a}, B. Liszka², M. Szubka¹, K. Jurkiewicz¹

a mjamshaid.shabbir@us.edu.pl

Keywords: biomass-derived carbon, structure, catalytic graphitization

The use of renewable, lignocellulosic, or agricultural waste sources as carbon feedstock not only supports circular economy principles but also reduces the carbon footprint and supports the production of environmentally friendly materials. In the field of carbon materials, this can be achieved through the use of cheap and abundant biomass-derived precursors, coupled with catalytic graphitization techniques that enable the formation of graphitic carbon structures at even lower temperatures (< 2000°C) than the temperatures used for artificial graphite production (~3000°C).

Our recent studies demonstrated that it is possible to obtain dense, highly-ordered graphite-like materials from conventional precursors of non-graphitizing carbons, such as sucrose and furfuryl alcohol, by using Si-assisted catalytic graphitization [1,2], while standard graphitization of these precursors leads to porous and disordered, at the atomic scale, fullerene-like carbons. In this contribution, the structural characterization of the banana-peel-derived carbon materials produced via standard carbonization under protective Ar atmosphere, at various temperatures (< 2000°C), will be presented. Moreover, the heat treatment of the banana-peel-derived materials in the presence of CaCO₃ particles was performed in order to evaluate their possible catalytic graphitization effect on the structure of the carbon matrix as well as the porosity. Ca is nowadays considered as an effective catalyst for graphitization of disordered carbons at low temperatures (< 2000°C).

The results of the performed X-ray diffraction and Raman spectroscopy structural studies will be presented, which were used to characterize the transformation of the atomic-scale structure of the studied banana-peel-based carbon materials heat-treated at various temperatures. Moreover, by supporting energy-dispersive X-ray spectroscopy measurements, it was possible to characterize their elemental and phase composition. The effect of the Ca catalyst on the atomic-scale structure will be evaluated. Moreover, the aim of these

¹ Institute of Physics, Faculty of Science and Technology, University of Silesia in Katowice, ul. 75 Pułku Piechoty 1, Chorzów, Poland

² Faculty of Natural Sciences, University of Silesia in Katowice, ul. Będzińska 60, Sosnowiec, Poland

studies is to determine the impact of catalytic graphitization on the porosity of these materials. Since their microporosity is mainly closed, it cannot be probed by gas adsorption methods. Therefore, the results of preliminary small-angle X-ray scattering studies will be presented to reveal the changes in the porous structure.

The obtained results underscore the potential of such graphitized carbon materials from biomass as promising anode candidates for sodium-, potassium, and lithium-ion cells, where the atomic arrangement and porosity are key to optimizing ion transport and storage capacity.

Acknowledgment: Conference participation was supported by the GreenMat project, co-funded by the European Union under the program "European Funds for Silesia 2021–2027

- [1] K. Jurkiewicz., et al. Advanced Functional Materials 34 (2024), 2410409.
- [2] K. Jurkiewicz., et al. Diamond and Related Materials 155 (2025), 112236.

Oxidation of SiC-containing refractory concretes

K. Rogalewska^{1a}, K. Dudek¹, J. Podwórny¹, R. Kusiorowski¹, A. Gerle¹

^a karolina.rogalewska@icimb.lukasiewicz.gov.pl

Keywords: silicon carbide, oxidation, refractory concrete

SiC is characterized by a very large number of polytypes — over 200 have been identified to this day. The most common forms crystallize in the cubic, hexagonal, and rhombohedral systems. Silicon Carbide is an extremely hard and highly refractory material, which results from its covalent, tetrahedral network composed of tetravalent atoms. Each silicon atom is surrounded by four carbon atoms, and each carbon atom by four silicon atoms. Together, they form three-dimensional shapes known as tetrahedra [1].

In dry air and at high temperatures, the dominant mechanism is passive oxidation, with amorphous silica (SiO_2) and carbon monoxide (CO) as the main products. Under typical conditions, silica forms protective layers around SiC grains or bondings between them. However, metal oxides may react with silica, damaging protective layers and accelerating oxidation, either through chemical interaction or by inducing cristobalite crystallization. In some cases, they may instead promote the formation of a dense, viscous layer that acts protectively [1,2].

Castables containing-SiC have been studied for many years, though not all were designed for high-temperature applications. Compared to oxide-based refractories, SiC castables offers excellent mechanical properties, including high strength, thermal shock resistance, and abrasion resistance. SiC materials also show good resistance to corrosion and oxidation. Oxidation can have degrading influence on mechanical properties, it can cause swelling, generating internal stresses. Inspections of industrial linings have shown that significant degradation may occur after several years of use due to the high expansion of oxidation products. Even a thin silica layer forming on each SiC grain can lead to macroscopic expansion, especially in porous materials with fine SiC particles. This process affects both the surface and bulk of the material due to high open porosity [2].

The aim of the work was to investigate the oxidation mechanism of silicon carbide used as a component of refractory concrete for high-temperature applications.

¹ Lukasiewicz Research Network – Institute of Ceramics and Building Materials, Center of Refractory Materials, Poland

Comparative studies were conducted using samples containing different amounts of SiC. The research included X-ray diffraction (XRD) for phase analysis, scanning electron microscopy (SEM) with energy dispersive spectroscopy (EDS) for microstructural analysis, X-ray fluorescence (XRF) for chemical composition, thermal analysis (DTA/TG). Measurements of physical and mechanical properties: porosity, bulk density and gas permability.

The results revealed that during firing, fine SiC particles start to sinter, and silicon carbide oxidizes, forming a silica layer around the grains. This oxide layer, which can be amorphous or partly crystalline causes local changes, especially at grain boundaries. The material becomes denser, and pores starts to close. This process is not uniform, which leads to an uneven distribution of pores in the sample.

- [1] A. J. Ruys, Silicon Carbide Ceramics: *Structure, Properties and Manufacturing*, in: Advanced Ceramic Materials, Elsevier, Amsterdam, 2023.
- [2] O. Gallet-Doncieux, C. Bahloul, C. Gault, M. Huger, T. Chotard, *Investigations of SiC aggregates oxidation: Influence on SiC castables refractories lifetime at high temperature*, Journal of the European Ceramic Society, nr (32), 2012, 737–743.

Structure, microstructure and mechanical performance of Zr-Nb-Mo Alloys: effect of composition and heat treatment

<u>J. Zając^{1a}</u>, I. Matuła¹, A. Barylski¹, K. Aniołek¹, M. Nabiałek², G. Dercz¹

a julia.zajac@us.edu.pl

Keywords: Zr alloys, XRD, microstructure

Zirconium based alloys are considered highly promising materials owing to their advantageous physicochemical properties, especially in applications within nuclear, chemical and medical industries. In this work, the development and structural characterisation of novel Zr-Nb-Mo alloys with varying Mo content, examined in both initial and water quenched state, is presented. The investigation consists of microstructural studies using scanning electron microscopy (SEM) and optical microscopy (OM), X-ray diffraction (XRD) assessment of qualitative and quantitative phase composition, energy dispersive spectroscopy (SEM-EDS) analysis of elemental distribution and mechanical evaluation through the use of Micro Combi Tester MCT³ and TRN tribometer.

Results demonstrate that increasing Mo content effectively hinders grain growth and promotes the formation of additional phases in the alloys, while water quenching also impacts the structure causing the ternary phase to appear in alloys with lower Mo content. Furthermore, heat treatment enhances microstructural and chemical homogeneity. The observed correlation between Mo doping and phase evolution was found to significantly influence mechanical and tribological performance, with systematic improvements in wear, hardness and elastic modulus, especially after quenching. These findings put an emphasis on the potential of Zr-Nb-Mo alloys as advanced materials, while highlighting the critical role of crystallographic investigation in tailoring their properties.

Acknowledgment: Conference participation was supported by the GreenMat project, co-funded by the European Union under the program "European Funds for Silesia 2021–2027

¹ Institute of Materials Engineering, Faculty of Science and Technology, University of Silesia in Katowice, Poland

² Department of Physics, Częstochowa University of Technology, Poland

Influence of short-term annealing on the physical and chemical properties of amorphous metal alloys based on aluminium

Kh. Khrushchyk^{1,2a}, P. Świec², J. Kubisztal², K. Balin², K. Aniołek², Yu. Kulyk¹, M. Karolus², L. Boichyshyn¹

^a khrystyna.khrushchyk@us.edu.pl

¹Faculty of Chemistry, Department of Physical and Colloidal Chemistry, Ivan Franko National University of Lviv, 6 Kyryla and Mefodiia Str., 79005, Lviv, Ukraine, ²Faculty of Science and Technology, Institute of Materials Engineering, University of Silesia in Katowice, 1A Pulku Piechoty Str., 41500, Chorzow, Poland

Keywords: amorphous metal alloy (AMA), crystallization, heat treatment, isothermal annealing

The objects of the investigations were AMAs alloys in the form ribbons with a thickness and width of 20-25 μ m and 3 mm, respectively, which were obtained at the G. V. Kurdyumov Institute for Metal Physics of the Ukrainian Academy of Sciences (Kyiv) by melt spinning method in a helium atmosphere on a copper drum rotating at a speed of ~30 m/s. The melt was prepared from pure metals and binary compounds REAl₃ (RE = Y, Gd). The purity of the starting metals was as follows: Al (99.999 wt.%), Ni (99.99 wt.%), Y (99.96 wt.%), Gd (99.96 wt.%) and Fe (99.99 wt. %).

In this work, the influence of rare earths and transition metals on the kinetics of stable crystallisation for the amorphous metal alloys (AMAs) with the following composition: Al₈₇Y₄Gd₁Ni₈. Isothermal annealing (during 5, 15, 30, 45, 60 min) were performed at certain temperatures with heating rate 20 K/min determined from the DSC curves, which are characteristic of stable growth of crystals of the secondary crystallization stage and equal to 611±2 K. Assessed the risks of AMA annealing on electrochemical properties at 0.3% NaCl. A profile analysis of the surface of the amorphous alloy Al₈₇Y₄Gd₁Ni₈ showed significant changes in topography depending on the heat treatment mode. In the as-cast state, the surface is characterised by relatively low roughness and a relatively uniform distribution of protrusions and depressions, which corresponds to a compact protective film. Short heat treatment for 5 minutes at T=611±2 K leads to temporary film thickening of the surface of AMA and an almost perfect double layer (n_{dl}=0.99), while roughness increases to 7.5, reflecting the increased active contact area with the electrolyte. Prolonged treatment (15 minutes) causes a sharp decrease in film resistance and charge transfer to $80 \Omega \cdot \text{cm}^2$ and 2.9×10^3 Ω ·cm², respectively, indicating film disruption and increased corrosion activity; at the same time, an increase in CPE-f-T (Q_f) and a decrease in n_f are observed, reflecting high surface heterogeneity, while roughness decreases to 0.26.

Acknowledgment: Conference participation was supported by the GreenMat project, co-funded by the European Union under the program "European Funds for Silesia 2021–2027

The synthesis of binary transition-metal hydrides through self-shearing reactive milling

I. Wyrębska^{1a}, J. Dworecka-Wójcik¹, A. Baran¹, M. Polański¹

a iwona.wvrebska@wat.edu.pl

Keywords: hydrogen storage, reactive milling, transition metal hydride

Self-shearing reactive milling (SSRM) is a mechanochemical process based on the intensive mixing of hydrogen-absorbing materials under hydrogen pressure. No grinding media, such as commonly used balls, are used. As recently discussed [1], the conversion of milled metals or intermetallic alloys into stoichiometric hydrides is allowed in most cases. During SSRM, the exposure of fresh, active surfaces of particles occurs due to their wear, which is caused by collisions with other particles and the internal surface of the cylinder. This method allows the manufacturing of very pure hydrides at room temperature and moderate pressure without capacity loss and contamination.

This work shows the syntheses of zirconium, hafnium, vanadium, niobium, and tantalum hydrides by intensive mixing under hydrogen pressure at room temperature with the use of a planetary mill without grinding media. Depending on the material, up to 90 h was required to fully convert metals to metal monoand dihydrides and their mixtures. During each synthesis, total hydrogen absorption was calculated based on a pressure drop in the vial measured during milling by the wireless sensor. The phase compositions of the products were characterized by X-ray diffraction (XRD), and the morphologies were observed by scanning electron microscopy (SEM). Additionally, the hydrogen content in the final product was determined via thermogravimetric analysis (TGA). It was demonstrated that SSRM can be easily adapted to most of the transition metal hydride syntheses without the necessity of using harsh pressure and temperature conditions.

[1] Patel, A.K., et al., Just shake or stir. About the simplest solution for the activation and hydrogenation of an FeTi hydrogen storage alloy. International Journal of Hydrogen Energy, 2022. 47(8): p. 5361-5371.

¹ Faculty of New Technologies and Chemistry, Military University of Technology, 2 Kaliskiego Street, 00-908 Warsaw, Poland

Tuesday 9th September

9:30	Randi Holmestad – Studies of Precipitates in age-hardenable Aluminium alloys by advanced TEM
10:20	Jakub Hawliczek – Ultrasonic Atomization: A Flexible Approach for Precious and Reactive Metals
10:40	Marek Polański – Spontaneous reactions of titanium alloys with hydrogen at room temperature
11:00	Coffee break
11:30	Manabu Ishimaru – Electron diffraction study of short-range order in ion-irradiated ceramics
12:20	Hanna Krężel & Felice D'Alia – Japan Electron Optics Laboratory – from past to present
12:40	Karolina Jurkiewicz – X-ray diffraction studies of amorphous pharmaceuticals
13:00	Patryk Wróbel – Advanced methods of analyzing the structure and phases of materials: XRD solutions offered by SCANMAT and LANScientific
13:20	Lunch
14:00	Magdalena Laskowska – Structural Ordering in Mesoporous Silica: From Liquid Crystal Templating to Functional Nanomaterials
14:20	Liliana Dobrzańska – Adaptive and selective crystals of homothiacalix[4]arene
14:40	Krystian Prusik – Structural and magnetic evolution of the NiMnCoIn alloy obtained by mechanical alloying
15:20	Anna Jarzębska – Crystallographic Insights into the Mechanical Behaviour of Absorbable Zinc Alloys
15:40	Rafal Babilas – Effect of cooling rate on the structure, corrosion resistance and nanomechanical properties of CoCrFeNi(Nb,Mo,B,Si) high entropy alloys
16:00	Coffee break & Poster session

19:00 Gala dinner

Studies of Precipitates in age-hardenable Aluminium alloys by advanced TEM

R. Holmestad^{1a}, C. D. Marioara², Sigmund J. Andersen²

a randi.holmestad@ntnu.no

Keywords: aluminium alloys, TEM, precipitation

The precipitation behavior in age-hardenable 6xxx (Al-Mg-Si) aluminium alloys is central to their mechanical performance. We performed atomic-scale characterization of early-stage clusters, Guinier–Preston (GP) zones, and metastable precipitates using advanced transmission electron microscopy (TEM) techniques. Aberration-corrected low-angle and high-angle annular dark-field scanning TEM (LAADF-STEM and HAADF-STEM) were employed to resolve nanoscale crystal structures in naturally aged and pre-baked conditions. The analysis reveals several cluster morphologies, including disordered Frank-Kasper (DFK) structures, and GP-zones composed of β'' structural units (eyes), which act as precursors to the main hardening phase [1].

Density functional theory calculations support experimental observations, confirming that β'' -like configurations with Mg/Si ratios close to 1 are energetically favorable. Pre-baking is shown to promote the formation of multi-eye GP-zones, which enhance nucleation of β'' needles during subsequent artificial aging. In contrast, natural aging leads to a higher fraction of less favorable DFK-type clusters, correlating with a delayed hardness response.

To support structural analysis, the AutomAl 6000 software was used for semiautomatic labeling of HAADF-STEM images, enabling efficient identification of atomic columns and precipitate motifs [2]. Scanning precession electron diffraction was also used to facilitate statistical evaluation of precipitate types and their evolution across different thermal treatments.

The presentation will provide new insights into the early stages of precipitation in 6xxx alloys and demonstrate the synergy between advanced microscopy, computational modeling, and automated image analysis in alloy design and optimization [3].

- [1] C.D. Marioara et al., Acta Mater. 269 (2024), 119811.
- [2] H. Tvedt et al., Ultramicr. 236 (2022), 113493.
- [3] We acknowledge the Research Council of Norway, project number 197405.

¹ Department of Physics, Norwegian University of Science and Technology (NTNU), Trondheim, Norway

² SINTEF Industry, Trondheim, Norway

Ultrasonic atomization a flexible approach for precious and reactive metals

J. Hawliczek^{1a}, A. Eckhoff^{1b}

^a jakub.hawliczek@3d-lab.pl ^b alexander.eckhoff@arcway.pl

¹ 3D Lab Sp. z o.o. & Arcway Sp. z o.o., Warsaw, Poland

Keywords: ultrasonic atomization, metallurgy

Additive Manufacturing and powder metallurgy research are becoming increasingly dependent on the availability of high-quality, application-specific metal powders. Ultrasonic atomization is a disruptive technology that enables controlled production of spherical powders with high flowability, low oxygen content, and narrow particle size distribution (PSD). This opens the door for precise material studies, including structural and crystallographic investigations.

This presentation highlights the role of UA in advancing research into difficult-to-atomize materials. We show how the technology supports the safe and economical preparation of powders from precious metals (e.g. Au, Pt), which are impractical to process at scale using GA or WA. With low oxygen levels (<10 ppm) and high recovery, UA allows small-scale synthesis without compromising purity — a key requirement for both crystallographic studies and functional validation in AM.

We also explore UA's role in enabling the study of reactive metals like magnesium and titanium. These materials present significant risks, including oxidation and explosion potential. Our work emphasizes the importance of combining process control with a deep understanding of material behavior, especially when balancing powder morphology, chemical stability, and operational safety.

The ultrasonic atomization was conducted using the ATO Suite (ATO Lab Plus, ATO Cast, IMS), equipped with controlled-atmosphere chambers and interchangeable crucibles. Multiple material batches (e.g., CuAlNiFe, CoCrFeMo, Nb, Au, Mg alloys) were processed. Comprehensive characterization included SEM imaging, EDS analysis, laser diffraction for PSD, and oxygen content measurement. Additionally, internal material reports were compiled post-process, summarizing all physical and chemical metrics.

All studied powders showed high sphericity (>95%), narrow PSD distributions, and oxygen content similar to feedstock. HEA maintained phase uniformity and

compositional stability, while maintaininh excellent flowability and sinterability for AM. Customer case studies confirmed successful

prototypes of implants and In one case, successful use of gold-based alloy powders in customized jewelry AM with material recovery.

We argue that UA expands the palette of materials accessible for 3D printing and powder metallurgy — from jewelry alloys to magnesium implants — but that scientific research is essential to define limits and optimize parameters.

Spontaneous reactions of titanium alloys with hydrogen at room temperature

I. Wyrębska¹, R. Chulist², D. Siemiaszko¹, P. Płatek³, M. Polański^{1*}

a marek.polanski@,wat.edu.pl

Keywords: hydrogen storage, mechanosynthesis, reactive milling, titanium hydride, hydrides

This study presents the results of investigations of the spontaneous reaction mechanisms between hydrogen and titanium, as well as selected titanium alloys (Ti6Al4V and Ti 5553), under room-temperature conditions in a hydrogen atmosphere using a planetary mill without conventional milling media. It was demonstrated that titanium particles undergoing self-induced milling readily absorb hydrogen and transform into stoichiometric titanium dihydride (TiH₂). Once initiated, the reaction proceeds spontaneously, even without further agitation, with initiation linked to the removal of surface oxides and strongly dependent on mixing intensity. Thermogravimetric measurements and X-ray diffraction confirmed the complete transformation of titanium into the hydride phase. Among the alloys tested, the metastable β-phase Ti-5553 alloy showed particularly high reactivity, absorbing hydrogen both as a hydride and in solid solution (>1.3 wt.%). Notably, an unexpected transformation route was observed in quenched α'-Ti64 alloy: instead of direct formation of hydride from α' , exposure to hydrogen resulted in the emergence of the titanium which β phase, indicating an alternative hydrogen-assisted phase transition pathway. Despite undergoing phase changes, the particles of alloys retained their original shape and structural cohesion, making the resulting spherical titanium hydride powders promising candidates for additive manufacturing applications, including porous structures and metallic foams.

¹ Institute of Materials Science and Engineering, Faculty of Advanced Technologies and Chemistry, Military University of Technology, Kaliskiego 2, 00-908 Warsaw, Poland,

AGH University of Science and Technology, Faculty of Metals Engineering and Industrial Computer Science, al. A. Mickiewicza 30, 30-059 Krakow, Poland
 Military University of Technology, Faculty of Mechatronics, Armament and Aerospace, Kaliskiego 2, 00-908 Warsaw, Poland,

Electron diffraction study of short-range order in ion-irradiated ceramics

M. Ishimaru

ishimaru@post.matsc.kyutech.ac.jp

Department of Materials Science and Engineering, Kyushu Institute of Technology, Fukuoka, Japan

Keywords: Radiation effects, order-to-disorder phase transformation, amorphous

When crystalline materials with long-range order are exposed to radiation environments, their structure changes to a short-range ordered state with damage accumulation. Knowledge of radiation-induced structural changes is of technological importance for realizing desirable material properties and for predicting the fate of materials under radiation environments. Information on short-range ordered structures appears as diffuse scattering in diffraction patterns, but its intensity is so weak that the diffuse scattering associated with disordering has not been well investigated. Electron diffraction has the advantage of detecting weak scattering intensities, because of the strong interaction between the matter and electrons. Furthermore, the short wavelength of high-energy electrons enables us to obtain diffraction intensity profiles up to high scattering angles in the reciprocal lattice space, which is useful for precise amorphous structure analysis. We have been analyzing the structures of radiation-induced metastable crystalline and amorphous phases using transmission electron microscopy. In this seminar, we will report (1) radiationinduced amorphous structures studied by a quantitative analysis of halo intensities [1] and (2) short-range ordered metastable crystalline phase formed during disordering processes [2-5].

- [1] M. Ishimaru, R. Nakamura, Y. Zhang, W. J Weber, N. J. Ianno, M. Nastasi, J. Eur. Ceram. Soc. 42 (2022) 376.
- [2] M. Iwasaki, Y. Kanazawa, D. Manago, M. K. Patel, G. Baldinozzi, K. E. Sickafus,
- [3] M. Ishimaru, J. Appl. Phys. 132 (2022) 075901.
- [4] M. Iwasaki, M. K. Patel, G. Baldinozzi, K. E. Sickafus, M. Ishimaru. J. Eur. Ceram. Soc. 44 (2024) 3131.
- [5] T. Izumi, M. Iwasaki, M. K. Patel, G. Baldinozzi, C. Grygiel, M. Ishimaru, Acta Mater. 284 (2025) 120581.

X-ray diffraction studies of amorphous pharmaceuticals

K. Jurkiewicz¹a, A. Janowska¹, T. Lamrani¹, P. Jesionek-Ratka², E. Ozimina-Kamińska² and K. Kamiński¹

a karolina.jurkiewicz@us.edu.pl

Keywords: X-ray diffraction, amorphous-like structure, molecular dynamics

One approach to address the problem of poor solubility of many amorphous pharmaceutical ingredients (APIs) is amorphization of their structure. However, there is still a very poor understanding of the relationship between the features of the local arrangement of molecules in the amorphous states, and the properties of such systems, such as molecular mobility, physical stability, dissolution/solubility, and, consequently, the therapeutic efficiency. The intra-and inter-molecular structural changes in API metastable glasses associated with manufacturing and storage, for example thermodynamic history, can significantly affect their structure, which exhibit only a limited order, so cannot be resolved by standard crystallography methods.

High energy total X-ray diffraction (XRD) studies of amorphous pharmaceuticals are relatively new application that builds on the long history of Pair Distribution Function (PDF) analysis, and enables more accurate investigations of materials with a limited atomic order. What is more, recent achievements of high-pressure X-ray diffraction in Diamond Anvil Cells (DACs) have made it possible to study of APIs at high-pressure conditions. As a result, new polymorphic forms of many APIs have been discovered. Moreover, studies of liquid APIs under high-pressure are possible, while it is well-known that the choice of the thermodynamic path (temperature and pressure conditions) of glass production affects its properties. Compression may significantly influence the structure and dynamics of supramolecular clusters, as well as the character and organization of hydrogen bonds. However, there is poor understanding of the structural differences between the ordinary glasses produced via vitrification at ambient pressure and the so-called pressure-densified glasses produced by vitrification of pressurized liquid.

Here we present temperature- and pressure-dependent XRD studies (please see Fig. 1) of two selected APIs, probucol and lorated lorated ine, both possessing a flexible unit in their molecules, which enables adopting different molecular conformations. Recent papers by some of us [1,2] demonstrated that liquid phases of these compounds show extraordinary differences in their molecular

¹ University of Silesia in Katowice, Institute of Physics, Chorzów, Poland

² Medical University of Silesia, Faculty of Pharmaceutical Sciences, Sosnowiec, Poland

dynamics under ambient and high pressure conditions. Our studies by XRD provided a deeper insight into microscopic origin of the observed changes in their molecular dynamics under compression. Moreover, we tested the hypothesis that the structural features of glasses produced via various thermodynamic routes are inherited from the corresponding liquid states.

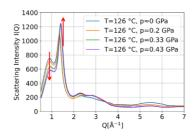


Fig. 1 Comparison of the experimental and model-based structure factors for supercooled liquid probucol.

The interpretation of the behaviour of XRD patterns under various thermodynamic conditions was supported by the molecular dynamics simulations. The models of the arrangement of molecules at various thermodynamic conditions were optimized so that the structure factors calculated on their basis were set together with the structure factors derived from experimental diffraction data (please see Fig. 2). Based on these models, the descriptions of the structural transformation of the structure of probucol and loratadine compounds from the liquid state to the glass state, via different thermodynamic routes, was possible.

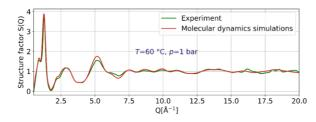


Fig. 2 Comparison of the experimental and model-based structure factors for supercooled liquid probucol.

Acknowledgement:

This research was funded by the National Science Centre (Poland), grant number: Opus 21 No. 2021/41/B/NZ7/01654. We gratefully acknowledge Polish high-performance computing infrastructure PLGrid (HPC Center: ACK Cyfronet AGH) for providing computer facilities and support within computational grants no. PLG/2025/018012J and PLG/2024/016967.

- [1] D. Heczko, et al. Journal of Molecular Liquids 376 (2023): 121377.
- [2] A. Minecka, et al. Journal of Molecular Liquids 321 (2021): 114626.

Structural ordering in mesoporous silica: from liquid crystal templating to functional nanomaterials

M. Laskowska^{1a}, M. Zubko², A. Karczmarska¹, M. Doskocz¹, and Ł. Laskowski¹

a magdalena.laskowska@ifj.edu.pl

 Institute of Nuclear Physics Polish Academy of Sciences, 31-342 Krakow, Poland
 Institute of Materials Engineering, Faculty of Science and Technology, University of Silesia, Chorzów 41-500, Poland

Keywords: nanomaterials, ordered mesoporous silica, functional materials

Ordered mesoporous silica materials are widely studied for their unique combination of high surface area, tuneable pore sizes, and long-range structural order. Their synthesis is typically based on liquid crystal templating (LCT) — a strategy that harnesses the self-assembly of surfactants or block copolymers into mesophases to guide the organization of silica precursors into nanostructures with defined symmetry [1].

Since the discovery of the first ordered mesoporous silica material, called MCM-41, in the early 1990s, these materials have attracted growing interest due to their uniform pore architectures, typically hexagonal, cubic, or lamellar, derived from liquid crystalline templates. Unlike classical crystalline solids, the periodicity in mesoporous silicas arises from their pore arrangement rather than atomic lattice order, positioning them at the interface between soft matter and solid-state materials [2].

The relevance of such structural control is discussed in the context of structure—property relationships and the design of new functional nanomaterials based on ordered silica frameworks. Applications of such materials include catalysis, adsorption, drug delivery, and sensing, where structural regularity, chemical stability, and tuneable porosity enhance performance. Moreover, templating strategies allow for precise control over pore connectivity and accessibility, which is crucial for selective transport and reactivity. Surface functionalization further broadens their potential in biomedicine, environmental technologies, and energy-related systems. Altogether, ordered mesoporous silicas offer a versatile platform for creating advanced materials with tailored properties linked directly to their mesostructural organization.

The applicational potential of such functionalized silica matrices will be discussed on the example of silica SBA-15 with propyl-phosphonate and propyl-carboxyl functional groups. This material is a unique example of a base

for single-atom catalysts, which may find wide application in medicine and industry. A detailed analysis of the molecular structure of the presented material and the influence of spatial confinement of functional groups on the material properties will be discussed based on the results of transmission and scanning electron microscopy, energy dispersive X-ray spectroscopy, low-angle X-ray diffraction, nitrogen sorption analysis, and vibrational spectroscopy [3-4].

- [1] M. Nagaraj, Crystals 10 (2020), p. 648;
- [2] C. T. Kresge, M. E. Leonowicz, W. J. Roth, J. C. Vartuli & J. S. Beck, Nature 359 (1992), p. 710–712;
- [4] L. Laskowski, Magdalena Laskowska, et al., Journal of Nanomaterials 1 (2017) p. 1287698;
- [5] M Laskowska, et al., Nanoscale 9 (2017), p. 12110-12123.

Adaptive and selective crystals of homothiacalix[4] arene

L. Dobrzańska 1a and R. Maria Losus 1

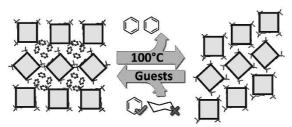
a lianger@umk.pl

¹ Faculty of Chemistry, Nicolaus Copernicus University in Toruń, Gagarina 7, 87-100 Toruń. Poland

Keywords: adaptive crystals, calixarenes, sorption

Calixarenes have been extensively studied as host molecules in solution and the solid state for many decades due to their facile synthesis, well-defined and adaptable cavities, strong guest-binding capabilities, and structural flexibility. [1] The latter has not been studied as broadly in the solid state as in solution, and revealing host adaptivity in single-crystals of these macrocycles upon external triggering is still exceptional. Two of our earlier reports on conformational changes taking place in the crystal unity of calixarenes, revealed for homodithiacalixarene and its selena analogue, are still the only examples presenting such molecular rearrangements for this group of compounds. [2,3] The potential of structural adaptability renders crystalline material based on calixarenes promising for future applications in gas storage, molecular separation, or sensing.

In this context, we would like to present results obtained for homothiacalix[4] arene crystals, which show high selectivity in the sorption of guest molecules.



Acknowledgement:

We would like to thank the National Science Centre – Poland for grant no. 2014/14/E/ST5/00611 and the program Excellence Initiative - Research University for funding the research group of Crystal Engineering and Advanced Solid-State Characterization.

- [1] X.-N. Han, Y. Han and C.-F. Chen, Chem. Soc. Rev. **52** (2023), 3265.
- [2] J. Thomas, G. Reekmans, P. Adriaensens, L. Van Meervelt, M. Smet, W. Maes, W. Dehaen and L. Dobrzańska, Angew. Chem., Int. Ed. 52 (2013), 10237.
- [3] J. Thomas, L. Dobrzańska, L. Van Meervelt, M. A. Quevedo, K. Woźniak, M.
- [4] Stachowicz, M. Smet, W. Maes and W. Dehaen, Chem. Eur. J. 22 (2016), 979.

Structural and magnetic evolution of the NiMnCoIn alloy obtained by mechanical alloying

K. Prusik la, E. Matyja , Z. Stokłosa , M. Zubko , P. Świec , G.Dercz

a krystian.prusik@us.edu.pl

Keywords: mechanical alloying, crystallisation kinetics, magnetic shape memory alloys;

NiCoMnIn alloys are a group of magnetic shape memory alloys (MSMAs), which exhibit a reversible martensitic transformation that can be induced by variations in temperature, applied mechanical strain, or magnetic fields. This transformation results in significant and controllable macroscopic shape changes, which are of interest for various functional applications [1,2] or may be used in a powder state in a metal printing technique.

This study investigates the structural and magnetic evolution of the Ni_{45.5}Co_{4.5}Mn_{36.6}In_{13.4} alloy (at.%) powders produced via mechanical alloying (MA). The powders, subjected to 70 and 100 hours of MA, were characterised by a heterogeneous microstructure comprising both amorphous and nanocrystalline body-centred cubic (bcc) phases. Relaxation phenomena in the as-milled powders were observed, exhibiting a logarithmic increase as a function of annealing time. Annealing treatments at temperatures above 440°C induced several significant microstructural transformations, including the ordering of L2₁ Heusler phase, dissolution of residual nickel and manganese, formation of tetragonal MnNi phases, and precipitation of γ phases.

In addition to post-annealing analyses, in-situ transmission electron microscopy (TEM) experiments were performed to elucidate the evolution of the microstructure as a function of temperature. Furthermore, magnetic characterisation, including measurements of magnetisation as a function of temperature and magnetic field, was employed to investigate the magnetic properties correlated with the microstructural development and phase evolution. The activation energies associated with the B2 \rightarrow L21 ordering transformation were determined. These combined structural, thermal, and magnetic investigations offer valuable insights into the thermomechanical processing and stability of Ni–Co–Mn–In alloys, with implications for their functional properties in magnetic shape memory applications.

¹ Institute of Materials Engineering, University of Silesia in Katowice, 41-500 Chorzów. Poland

Acknowledgment: Conference participation was supported by the GreenMat project, co-funded by the European Union under the program "European Funds for Silesia 2021–2027

- [1] K. Ulakko et. al., Mater. J. Mater. Engin. Perform. 5 (1996), 405-409.
- [2] R. Kainuma, Y. Imano, W. Ito, Y. Sutou, Nature Vol 439 (2006), 957-960.

Crystallographic insights into the mechanical behaviour of absorbable zinc alloys

A. Jarzębska^{1a}, M. Gieleciak¹, Ł. Maj¹, M. Bieda¹, R.Chulist², J. Skiba³

a a.jarzebska@imim.pl

Keywords: absorbable zinc alloys, crystallographic texture, strain-rate sensitivity

Zinc alloys have recently attracted interest for use in absorbable implants due to their favourable corrosion rate. This allows them to remain intact during tissue healing and subsequently degrade safely in the body. However, their limited mechanical properties and strain-rate sensitivity hinder broader application. Previous studies have shown that combining alloying additions with hydrostatic extrusion (HSE) can enhance the mechanical properties of Zn-based materials to meet biomedical requirements. However, the stability of such processed materials has not been fully addressed. This study addresses that gap by exploring the impact of alloying on strain-rate sensitivity.

Pure Zn and two different alloys—Zn-Mg and Zn-Mg-Cu—were prepared and subjected to multi-pass HSE. Mechanical properties were evaluated via tensile tests using a Zwick/Roell Z250 machine at varying strain rates. Microstructural characterization was performed using EBSD in an FEI Quanta 3D FEGSEM, TEM in an FEI Tecnai G2 200kV FEG microscope. Crystallographic texture was analyzed using high-energy synchrotron X-ray diffraction at DESY, Hamburg.

The results revealed a composite-like microstructure composed of alternating bands of refined α - or η -Zn grains and the hard Mg_2Zn_{11} intermetallic phase, along with a double-fiber texture. These features contribute to improved strength and ductility. Despite these enhancements, the materials also exhibited increased strain-rate sensitivity with increase of the number of alloying additions. This behaviour may be linked to additional solid solution strengthening in the ternary alloy, which facilitates dynamic recrystallization.

Acknowledgement: This work was supported by the Institute of Metallurgy and Materials Science, Polish Academy of Sciences, within a statutory work Z-6.

¹ Institute of Metallurgy and Materials Science, Polish Academy of Sciences, Krakow, Poland

² Faculty of Metals Engineering and Industrial Computer Science, AGH University of Krakow, Krakow, Poland

³ Institute of High Pressure Physics, Polish Academy of Sciences, Warszawa, Poland

Effect of cooling rate on the structure, corrosion resistance and nanomechanical properties of CoCrFeNi(Nb,Mo,B,Si) high entropy alloys

R. Babilas^{1a}, K. Młynarek-Żak², E. Wyszkowska³ and J. Bicz¹

a rafal.babilas@polsl.pl

Keywords: High entropy alloys; Electrochemical measurements; Nanoindentation

The high entropy alloys (HEAs) represent a novel group of metallic engineering materials that have received increasing attention in recent years. A concept of high-entropy alloy involves the use of five or more principal elements in equimolar or near-equimolar ratios. As a result, these alloys characterize with a high value of the configurational entropy, which contributes to stabilization of single phases of FCC, BCC, and HCP phases. In particular, their high-temperature microstructural stability, long-term fatigue resistance, and high oxidation and wear resistance make them promising materials for advanced structural elements. Furthermore, HEAs can be characterised with improved irradiation resistance, creating perspectives for their use as structural materials in nuclear applications. The possible use of HEAs in electrocatalysis is also being considered, which is derived from its high corrosion resistance and notable catalytic activity. HEAs are also expected to be potential hydrogen storage materials [1-6].

Equimolar CoCrFeNiX high entropy alloys (X = Mo, Nb, B, and Si) were prepared by induction melting and copper die casting to determine the effect of cooling rate on the structure and anticorrosion and mechanical properties of ingots and plates. The investigated HEAs in the form of ingots were obtained by the induction melting method with the use of a NG-40 induction generator, under an argon atmosphere. The ingots were solidified with a low cooling rate using Al_2O_3 crucibles. Plates with a thickness of 1 mm were prepared by remelting the ingots obtained ingots and low pressure casting using a water cooled copper mould with a cooling rate $\sim 10^3$ K/s.

¹ Department of Engineering Materials and Biomaterials, Silesian University of Technology, Konarskiego 18a St., Gliwice, Poland

² Department of Engineering Processes Automation and Integrated Manufacturing Systems, Silesian University of Technology, Konarskiego 18a St., Gliwice, Poland ³ National Centre for Nuclear Research, NOMATEN CoE MAB+, Andrzeja Soltana 7 St., Otwock-Świerk, Poland

The structure was investigated extensively using X-ray diffraction (XRD), scanning electron microscopy (SEM), transmission electron microscopy (TEM) and Mössbauer spectroscopy (MS). To evaluate the corrosion resistance of the alloys investigated, electrochemical measurements were performed in the environments of 3.5 and 5% sodium chloride solution environments at a temperature of 25 °C. The corrosion potential and the corrosion current density were also determined using the Tafel extrapolation method. To complete the polarization tests, electrochemical impedance spectroscopy (EIS) was performed at open-circuit potentials with an amplitude adjusted at 5 mV over a frequency range of 10⁵ - 10⁻² Hz. Moreover, scanning Kelvin probe force microscopy (SKPFM) was used to determine the interaction between the phase structure and potential differences. Nanomechanical tests (hardness and Young's modulus) were conducted on a NanoTest Vantage apparatus equipped with a diamond Berkovitch indenter.

The application of rapid solidification contributed to the refinement and homogenisation of the structure for HEAs in the form of plates. High entropy alloys with Mo, Nb, and B have a multiphase structure consisting of FCC and intermetallic phases. The formation of a dual-phase structure consisting of only intermetallic phases was observed for the CoCrFeNiSi alloy. The CoCrFeNiSi alloy in ingot form is characterized by the highest corrosion resistance in solutions of 3.5 and 5% NaCl. The EIS study indicated the formation of a stable and protective passivation layer on the CoCrFeNiSi alloy. The most favourable nanomechanical properties characterize the plates with B and Si additions. The refinement of the structure for rapid solidificated samples of studied HEAs has a positive effect on hardness and corrosion resistance.

Acknowledgement: The work was supported by the National Science Centre of Poland under research project no. 2022/47/B/ST8/02465.

- [1] D.B. Miracle and O.N. Senkov, , Acta Mater. 122 (2017) p. 448-511.
- [2] B. Yu, Y. Ren, Y. Zeng, W. Ma, K. Morita, S. Zhan, Y. Lei, G. Lv, S. Li and J. Wu,
- [3] J. Mat. Res. Techol. 29 (2024) p. 2689-2719.
- [4] T. Sonar, M. Ivanov, E. Trofimov, A. Tingaev and I. Suleymanova, Mater. Sci. Energy Technol. 7 (2024) p. 35-60.
- [5] Y. Lin, T. Yang, L. Lang, Ch. Shan, H. Deng, W. Hu and F. Gao, Acta Mater. 196 (2020) p. 133-143.
- [6] E.J. Pickering, A.W. Carruthers, P.J. Barron, S.C. Middleburgh, D.E.J. Armstrong and A.S. Gandy, Entropy 23(1) (2021) p. 98.
- [7] R. Babilas, J. Bicz, A. Radoń, M. Kądziołka-Gaweł, D. Łukowiec, K. Matus, E. Wyszkowska, Ł. Kurpaska, D. Rudomilova, K. Młynarek-Żak, Elect. Acta 525 (2025) 145933.

Advanced methods of analyzing the structure and phases of materials: XRD solutions offered by SCANMAT and LANScientific

P. Wróbel

SCANMAT, Warsaw, Poland

Keywords: X-ray diffraction (XRD), advanced material analysis

X-ray diffraction (XRD) remains one of the key methods used in the analysis of crystal structure and phase identification of solid materials. With the development of instrumentation technology, XRD systems are becoming increasingly efficient, compact, and adapted to a variety of applications, from basic research to industrial quality control. The presentation will introduce selected XRD solutions and other techniques offered by Scanmat in cooperation with LANScientific.

Wednesday 10th September

- 9:30 **Krzysztof Woźniak** Hidden complexity in Structures of Ices by Quantum Crystallography and PDF
- 10:20 **Maciej Grzywa** Quantitative Phase Analysis of Zeolites using X-ray Powder Diffraction (XRPD)
- 10:40 **Joanna Grelska** High-pressure polymorphism discovered in n-butanol
- 11:00 Coffee break
- 11:30 **Łukasz Laskowski** The 2D solid solvent: a novel approach to preparation functional nanomaterials
- 11:50 **Radosław Kamiński** Our recent developments towards ultrafast time-resolved small-molecule crystallography
- 12:10 **Tomas Moravek** TESCAN TENSOR Advances in precession-assisted electron diffraction technology
- 12:30 Marek Kojdecki Crystalline microstructure of mullite in whiteware triaxial porcelains method of investigation and characteristics of materials
- 12:50 Closing ceremony
- 13:00 Lunch

Hidden complexity in Structures of Ices by Quantum Crystallography and PDF

<u>K. Woźniak^{1a}.</u> W. A. Sławiński¹, G. Łach², R. Gajda¹, M. Chodkiewicz¹, P. Rejnhardt, M. Arhangelskis¹, Ch. Ridley^{3,5} and C. L Bull^{3,4}

a kwozniak@chem.uw.edu.pl

¹ University of Warsaw, Departm. of Chem., Pasteura 1, 02093 Warszawa, Poland. ²University of Warsaw, Departm of Phys., Pasteura 5, 02093 Warszawa, Poland. ³ISIS Neutron and Muon Source, STFC, Rutherford Appleton Laboratory; Harwell Campus, Didcot, Oxfordshire, OX11 0QX, UK.

 4 EaStCHEM School of Chemistry, University of Edinburgh; Joseph Black Building, Edinburgh EH9 3FJ, Scotland, UK.

Keywords: Ice, HAR, PDF

Ice is the solid form of water (H₂O), a substance fundamental to life on Earth. The most familiar form of ice is the hexagonally structured ice I_h, which forms in our everyday environment in the form of snowflakes and ice cubes. However, water can crystallize into at least 21 distinct phases, unique in structure, depending on the temperature/pressure and route of formation. The different phases are denoted by Roman numerals (e.g., Ice I_h, II, III etc.), and have found relevance across a diverse range of different research areas, from geology and planetary science to fundamental physics. Hydrogen bonds are responsible for many unique properties of water (and ices), such as its high melting and boiling points relative to other small molecules, and its lower density in solid compared to liquid form. Understanding hydrogen bonding in ice thus paved the way for broader research into the significance of hydrogen bonding in various chemical and biological systems. The presence of different ices in the outer solar system and beyond provides information about the formation and evolution of celestial bodies, as well as on the potential for life in extreme environments. Studies of ices also have practical implications in understanding natural phenomena on Earth, such as the formation of glaciers and the behaviour of water in different atmospheric and environmental conditions as well as formation and decay of methane clathrate deposits.

At pressures exceeding 2–3 GPa, water molecules arrange themselves into cubic ice VII (Fig. 1a, space group Pn-3m)[1,2]. This is one of the densest ice structures (ca. 1.50g/cm³) with ices X and XI (2.51g/cm³ and >2.51g/cm³, respectively). Ice VII plays a role in the water-rich interiors of Jupiter's moon

⁵Spallation Neutron Source, Oak Ridge Nat. Lab., Oak Ridge, Tennessee 37830, USA.

Europa and Saturn's moon Enceladus and other planetary bodies. This highpressure polymorph of ice, is known for its disordered hydrogen positions, yet the nature of this disorder has remained unresolved.

In this contribution will present details of structures of ices (VI[3], VII[1,2], Ih [4]) obtained with quantum-crystallographic Hirshfeld Atom Refinement against single crystal X-ray, electron and neutron diffraction data. We will also present the first quantitative characterisation of disorder in D₂O ice VII and VI obtained through a combination of Pair Distribution Function (PDF) analysis, Reverse Monte Carlo (RMC) modelling, and high-pressure neutron scattering. Our results provide a detailed decomposition of both the average and local atomic structures of Ice VII, revealing a previously unquantified level of structural disorder. These findings are corroborated by density functional theory (DFT) calculations, offering a comprehensive understanding of the structural behaviour of Ice VII under extreme conditions.

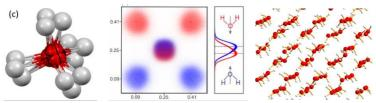


Figure 1 (from the left); Disordered model of ice VII refined by HAR (the average structure), distribution of oxygen atoms in ice VII from PDF and RMC refinement and unique positions of water molecules in ice VII (local structure).

Acknowledgement: KW, RG and PR gratefully acknowledge support by the National Science Centre, Poland, through OPUS 21 grant No. DEC-2021/41/B/ST4/03010.

- [1] R. Gajda, M. Chodkiewicza, D. Zhang, P. Nguyen, V. Prakapenka, K. Wozniak, Structure of ICE VII with Hirshfeld Atom Refinement, IUCRJ, 12(3) (2025) 288-294, https://doi.org/10.1107/S2052252525002581
- [2] W. A. Sławiński, G. Łach, R. Gajda, M. Chodkiewicz, P. Rejnhardt, M. Arhangelskis, C. Ridley, C. L Bull, K. Woźniak, Hidden complexity in D2O Ice VII, Nature Comm., (2025) submitted.
- [3] M. L. Chodkiewicz, R. Gajda, B. Lavina, S. Tkachev, V. B. Prakapenka, P. Dera, K. Woźniak, Accurate crystal structure of ice VI from X-ray diffraction with Hirshfeld atom refinement, IUCRJ, 9 (2022) 573-579, IUCRJ Highlight, https://doi.org/10.1107/S2052252522006662
- [4] M. L. Chodkiewicz, B. Gruza, K. K. Jha, P.M. Dominiak, K. Woźniak, Hirshfeld atom refinement and dynamical refinement of hexagonal ice structure from electron diffraction data, IUCRJ, 11(5) (2024) 730-736, https://doi.org/10.1107/S20522525240068

Quantitative phase analysis of zeolites using X-ray Powder Diffraction (XRPD)

M. Grzywa

maciej.grzywa@rigaku.com

Rigaku Europe SE, Neu-Isenburg, Germany

Keywords: zeolites, quantitative phase analysis, Direct-Derivation method

Zeolites, classified as porous aluminosilicate minerals, are extensively employed in industrial applications owing to their unique structural properties, including high surface area, thermal stability, and ion-exchange capabilities. These materials are used in various fields, including catalysis, adsorption and separation, ion exchange, medicine, construction, and agriculture.

This study focuses on the quantitative phase analysis of zeolites utilizing the X-ray powder diffraction (XRPD) technique. XRPD is a robust method for characterizing the crystalline structure of materials, facilitating the identification and quantification of different phases within a sample. Through the application of X-ray powder diffraction, precise quantification of zeolitic phases was achieved using various methods (e.g., Rietveld, Direct-Derivation [1]) with the SmartLab Studio II software, providing insights into the purity and composition of the samples.

The XRPD data for the analysis were collected using a Rigaku MiniFlex 600 advanced X-ray benchtop diffractometer equipped with the 1-D D/teX Ultra2 detector, as well as a Rigaku SmartLab SE diffractometer.

This presentation introduces various quantitative analysis methods, with a particular focus on the Direct-Derivation method. It underscores the importance of accurate phase quantification in the development, production, and application of zeolite-based materials.

- [1] H. Toraya, J. Appl. Cryst., 55 (2022), p. 439
- [2] H. Toraya, Powder Diffraction, 36 (3) (2021), p. 159
- [3] H. Toraya, J. Appl. Cryst., 53, (2020), p. 1225

High-pressure polymorphism discovered in n-butanol

<u>J. Grelska^{1a}</u>, R. Gajda¹, M. Arhangelskis¹, K. Jurkiewicz², K. Woźniak¹ and W.A. Sławiński¹

a j.grelska@uw.edu.pl

Keywords: polymorphism, high-pressure, hydrogen bonds

N-butanol, the fourth member of linear-chain primary monohydroxy alcohols, exhibits a strong tendency toward vitrification, hindering crystallization under ambient conditions. A low-temperature crystalline phase (PI at 110 K) has been previously identified [1], forming from intermediate glacial state. This study reports crystallization of n-butanol under high-pressure conditions, resulting in two newly discovered high-pressure polymorphs, both structurally different from low-temperature form.

The high-pressure phase transition occurs at \sim 2 GPa, producing a more ordered structure with four times smaller unit cell volume while retaining P21/c space group. Comparative analysis shows that polymorphism under varied thermodynamics conditions is common among monohydroxy alcohols, which crystal structure is governed by infinite chains of hydrogen bonds [2]. Hydrogen bonds also dominate molecular aggregation in liquid state of these compounds [3].

High-pressure crystallization of n-butanol in a diamond anvil cell was first observed in a powder diffraction experiment at ESRF [4]. Subsequently, single crystals at high-pressure were produced and two structural forms were resolved. Raman spectroscopy was used as a complementary method to characterize each form. The results show significant role of hydrogen bonds in determining the crystal structure. The findings contribute to the understanding of polymorphism in hydrogen-bonded compounds and highlight the structural diversity accessible through high-pressure crystallization.

- [1] P. Derollez, A. Hédoux, Y. Guinet, F. Danède and L. Paccou, Acta Cryst. B Structural Science 69.2 (2013), 195.
- [2] D.R. Allan and S.J. Clark, Physical Review B 60.9 (1999), 6328.
- [3] J. Grelska, K. Jurkiewicz, A. Burian, and S. Pawlus, The Journal of Physical Chemistry B 126.19 (2022), 3563.
- [4] The access to ESRF was financed by the Polish Ministry of Education and Science (dec. no. 2021/WK/11).

Faculty of Chemistry, University of Warsaw, Warsaw, Poland
 August Chełkowski Institute of Physics, Faculty of Science and Technology, University of Silesia in Katowice, Chorzów, Poland

The 2D solid solvent: a novel approach to preparation functional nanomaterials

Ł. Laskowski

lukasz.laskowski@ifj.edu.pl

The Henryk Niewodniczański Institute of Nuclear Physics Polish Academy of Sciences

Keywords: Molecular engineering – Self-organization – 2D solid solvent

Within a framework of this presentation, the audience will be guided through the methods of molecular engineering. The key to the bottom-up approach for molecular engineering is to design synthesis in such a way that atoms create assumed molecular structure by themselves through the self-organization process. This concept can be applied to operate a position of individual atoms and molecules, preserving assumed distribution of the building blocks (atoms) and control distance between them. Then, we can observe them as separate objects, investigate the interaction between them as a function of intermolecular distance and utilize the properties of individual molecules, which often differs tremendously from their bulk characteristics.

All this above sounds promising but how to achieve this in practice? Let us imagine a solid material with regularly distributed anchoring units separated by a specific distance, which can catch particular atoms or molecules and keep them separated. One association which comes to mind is some kind of a solvent since the last one is able to coordinate the molecules in such a way that they are separated and to create a solvation complex. In the case of a liquid, nevertheless, dissolved molecules are difficult to investigate since they are not immobilized. The compound we are searching for should have such a form that allows for rigid immobilization of nano-objects. This way the objects could be used for specific purposes at specific time and place. It should be some kind of a "solid solvent".

In this lecture, the concept of 2D solid solvent will be presented. Such materials can be fabricated based on functionalized nanostructured materials, such as silica or alumina. A few examples of functional materials being in fact 2D solid solvents will be shown, along with an explanation of their structure, functionality, description the fabrication route and justification the purposefulness of their production. Also, the role of molecular engineering in the fabrication process will be clarified here.

Our recent developments towards ultrafast time-resolved small-molecule crystallography

R. Kamiński^{1a}, K. N. Jarzembska¹, D. Szarejko¹, P. Łaski¹

a rkaminski85@uw.edu.pl

Keywords: photocrystallography, time-resolved diffraction, XFEL

Ultrafast X-ray based techniques allow for tracing of short-lived light-induced molecular species from several ms to even sub-ps/fs time-scale. Whereas the former are recently becoming possible even at the laboratory sources — with proper instrumentation provided — the latter require use of the large-scale facilities, synchrotrons and X-ray free-electron lasers (XFELs) in particular. Synchrotrons provide X-ray pulses as short as about 100 ps, and coupled with the polychromatic narrow-band ('pink') Laue technique can provide an excellent data for further analyses. In turn, XFELs, by their fundamental principles provide X-ray pulses of unprecedented intensity and as short as about 12 fs.

In this contribution I will concentrate on our recent developments in terms of data processing and sample delivery for both of the above-mentioned techniques, which we utilize in our research. For the data processing we advanced the Laue diffraction method towards small-molecule crystals, where the diffraction patterns are 'sparse' compared to the macromolecular crystals. I will present our efforts towards new seed-skewness Bragg spot integration method [1], instrument model refinement [2] and our most recent attempts for finding a crystal orientation in Laue polychromatic experiments.

XFEL studies will concern polycrystalline thin-film diffraction with sub-ps time resolution of a model Fe^{II} spin-crossover complex [3]. Our initial results yielded an excellent comparison of XFEL results with the ones obtained independently via ultrafast electron diffraction. Furthermore, we explore more possibilities to use the rotation method for such experiments, and how our integration techniques can be applied for the XFEL data.

Acknowledgement: Authors acknowledge the National Science Centre (Poland) (2016/21/D/ST4/03753, 2020/38/E/ST4/00400) and the Ministry of Science and Higher Education (Poland) for financial support (agt. No. 2022/WK/13).

¹ University of Warsaw, Faculty of Chemistry, Warsaw, Poland

- [1] D. Szarejko, R. Kamiński et al., J. Synchrotron Rad. 27 (2020), p. 405.
- [2] R. Kamiński, D. Szarejko et al., J. Appl. Cryst. 53 (2020), p.1370.
- [3] D. Vinci, K. Ridier et al., Nat. Commun. 16 (2025) p. 2043.

TESCAN TENSOR – Advances in precession-assisted electron diffraction technology

T. Morávek*1, D. Němeček1, B. Clarke1

a tomas.moravek@tescan.com

¹ TESCAN GROUP, a.s., Libušina třída 863/21, Brno, Czech Republic

Keywords: diffraction microscope, Tensor, 3DED

Technology advances and method developments drive the increasing interest in applications of electron diffraction for characterization of crystalline phases and structure determination of synthetic compounds. The new analytical STEM and diffraction microscope, TESCAN TENSOR, is the first microscope with fully integrated electron beam precession that diminishes the effects of dynamical scattering in collected electron diffraction datasets. Consequently, the quality of (initial) kinematical refinements is significantly improved. Moreover, TENSOR is equipped with a FEG electron source that can provide a parallel beam well below 100-nm in diameter and thus determine the structure even from individual grains in polycrystalline materials.

Crystalline microstructure of mullite in whiteware triaxial porcelains – method of investigation and characteristics of materials

J. Bastida¹, A. Caballero², M.A. Kojdecki^{3a} and A. Sanz¹

a Marek.Kojdecki@wat.edu.pl

Keywords: crystalline microstructure, mullite, porcelain

The aim of this work is the presentation of both the method for determining crystalline microstructure and the results of its application to the systematic study of mullites in series of porcelain samples.

The development of mullite in triaxial whiteware porcelains produced of mixtures containing 53% weight of kaolin (of high crystallinity kaolinite B, or of low crystallinity kaolinite minerals M), 14% of quartz (of small grains P or of big grains G) and 33% of feldspar (with lithium content C or without it S) were studied. Cylindrical samples were prepared by casting and subsequent drying. Samples were treated at two firing cycles: slow (L) with heating rate of 2°C/min and stay at maximal temperature for 180 minutes or fast (R) with heating rate of 5°C/min and stay at maximal temperature for 90 minutes, both at one of four maximal temperatures: T1=1270°C, T2 = 1300°C, T3 = 1320°C, T4 = 1340°C (all typical of industrial processing). In this way sixty-four different porcelain specimens were obtained (labelled as e.g. BGCL1, MPSR2) [1]. Porcelain samples were ground and investigated by X-ray diffraction and other techniques. Influence of firing temperature and different compositions on crystalline microstructure of mullite was observed. Size distributions and shapes of crystallites and second-order strain distributions were determined by applying multi-peak analysis of X-ray diffraction patterns [2] [3].

Crystallites were modelled in form of spheres, cylinders or prisms. Prisms (found to be most probable shape in most samples) were modelled with edges parallel to main crystallographic axes of corresponding lengths A, B, C with aspect ratios B/A=1.02 fixed and C/A modelled. Mean volume-weighted standardised crystallite size T [Å] (equal to cube root of volume) of mullite was used to compare the samples and is shown in the first table. Cylinder with aspect ratio H/D (hight to diameter) modelled was found in most cases almost equally probable as corresponding prism.

¹ Departament de Botànica i Geologia Universitat de València, Valencia, Spain

² Instituto de Cerámica y Vidrio, CSIC, Madrid, Spain

³ Instytut Matematyki i Kryptologii, Wojskowa Akademia Techniczna, Warsaw, Poland

All samples featured bimodality of volume-weighted size distributions of mullite crystallites. All firing cycles produced secondary mullite (3Al2O3·2SiO2) but primary mullite (2Al2O3·SiO2) appeared also at early stages of processing and finally transformed into secondary one. These processes resulted in formation of two fractions of crystallites with logarithmic-normal size distributions. Mean volume-weighted standardised sizes [Å] of mullite crystallites for whole sample and for each fraction, mean-absolute second-order strain [%] and mean aspect ratio of prismatic crystallites for BPS series of samples were collected in the second table to illustrate complex dependence of mullite microstructure on composition and firing cycle.

Table 1. Mean volume-weighted standardised crystallite size T [Å] of mullite.

			0						
Cycle	T max	BGS	BGC	BPS	BPC	MGS	MGC	MPS	MPC
L1	1270	601	666	313	488	517	468	559	810
L2	1300	597	898	411	663	546	474	467	404
L3	1320	547	710	422	530	464	770	504	504
L4	1340	514	563	462	777	460	837	514	535
R1	1270	500	625	380	417	378	435	496	382
R2	1300	509	556	437	518	437	568	546	616
R3	1320	625	532	403	688	451	519	464	507
R4	1340	607	478	489	650	565	543	563	495

Table 2. Average characteristics of mullite in the samples of BPS series.

	BPSL1	BPSL2	BPSL3	BPSL4	BPSR1	BPSR2	BPSR3	BPSR4
Mean size: total	313	411	422	462	380	437	403	489
first fraction	273	321	180	355	291	176	246	343
second fraction	377	521	493	567	454	467	517	606
Mean strain	0.099	0.080	0.086	0.080	0.089	0.087	0.085	0.082
Prism aspect ratio	1.4	2.0	1.7	1.9	1.7	1.7	1.8	1.5

The results of investigations of the porcelain samples by simplified methods of microstructure analysis were previously published [4,5].

- [1] A. Sanz, Study of crystallite size in industrial porcelains, PhD thesis (in Spanish), 2015, University of Valencia (Spain).
- [2] M.A. Kojdecki, J. Bastida, P. Pardo and P. Amorós, J. Appl. Cryst. 38 (2005), p. 888-899.
- [3] M.A. Kojdecki, E. Ruiz de Sola, F.J. Serrano, V. Delgado Pinar, M.M. Reventós, V.J. Esteve, J. Appl. Cryst. 40 (2007), p. 260–276.
- [4] A. Sanz, J. Bastida, A. Caballero and M.A. Kojdecki, Clay Minerals 53 (2018), p. 471-485.
- [5] A. Sanz, J. Bastida, A. Caballero and M.A. Kojdecki, Appl. Clay Sci. 198 (2020), 105805, p. 1-9.

Poster session 9th September

- P.01 **R. Albrecht**: High-resolution misorientation mapping in single-crystal superalloys via X-ray diffraction imaging
- P.02 **R. Albrecht:** Practical applications of XRD phase analysis in the recycling industry of lead-acid batteries
- P.03 **K. Aniolek:** Surface characterization of titanium Grade 2 after cyclic oxidation
- P.04 **A. Antolak-Dudka**: Room temperature mechanical nitridation of titanium and its alloys by self-shearing reactive milling under nitrogen pressure
- P.05 **M. Bara:** Structure of AAO-Cu coatings produced on EN AW-5251 aluminum alloy substrate
- P.06 **W. Bednarczyk**: Micromechanical investigation of deformation mechanisms in bioresorbable Zn alloys with EBSD-based microstructure analysis
- P.07 **R. Bernat**: Modulation of piribedil stability and bioavailability by hydrophilic and amphiphilic excipients
- P.08 **L. Boichyshyn**: Influence of Fe alloying on phase transformation mechanisms in amorphous Co–Si–B alloys
- P.09 A. Chrobak: Novel method for obtaining metallic composites
- P.10 **D. Chrobak**: Distinguishing crystal structures using ordinal patterns
- P.11 **G. Dercz**: Design, synthesis, and characterization of novel core-shell based materials for prospective medical applications
- P.12 **K. Duch**: Comparison of the impact of training in normal conditions and normobaric hypoxia on thermal profiles of changes in the heat capacity of human blood serum.
- P.13 **K. Dudek**: From phase change to microstructure and properties of corundum monolitics: transformations in the matrix
- P.14 **M. Dulski**: Mesoporous SBA-15 silica functionalization for selective silver ion adsorption
- P.15 **T. Durejko**: The influence of multi-sample DED manufacturing process on microstructure of Ti-5553 alloy
- P.16 **J. Dworecka-Wójcik**: Phase evolution and challenges in phase characterization of heat-treated additively manufactured 18Ni300 maraging steel.

- P.17 **K. Gancarczyk**: Evaluation of microstructure, crystal orientation and creep resistance in nickel-based single crystal turbine blades
- P.18 **K. Glowka**: The analysis of the martensite tetragonality in steels using EBSD
- P.19 **S. Golba**: Template assisted synthesis of nanostructured polypyrrole powder
- P.20 **A. Gradzik**: Effect of tungsten carbide addition on phase composition and wear resistance of Inconel 738LC nickel-based alloy layer deposited by laser cladding
- P.21 **W. Gurdziel**: Analysis of the influence of compositional changes in Co1–xNixSi2 single crystals on key material properties
- P.22 **J. Jurek-Suliga**: The influence of structure morphology on the functional properties of selected self-adhesive hydrogels used in the treatment of thermal burns
- P.23 **M. Karolus**: Structural analysis and corrosion resistance of zinc coatings on DC01 steel depending on the thickness of the deposited layer
- P.24 **S. Kolodziej**: Multiscale analysis of defect structures in single-crystalline CMSX-4 superalloys
- P.25 **J. Korzekwa**: Utilisation of porous AAO structure for tribological application
- P.26 **B. Kościelniak**: Microstructure and oxidation resistance of DMV 617 mod superalloy in a steam environment at 750 °C
- P.27 **L. Kozielski**: Artificial intelligence to power the future of materials science and engineering
- P.28 **J. Krawczyk**: Dendritic structure and chemical composition in the cooling bores area of single-crystalline turbine blades
- P.29 **J. Kubisztal**: High-entropy powder (Mn, Fe, Co, Ni, Cu)₃O₄ in a porous Ni matrix as an oxygen evolution electrocatalyst
- P.30 **M. Kubisztal**: Intragranular and intergranular contributions to charge transport and temperature sensitivity of Mn-Ni-Fe spinel oxide
- P.31 **S. Kulesza**: Comparative analysis of structural properties of zirconia powder reflected in its XRD spectra
- P.32 **I. Laszko**: Synthesis of biocompatible metal-metal composite with variable size of reinforcing particles

- P.33 **L. Maj**: Micro-arc oxidation of plastically deformed titanium for future dental implants: effect of Ag nanoparticles on microstructure and properties
- P.34 **I. Matula**: The gradient titanium-based materials for potential medical applications produced by modified powder metallurgy method
- P.35 **E. Matyja**: Structure, Martensitic Transformation, and Properties of Ni-Co-Mn-In-Fe-Cr Magnetic Shape Memory Alloys
- P.36 **W. Michalik**: Design and fabrication of biocompatible metal-metal composite with □ titanium alloy as reinforcing fraction
- P.37 **J. Nawrocki**: The Effect of Withdrawal Rate on Crystal Structure Perfection and Microstructure of Single Crystal Castings Made from High Ni Content Alloy
- P.38 **L. Orszulak**: Polyvinylpyrrolidone with diverse topologies as effective polymer matrices for tuning desired properties of liquid crystalline drugs
- P.39 **D. Orzel**: The influence of the thermomechanical processing on the microstructure and grain boundary character distribution of Zn0.1Cu alloy
- P.40 **M. Oualid**: Crystal structure of a new hybrid compound based on an iodido-plumbate(II) anionic motif
- P.41 **R. Paszkowski:** Influence of plastic deformation method on the microstructure and mechanical properties of Duplex stainless steel
- P.42 **M. Pęska**: Structural Investigation of Mg₆Pd_{1-x}Pt_x Alloys for Hydrogen Storage Applications
- P.43 **K. Rogalewska**: Characterization of refractory concrete with high silicon carbide (sic) content
- P.44 **N. Rońda**: The influence of thermal history on the phase composition and mechanical properties of parts additively manufactured by Wire Arc Additive Manufacturing
- P.45 **P. Salwa**: Analysis of martensite tetragonality in medium-carbon steels using EBSD mapping.
- P.46 **D. Siemiaszko**: Texture of feal sintered samples prepared using the pressure-assisted induction sintering (PAIS) method
- P.47 **A. Stróż**: Structural characterization of anodic oxide nanotube layers for potential biomedical applications

- P.48 **R. Strzalka**: Synthesis and structure analysis of znmger P-type quasicrystal
- P.49 A. Szeremeta: Doping influence on structural ferroelectric phase transitions and electrical features of barium calcium titanate
- P.50 M. Szklarska: Bioactive composite coatings of natural polymers with zno and Ag particles on titanium alloys obtained by electrophoretic deposition
- P.51 **B. Terlecki**: Mechanism of Plastic Deformation in New Designed TWIP High Manganese Steels
- P.52 **B. Terlecki**: Integrated Experimental Stereological Quantification and Critical Methodological Review of the γ' Phase in Single-Crystal Nickel-Based
- P.53 **K. Wójciak**: Translational symmetry a way to efficient EBSD diffraction pattern analysis
- P.54 **G. Ziółkowski**: Magnetic properties of Fe-Nb-B-RE melt spun ribbons
- P.55 **M. Zubko**: Microstructure of lanitiysi: a La-containing High-Entropy Alloy

High-resolution misorientation mapping in single-crystal superalloys via X-ray diffraction imaging

R. Albrecht¹.a, K. Gancarczyk², A. Gradzik² and J. Maszybrocka¹

a robert.albrecht@us.edu.pl

Keywords: single-crystal, superalloys, X-ray diffraction

High-resolution X-ray diffraction imaging (HR-XDI)—an extension of classical X-ray topography—achieves arcsecond-level angular sensitivity with micrometre-scale spatial resolution over millimetre-scale fields of view. Applied to Ni- and Ti-based single crystals produced by directional solidification methods, the technique resolves micro-scale mosaicity and residual-stress-affected regions through systematic changes in intensity/contrast and subtle Bragg-angle shifts. Using as-cast CMSX-4 rods fabricated at different withdrawal rates, we quantify dendrite misorientations and reveal the inheritance of misorientation as a function of withdrawal rate. In addition, by employing misorientation mapping in a Gum Metal–type Ti β -alloy single crystal grown by the optical floating-zone technique, we clearly present the subgrain structure with misorientations not exceeding 1° .

These results position HR-XDI as a practical and sensitive tool for quality control and process—structure linkage in single-crystal alloys, complementing EBSD and Laue methods by delivering large-area, sub-degree orientation maps with elastic-strain sensitivity directly on near-net-shape components.

¹ Institute of Materials Engineering, University of Silesia, 75 Pułku Piechoty 1A, Chorzów, 41-500, Poland

² Department of Materials Science, Rzeszow University of Technology, Al. Powstancow Warszawy 12, 35-959 Rzeszow, Poland

Practical Applications of XRD Phase Analysis in the Recycling Industry of Lead-Acid Batteries

R. Albrecht^{1a}, D. Malecha^{2,3}, M. Płońska¹, S. Małecki²

a robert.albrecht@us.edu.pl

Keywords: aluminum, lead-acid battery, XRD

The lead refining process, practiced for decades, has traditionally relied on oxidation methods. However, recent efforts have focused on developing alternative approaches aimed at selectively removing antimony while retaining tin in the alloy [1–4]. This study demonstrates the application of X-ray diffraction (XRD) phase analysis to characterize slags generated during industrial-scale lead refining processes involving aluminum scrap addition, in the context of lead-acid battery recycling. Particular emphasis was placed on the identification of the Al-Sb intermetallic phase, whose formation was confirmed through XRD analysis and complemented by microscopic observations with point analysis. Furthermore, DSC-TGA thermal analysis was performed on metallic slag collected directly after aluminum scrap addition to the lead-tin bath. The results unambiguously confirmed the binding of antimony with aluminum under industrial refining conditions, offering new perspectives for more efficient and selective lead purification methods in recycling processes.

- [1] D. Malecha, S. Małecki, P. Jarosz, R. Kowalik, P. Żabiński, Recovery of Pure Lead-Tin Alloy from Recycling Spent Lead-Acid Batteries, Materials 16 (2023) 5882. https://doi.org/10.3390/ma16175882.
- [2] D. Malecha, P. Świec, R. Albrecht, P. Jarosz, S. Małecki, Refining of Secondary Pb with Retention of Sn Using Al and Ca Additions, JOM 77 (2025) 3249–3261. https://doi.org/10.1007/s11837-024-06892-w.
- [3] D. Malecha, M. Zubko, P. Żabiński, S. Małecki, Analysis of the Lead Refining Method Using Aluminum, Metallurgical and Materials Transactions A 56 (2025) 2957–2975. https://doi.org/10.1007/s11661-025-07813-5.

¹ Institute of Materials Engineering, University of Silesia, 75 Pułku Piechoty 1a, 41-500. Chorzow. Poland.

² Faculty of Non-Ferrous Metals AGH University of Krakow, al. Mickiewicza 30, 30-059 Krakow, Poland.

³ Baterpol S.A., ul. Obr. Westerplatte 108, 40-335 Katowice, Poland.

[4] D. Malecha, R. Albrecht, J. Lamb, S. Małecki, The Influence of Lead Refining Method on the Dross Content in the Metal, JOM 77 (2025). https://doi.org/10.1007/s11837-025-07558-x.

Surface characterization of titanium Grade 2 after cyclic oxidation

K. Aniołek^{1a}, G. Dercz¹

a krzysztof.aniołek@us.edu.pl

¹ Faculty of Science and Technology, Institute of Materials Engineering, University of Silesia, 75 Pulku Piechoty 1A, 41-500 Chorzów, Poland

Keywords: titanium Grade 2, cyclic oxidation, oxide layer

Titanium and its alloys belong to the group of metallic materials characterized by exceptional functional properties. The combination of low density, good corrosion resistance, along with favourable plasticity and mechanical properties, is an advantage leading to the increasing practical applications of these materials [1].

One of the main limitations in the technical and biomedical applications of titanium-based materials is their insufficient tribological properties, which significantly restricts, or in some cases completely excludes, their use in friction pairs. The fundamental problem is the high and unstable coefficient of friction as well as the tendency to adhesive wear [2,3].

One of the most effective techniques for improving both the biocompatibility and the mechanical and tribological properties of titanium and its alloys is the process of cyclic oxidation [4]. This method takes advantage of oxygen diffusion at elevated temperatures and enables the hardening of the surface layer through the formation of a relatively thick TiO₂ layer above the so-called oxygen diffusion zone. The formation of oxide layers on the surface of titanium and its alloys makes it possible to achieve significant improvement in corrosion resistance, biocompatibility, biological activity, surface topography, as well as mechanical and tribological properties [5,6].

This study presents the results of research on the cyclic oxidation process of titanium Grade 2. The morphology, phase composition, as well as the micromechanical and tribological properties of the obtained oxide layers were determined. The oxidation process was carried out at temperatures of 600°C, 650°C, and 700°C in 4 and 12 cycles. Microscopic examinations revealed that the size of the oxide particles increased with both the oxidation temperature and the number of cycles. Phase composition analysis after cyclic oxidation showed that the oxide layers formed on titanium consisted solely of TiO₂ (rutile). Micromechanical tests demonstrated that the presence of oxide layers obtained through cyclic oxidation led to a decrease in the total indentation work (Wtotal),

which indicates an increased resistance of the surface layer to deformation. It was shown that titanium Grade 2 after oxidation exhibited up to three times higher hardness. The Indentation Creep (CIT) parameter decreased with increasing oxidation temperature, which confirms enhanced creep resistance. The formation of protective oxide layers on the surface of titanium also resulted in improved tribological characteristics, both under dry sliding conditions and in lubricated contact (Ringer's solution). It was demonstrated that wear resistance increased with oxidation temperature and the number of cycles. However, in lubricated contact a greater reduction in wear (by approx. 50%) was observed compared to dry sliding tests.

- [1] Y. Zhou, Q.Y. Zhang, J.Q. Liu, X.H. Cui, J.G. Mo, S.Q. Wang. Wear characteristics of a thermally oxidized and vacuum diffusion heat treated coating on Ti–6Al–4V alloy. Wear 344-345 (2015) 9–21.
- [2] D.R. Unune, G.R. Brown, G.C. Reilly. Thermal based surface modification techniques for enhancing the corrosion and wear resistance of metallic implants: A review. Vacuum 203 (2022) 111298.
- [3] Y. Niu, X. Pang, S. Yue, S. Wang, C. Song, B. Shangguan, Y. Zhang. Improving tribological properties of Ti–Zr alloys under starved lubrication by combining thermal oxidation and laser surface texturing. Wear 496-497 (2022) 204279.
- [4] M.J. Kim, P. Yadav, D.B. Lee. Isothermal and cyclic oxidation of Ti-6Al-4V alloy. Defect Diffusion Forum 369 (2016) 99-103.
- [5] I. Kopova, J. Stráský, P. Harcuba, M. Landa, M. Janeček, L. Bačákova. Newly developed Ti–Nb–Zr–Ta–Si–Fe biomedical beta titanium alloys with increased strength and enhanced biocompatibility, Mater. Sci. Eng. C 60 (2016) 230–238.
- [6] S. Wang, Z. Liao, Y. Liu, W. Liu. Influence of thermal oxidation duration on the microstructure and fretting wear behavior of Ti6Al4V alloy. Materials Chemistry and Physics 159 (2015) 139–151.

Room temperature mechanical nitridation of titanium and its alloys by self-shearing reactive milling under nitrogen pressure

A. Antolak-Dudka^{1a}, M. Liszewska², S. Dyjak³, I. Wyrębska¹, T. Czujko¹ and M. Polański¹

a anna.dudka@wat.edu.pl

Keywords: reactive milling, titanium alloys, nitrogen, powder

Titanium and its alloys are widely used across various industries, including medicine and aerospace, due to their exceptional strength-to-density ratio, corrosion resistance and biocompatibility. However, despite these advantages, the surface of titanium is relatively soft and chemically reactive. To enhance surface properties such as hardness, wear resistance, and corrosion resistance, titanium nitride (TiN) coatings are commonly applied. Conventional methods for TiN deposition typically require high temperatures or aggressive processing environments and are generally limited to solid substrates. This has created a demand for alternative techniques capable of synthesizing titanium nitride under milder conditions, and particularly methods applicable to powder materials.

This work presents a novel approach for producing titanium nitride (TiN) on the surface of spherical Ti, Ti-6Al-4V, and Ti-5553 alloy powders via self-shearing reactive milling under nitrogen pressure. The process was conducted in a Fritsch P6 planetary mill without the use of grinding balls, for durations of up to 10 hours. Characterization of the processed powders using scanning electron microscopy (SEM), X-ray diffraction (XRD), Raman spectroscopy, and elemental analysis revealed that after 10 hours of self-milling a thin ceramic layer (~500 nm) of TiN was successfully formed on their surfaces. Simultaneously, the spherical morphology of the powder particles was retained.

The preservation of particle morphology is an additional point of interest, which opens up the possibility of utilizing these surface-modified powders in additive manufacturing techniques.

¹ Institute of Materials Science and Engineering, Military University of Technology, Kaliskiego 2, 00-908 Warsaw, Poland

² Institute of Optoelectronics, Military University of Technology, Kaliskiego 2, 00-908 Warsaw, Poland

³ Institute of Chemistry, Military University of Technology, Kaliskiego 2, 00-908 Warsaw, Poland

Structure of AAO-Cu coatings produced on EN AW-5251 aluminum alloy substrate

M. Bara^{1a}, J. Korzekwa¹, M. Niedźwiedź¹ and G. Dercz¹

a marek.bara@us.edu.pl

Keywords: coatings, AAO-Cu, structure

Among the many materials used in modern technology, light metal alloys, such as aluminum, are increasingly being used as structural materials. Electrolytic oxidation of aluminum alloys leads to the formation of hard coatings on their surfaces – AAO (anodic aluminum oxide). AAO coatings belong to a group of materials with a highly developed surface [1], and therefore can be a good material for modification [2], for example, with a phase with good lubricating properties, intended for sliding applications [3].

In this work, it was assumed that the AAO coating could be modified by introducing copper into its near-surface structure and then increasing its thickness. The AAO-Cu coatings were produced using three surface engineering processes. The method for producing AAO-Cu coatings is currently being prepared for patent protection, so the parameters of these processes are not disclosed.

As a result of the work carried out, Cu coatings with a thickness of $43.5 - 58 \,\mu m$ were obtained on AAO coatings (Fig. 1). The copper crystals form a compact structure (Fig. 2), and the coating demonstrates good adhesion to the substrate.

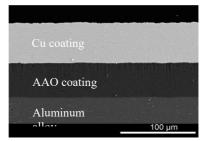


Fig. 1. Structure of the AAO-Cu coating.

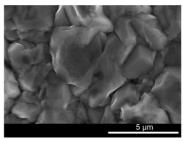


Fig. 2. Surface morphology of the AAO-Cu coating.

¹ Institute of Materials Engineering, Faculty of Science and Technology, University of Silesia in Katowice, 75 Pułku Piechoty 1a, 41-500 Chorzów, Poland;

Phase analysis (GIXRD) revealed a dominant Cu phase in all tested samples. A characteristic feature is a strongly increased ratio of the (111) to (200) reflection intensity, indicating a distinct [111] texture in the deposited layers, which is typical for thin metallic coatings. In several cases, additional Cu₂O and CuO phases were detected, associated with surface oxidation of copper. Selected coatings were subjected to tribological tests. The results showed that modification of AAO coatings with copper reduced the friction coefficient compared to the reference coating by as much as 55% (for continuous lubrication) and by 34% (for oil mist lubrication). Additionally, the modification of the AAO coating leads to a gradient change in the hardness of the surface structure of the coating and takes over part of the dynamic loads, protecting the brittle oxide coating against cracking.

A properly selected sliding surface of the friction pair, even with reduced lubrication, brings economic and ecological benefits, which are currently key issues.

- [1] Sulka GD. Highly Ordered Anodic Porous Alumina Formation by Self-Organized Anodizing. 2008. Epub ahead of print 2008.
- [2] Schlottig F, Textor M, Spencer ND, et al. Characterization of nanoscale metal structures obtained by template synthesis. 684–686.
- [3] Hu N, Ge S, Fang L. Tribological properties of nano-porous anodic aluminum oxide template. J Cent South Univ Technol 2011; 18: 1004–1008.

Micromechanical investigation of deformation mechanisms in bioresorbable Zn alloys with EBSD-based microstructure analysis

W. Bednarczyk^{1a}, G. Cios² and P. Bała^{1,2}

a bednarczyk@agh.edu.pl

Keywords: deformation mechanisms, micromechanics, zinc alloys

Zinc alloys are gaining increasing attention as promising candidates for temporary biodegradable metallic implants, such as bone-fixing plates or cardiovascular stents, due to their favourable biocompatibility and controlled degradation behaviour. However, the inherently low mechanical strength of conventional Zn alloys has historically limited detailed investigations into their deformation mechanisms, particularly in fine-grained microstructures.

In this study, we conduct a comprehensive micromechanical investigation of these mechanisms, focusing on the effects of solid solution strengthening, second-phase particles, and size-dependent plasticity, as revealed by micropillar compression. EBSD-based microstructural analysis is employed in conjunction with SEM, AFM, and nanoindentation techniques, including strain rate jump tests and spherical nanoindentation, to assess the contributions of grain boundary sliding and slip system activity to superplastic deformation across a wide strain rate range [1,2].

Our findings demonstrate that grain boundary sliding dominates tensile deformation in fine-grained Zn alloys, while strain rate sensitivity remains high (m ≈ 0.3) regardless of thermal treatment. Additionally,non-basal slip system activity was found to be minimal. Cross-platform strain rate jump tests performed on three different nanoindentation systems (Agilent G200, Alemnis, Femtotools) also confirm the potential for reliable cross-correlation of results between devices

¹ Faculty of Metals Engineering and Industrial Computer Science, AGH University of Krakow, Krakow, Poland

² Academic Centre for Materials and Nanotechnology, AGH University of Krakow, Krakow, Poland

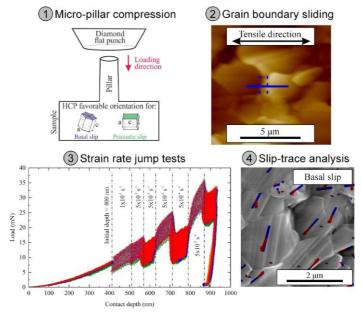


Figure 1 Techniques utilized in the investigation of deformation mechanisms in biodegradable ultrafine-grained Zn alloys

- [1] W. Bednarczyk, J. Kawałko, M. Wątroba, M. Szuwarzyński, P. Bała, Archives of Civil and Mechanical Engineering (2023) 23:253.
- [2] W. Bednarczyk, M. Wątroba, M. Jain, K. Mech, P. Bazarnik, P. Bała, J. Michler, K. Wieczerzak, Materials & Design (2023) 229:111897

Modulation of piribedil stability and bioavailability by hydrophilic and amphiphilic excipients

R. Bernat^{1a}, L. Orszulak², A. Minecka³, K. Jurkiewicz⁴, M. Tarnacka⁴, Grzegorz Garbacz⁵, Maciej Zubko¹, E. Kamińska³, K. Kamiński⁴

a roksana.bernat@us.edu,pl

Keywords: piribedil, drug-polymer binary mixtures, micellar systems

The poor bioavailability of many active pharmaceutical ingredients (APIs) has long posed a challenge for the pharmaceutical industry, especially for compounds in BCS classes II and IV, where low aqueous solubility is a major limitation. In response, various drug delivery systems (DDS) have been developed, including amorphous solid dispersions (ASDs) and micellar formulations, typically employing polymeric excipients. While molecular weight is often considered in excipient selection, other important polymer characteristics, including topology, microstructure, water affinity, and DDS type, remain less studied.

This study presents an innovative approach that utilizes polymers with different topologies and properties as potential matrices for the poorly water-soluble API - piribedil (PBD). We investigated ASDs as well as micellar systems composed of PBD and three different polymer matrices: (i) the commercially available amphiphilic copolymer Soluplus, (ii) self-synthesized hydrophilic linear polyvinylpyrrolidone (linPVP), and (iii) self-synthesized hydrophilic star-shaped PVP (starPVP). To obtain a comprehensive picture of the thermal and structural properties, intermolecular interactions, global molecular dynamics, and recrystallization processes of PBD in these binary systems, we applied various techniques such as differential scanning calorimetry (DSC), X-ray diffraction (XRD), dynamic light scattering (DLS), transmission electron miscroscopy (TEM). The primary objective of this study was to assess the

¹ Institute of Materials Engineering, Faculty of Science and Technology, University of Silesia in Katowice, Poland

² Institute of Chemistry, Faculty of Science and Technology, University of Silesia in Katowice, Poland

³ Department of Pharmacognosy and Phytochemistry, Faculty of Pharmaceutical Sciences in Sosnowiec, Medical University of Silesia in Katowice, Jagiellonska 4, 41-200 Sosnowiec, Poland

⁴ Institute of Physics, Faculty of Science and Technology, University of Silesia in Katowice, Poland

⁵ Chemische Fabrik Budenheim KG, Germany

influence of polymer type, molecular architecture, and formulation composition on the physical stability of amorphous PBD, its recrystallization kinetics, and drug release behaviour.

A particularly intriguing and highly relevant outcome of the investigation was the identification of a previously undescribed polymorphic form of PBD (form II), appearing in drug-polymer ASDs. DSC and XRD studies showed that PBD recrystallizes predominantly (in PVP systems) or exclusively (in Soluplus-based systems containing ≥20% polymer) into this novel polymorph with a melting temperature of ~363 K, slightly lower than that of the known form I (~370 K). Importantly, XRD and DSC measurements indicated that the amorphous form of PBD is most stable in ASDs with hydrophilic PVP, with starPVP providing marginally stronger inhibition of recrystallization than *lin*PVP. Further analyses confirmed the absence of specific API-polymer interactions, suggesting that the observed differences in crystallization kinetics are primarily governed by macromolecular architecture and the viscosity of the matrix. On the other hand, the amphiphilic polymer Soluplus proved most effective in generating stable micelles with narrow size distribution, where PBD also retained its amorphous state for a longer period than in PVP-based micelles. Drug release studies performed in a biorelevant FASSIF medium (pH = 6.5) demonstrated a clear enhancement of PBD solubility in all tested formulations compared with the neat crystalline API (~30%). Among ASDs, the PBD-Soluplus 60:40 w/w formulation reached ~50% release, whereas in micellar systems, the PBDstarPVP 1:2 (10:90) system achieved nearly complete release (~99%), accompanied by the most favourable sustained release profile for over ~20 hours, rather than the rapid 1-3.5-hour release observed for other formulations.

These outcomes contribute to a better understanding of how polymer architecture and formulation design affect the stability and performance of poorly soluble drugs, highlighting new opportunities for improving bioavailability through rational excipient selection.

Acknowledgements: The research was financed by the Ministry of Education and Science within the "Pearls of Science" Grant (No. PN/01/0078/2022) and by the National Center for Research and Development (Poland) within the Lider XII project (No. LIDER/28/0152/L-12/20/NCBR/2021).

Influence of Fe alloying on phase transformation mechanisms in amorphous Co–Si–B Alloys

L. Boichyshyn¹, M. Lopachak^{1a}, O. Hertsyk¹, M. Karolus²

amariia.lopachak@lnu.edu.ua

Keywords: amorphous alloys, phase transformations, nanocrystals

Cobalt-based amorphous alloys with silicon and boron attract significant attention due to their combination of high magnetic permeability, corrosion resistance, and the ability to form a nanocrystalline structure upon controlled annealing. Studying these alloys is important for the development of functional materials in microelectronics and energy applications.

The aim of this work was to investigate the thermal stability of the amorphous state, the sequence of phase transformations, and the kinetics of nanocrystal growth in $Co_{77}Si_{11}B_{12}$ and $Co_{72}Fe_5Si_{11}B_{12}$ ribbons using in-situ X-ray diffraction during vacuum heating. Short-range order parameters were determined from the position and width of the main maximum of the amorphous halo, while average nanocrystal sizes were calculated using the Scherrer equation.

For $Co_{77}Si_{11}B_{12}$, the amorphous state is stable up to ~500 °C. Further heating leads to the formation of defective α -Co (hcp) nanocrystals, Co_2Si at 550 °C, and a metastable Co_3B phase in the 600–650 °C range, which subsequently transforms into β -Co (fcc) and Co_2B . Above 700 °C, the system reaches an equilibrium state comprising β -Co + Co_2B + Co_2Si .

For $Co_{72}Fe_{5}Si_{11}B_{12}$, the amorphous state persists up to ~475 °C, after which a metastable bcc phase with lattice parameter a \approx 0.2806 nm appears, indicating Si dissolution in the solid solution. The formation of Co₂Si and β -Co is observed, and above 600 °C - Co₂B. At 750–800 °C, the structure evolves into the equilibrium multiphase system β -Co + Co₂B + Co₂Si.

Analysis of short-range order evolution showed that for $Co_{77}Si_{11}B_{12}$ the average interatomic distance remains nearly unchanged, while the size of short-range ordered regions reaches a maximum at $350\text{--}400\,^{\circ}C$, corresponding to the relaxation stage of the amorphous matrix. For $Co_{72}Fe_5Si_{11}B_{12}$, the appearance of the metastable bcc-like phase is the key factor determining subsequent crystallization kinetics.

¹Department of Physical and Colloid Chemistry Ivan Franko National University of Lviv, 79005 Lviv, Ukraine

²Institute of Materials Engineering, University of Silesia in Katowice, 41-500, Chorzów, Poland

Nanocrystal growth studies revealed that the average α-Co size in Co₇₇Si₁₁B₁₂ increases from 5 nm at 525 °C to over 100 nm at 700–800 °C, whereas in Co₇₂Fe₅Si₁₁B₁₂, metastable nanocrystals reach ~140 nm at 700 °C, indicating a limited number of nucleation sites and growth-dominated processes. High defect density in hcp-Co affects hcp↔fcc transitions and diffraction patterns.

Partial substitution of Co by Fe reduces the thermal stability of the amorphous state and changes the crystallization scenario via stepwise formation of the bcc phase. The results demonstrate the possibility of tailoring the structure and properties of Co–Si–B alloys through Fe alloying and thermal treatment, opening prospects for their application in microelectronics and magnetic devices [1–3].

- [1] Milica M. Vasić et al. Journal of Non-Crystalline Solids, 500 (2018) 326–335.
- [2] Lixia Wang et al. Journal of Materials Research, 8 (2014) 989–995.
- [3] Shuang Ma et al. Materials Today Communications, 48 (2025) 113540.

Novel method for obtaining metallic composites

A.Chrobak^{1a} and G.Ziółkowski2

a artur.chrobak@us.edu.pl

¹ Institute of Materials Engineering, University of Silesia in Katowice, 75 Pułku Piechoty 1A, 41-500 Chorzów, Poland

Keywords: composites, suction casting

Metallic composites occupy an important place in many fields of technology because they can combine multiple, often contradictory, properties, which is unheard of in homogeneous materials (alloys, solid solutions, compounds). Numerous methods exist for obtaining such composites. These include powder sintering methods, partial crystallization from the amorphous phase (crystallites in an amorphous matrix), additive laser techniques (surfaces), and so-called mechanical alloying by high-energy milling (powder systems). A composite must contain various phases with clearly defined boundaries. However, in the case of solid metal composites, difficulties arise due to the ease of formation of chemical compounds, alloys, or solid solutions of the individual components of the composite. These factors blur the interphase boundaries, and the resulting material does not meet the definition of a composite.

The presentation refers to a novel method for obtaining metallic composites using a modified vacuum suction technique [1,2]. The main idea of the modification is to apply separated partial crystallization of the composite ingredients that occurs in a special designed casting form. We present the original design of the apparatus and microstructure of exemplary systems such as Fe-Ni and (Dy-Fe-Nb-B)-Ni. It turned out that the new technique allows preparing metallic composites, and moreover, the microstructure can be influenced by technology parameters, as shown in the examples.

- [1] X. Wang, L.H. Dong, X.L. Ma, Y.F. Zheng, Microstructure, mechanical property and corrosion behaviors of interpenetrating C/Mg-Zn-Mn composite fabricated by suction casting, Materials Science and Engineering C 33 (2013) 618–625.
- [2] Tomasz Kozieł, Krzysztof Pajor, Łukasz Gondek, Cooling rate evaluation during solidification in the suction casting process, J Mater Res Technol. 2020;9(xx):13502–13508.

Distinguishing crystal structures using ordinal patterns

D. Chrobak^{1a}

a dariusz.chrobak@us.edu.pl

Keywords: crystal structures, high-pressure silicon phases, molecular dynamics

Thermal fluctuations limit the ability to identify crystal structures, even though an atom's trajectory contains information about its surroundings. This simple conclusion justifies the search for a method that can determine the type of structure to which an atom belongs by analysing its motion. Using molecular modelling, it can be shown that statistical analysis of the velocity trajectory of a single atom allows for distinguishing crystal structures. The proposed method utilizes the Shannon entropy of order patterns (OP) and was demonstrated using high-pressure silicon phases (Fig. 1). Identification of atoms occupying Wyckoff positions 2(c) and 6(f) of the r8 phase crystal showed an increase in the accuracy of the developed method with increasing trajectory length. The method for distinguishing crystal phases based on order patterns opens new possibilities in the study of solid-phase transformations.

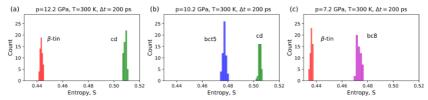


Fig. 1 Illustration of the operation of the OP-based method. Each two silicon phases were modelled at 300 K and under equilibrium pressure. Histograms were calculated for groups of several dozen atoms randomly selected from the crystals of cd (green), β -tin (red), bct5 (blue), and bc8 (purple). The panels demonstrate the relationship between the permutation entropy distributions and the equilibrium silicon phase pairs: β -tin/cd (a), bct5/cd (b), and β -tin/bc8 (c). Separation of the entropy histograms confirmed the effectiveness of the S method in studying the local atomic environment.

¹ Institute of Materials Engineering, Faculty of Science and Technology, University of Silesia in Katowice, Chorzów, Poland

Design, synthesis, and characterization of novel core-shell based materials for prospective medical applications

G. Dercz^{1a}, I. Matuła¹, M Zubko¹

a grzegorz.dercz@us.edu.pl

Keywords: core-shell, Rietveld method, TEM, XRD, SEM, powder metallurgy

This study presents the design, synthesis, and characterization of novel coreshell structured materials for potential biomedical applications. The materials were fabricated using powder metallurgy by ball milling elemental titanium and tantalum powders, followed by sintering at 1000 °C for 24 h. Optimization of process parameters showed that 60 h of milling provides a fully covered tantalum shell on titanium cores.

Comprehensive techniques assessed structural, chemical, and mechanical properties of synthesized materials. SEM, TEM, and FIB enabled high-resolution imaging, while XRD confirmed multi-phase structures. AFM analyzed surface topography. EDS and XRF determined chemical composition and elemental distribution within particles.

The synthesized particles exhibit a distinct core-shell architecture composed of a Ti-rich core, an intermediate Ti-Ta equilibrium region, and an outer Ta-enriched shell formed by interdiffusion during sintering. A two-phase ($\alpha+\beta$) Widmanstätten-type microstructure was identified, indicating complex phase evolution. Mechanical testing revealed significant variations in hardness and reduced Young's modulus across three regions corresponding to $\beta, \alpha+\beta,$ and α -Ti phases. The combination of lightweight architecture, tailored microstructures, and tunable mechanical properties highlights the potential of Ti-Ta core-shell materials for biomedical applications requiring enhanced corrosion resistance and mechanical performance.

The obtained results provide a solid basis for optimizing processing conditions and conducting characterization of core-shell structured materials designed for next-generation biomedical implants.

Acknowledgment: This work was supported by the Polish National Science Centre, Poland (Polish: Narodowe Centrum Nauki, abbr. NCN) under the research project OPUS-27 no. UMO-2024/53/B/ST11/00431.

¹ Institute of Materials Engineering, University of Silesia in Katowice, 75 Pułku Piechoty Street 1 A, 41-500 Chorzów, Poland;

Comparison of the impact of training in normal conditions and normobaric hypoxia on thermal profiles of changes in the heat capacity of human blood serum.

Klaudia Duch¹, Michał Krzysztofik², Ewa Sadowska-Krępa²

¹Uniwersytet Śląski w Katowicach, Wydział Nauk Ścisłych i Technicznych, Instytut Inżynierii Biomedycznej, ul. 75 Pułku Piechoty 1a, 41-500 Chorzów

²Akademia Wychowania Fizycznego w Katowicach, Katedra Nauk Fizjologiczno – Medycznych, Zakład Biomedycznych Podstaw Aktywności Fizycznej, ul. Mikołowska 72a, 40-065 Katowice

Keywords: training; normobaric hypoxia; blood serum; DSC; heat capacity

For several years, there have been reports on the possibility of using the differential scanning calorimetry (DSC) method in various areas of medical diagnostics and sports medicine based on thermal profiles of blood plasma/serum. In this study, an attempt was made to compare the DSC profiles and thermal parameters of athletes' sera.

Serum samples were collected from the blood of weightlifting athletes. Blood was collected at rest and after physical exercise, under normal conditions and under normobaric hypoxia.

The research was performed by differential scanning calorimetry (DSC) using a VP-DSC microcalorimeter (MicroCal Co, Northampton, MA). DSC measurements of aqueous serum solutions were performed in the temperature range from 20° to 100°C with a heating rate of 1°C/min and a pressure of approximately 1.8 atm.

The thermodynamic parameters of the tested endothermic transition were compared among participants (e.g. characteristic transition temperatures and corresponding heat capacities, enthalpy of the serum denaturation process, half-width of the transition).

A substantial inter-individual variability has been observed in the effects of hypoxia on DSC curves of athlete's serum. The exhaustive exercise in hypoxia has induced probably an acute-phase response in some cases.

From phase change to microstructure and properties of corundum monolitics: transformations in the matrix

K. Dudek^{1a}, J. Podwórny¹

^a karolina.dudek@icimb.lukasiewicz.gov.pl

¹ Lukasiewicz Research Network – Institute of Ceramics and Building Materials, Center of Refractory Materials, Poland

Keywords: HT-X-ray diffraction, X-ray dilatometry, phase transformation

Monolithic refractory materials with improved thermomechanical properties are of great interest in applications requiring high temperatures, where energy efficiency, raw material consumption and high production efficiency (time and quality) are key issues for maintaining high competitiveness. Such materials include, among others, a smart matrix [1], designed in such a way that during operation in high-temperature conditions they effectively compensate for the thermal stresses that arise and prevent their accumulation.

Monoliths are usually prepared on site and applied directly (e.g. as steel ladle linings), allowing for reduced production line downtime. After installation, the lining is dried and preheated, but to a temperature lower than its operating temperature. Monoliths with a high-alumina cement binder are based in the "green" state on the strength of the hydraulic bond, which completely decomposes during heating. After that material sinters and develops its final, high mechanical strength.

In practical applications, refractory linings are exposed to a temperature gradient - only the thin layer in direct contact with heat undergoes full sintering, while deeper regions remain merely dehydrated, and the cold-face one may still contain unreacted hydrates. This variation across the lining's cross-section results in non-uniform thermomechanical properties, leading to the accumulation of thermal stresses and, ultimately, material degradation through spalling process. In addition, the hot-face surface gradually erodes during service, causing the deeper transition zones to sinter as a result of the high temperature.

The aim of the work was to investigate the chemical reactions and phase transformations occurring in concrete with a smart matrix subjected to heating, as well as their influence on the state of stress in the material and changes in elastic properties during heating and cooling, in connection with the analysis of the microstructure.

High-temperature X-ray diffraction (HT-XRD) measurements were carried out over a temperature range of 25 to 1550 °C. These studies identified the temperature intervals for the formation and decomposition of secondary calcium aluminates (e.g., CA and CA₂), the reaction onset temperatures of raw materials, and the formation of high-temperature phases such as CA₆. The determined expansion tensors provided information on the behaviour of individual phases in the material, indicating potential areas of stress formation. These phase transformations were accompanied by changes in the material's elastic properties during both heating and cooling cycles, as observed through high-temperature resonance frequency and damping analysis (HT-RFDA).

The results indicated that, at high temperature, the material enters a viscoplastic state, which enables it to effectively accommodate thermal stresses and prevent their accumulation.

Acknowledgement:

This project was implemented under the CORNET initiative. It was funded by the National Centre for Research and Development (NCBR) in Poland and the German Federation of Industrial Research Associations (AiF). This project was carried out under the auspices of AiF and financed from the budget of the Federal Ministry of Economics and Technology (BMWi) within the framework of the programme for promoting collective industrial research (IGF), project No.175 EN

[1] F. Holleyn, O. Krause, M. Odziomek, E. Brochen, J. Podwórny, Improved sintering due to an intelligent matrix design of high-alumina refractory monolithics that is adjusted to the service conditions, Proceedings of the 61st International Colloquium on Refractories (2018)

Mesoporous SBA-15 silica functionalization for selective silver ion adsorption

M. Dulski^{1a}, A. Strach², R. Zaleski³, M. Gorgol³, E. Matyja¹, M. Laskowska⁴, V. Grebnevs⁵, and Ł. Laskowski⁴

a mateusz.dulski@us.edu.pl

¹Institute of Materials Engineering, 75 Pulku Piechoty 1A, 41-500 Chorzow, Poland ²Doctoral School, University of Silesia, Bankowa 14, 40-032 Katowice, Poland ³Department of Materials Physics, Maria Curie-Sklodowska University in Lublin, Akademicka 7/255, 20-031 Lublin, Poland ⁴Institute of Nuclear Physics Polish Academy of Sciences, 31-342 Kraków, Poland ⁵Faculty of Chemistry, University of Latvia, Jelgavas Street 1, LV-1004 Riga, Latvia

A state-of-the-art approach to tackling environmental pollution involves the development of bio-perforated, mesoporous SBA-15 silica, distinguished by its exceptionally high surface area (~800 m²/g). This material consists of amorphous silica featuring uniaxially ordered hexagonal approximately 5 nm in diameter that extend over micrometer lengths. The uniformity of these channels imparts excellent capillary properties, making SBA-15 highly effective for sorption applications. Being non-toxic and environmentally benign, SBA-15 offers versatile physicochemical characteristics that can be precisely tuned through chemical functionalization of both its inner and outer surfaces, thereby enhancing its suitability for a wide range of environmental remediation challenges.

The SBA-15 has been functionalized with varying concentrations (1.25–20%) of propyl-carboxylic groups to facilitate targeted chelation of silver ions. To optimize its structural design and performance, advanced characterization methods were employed. Small-Angle X-ray Scattering (SAXS) enabled accurate determination of pore size and distribution, while Positron Annihilation Lifetime Spectroscopy (PALS) provided detailed insights into the mesoporous network, including nanoscale porosity. Combined analysis from these techniques helped elucidate the diffusion pathways of silver ions within the material. Atomic Absorption Spectroscopy (AAS) was used to quantify metal uptake, assessing sorption efficiency, saturation, and desorption behavior. Complementary UV-VIS spectroscopy monitored the kinetics of silver ion interaction in real time, generating time-dependent uptake profiles across different pH conditions. Collectively, these techniques offer a comprehensive evaluation of SBA-15's sorption capabilities.

This innovative strategy, combining precise functionalization with thorough characterization, establishes SBA-15 as a sustainable and highly efficient material for metal ion sorption. Its advancement holds significant potential for environmental remediation efforts, contributing to healthier ecosystems and enhanced public health.

Acknowledgment: M.D. and L.L. are thankful for the financial support from the National Center of Science (NCN) based on 2020/37/B/ST8/03637.

The influence of multi-sample DED manufacturing process on microstructure of Ti-5553 alloy

<u>T. Durejko</u>^{1a}, I. Mierzejewska¹, A. Antolak-Dudka¹, D. Zasada¹, M. Kopeć

a tomasz.durejko@wat.edu.pl

¹ Institute of Materials Science and Engineering, Military University of Technology, Kaliskiego 2, 00-908 Warsaw, Poland

Titanium and its alloys exhibit outstanding properties such as high specific strength and stiffness, corrosion resistance, and good biocompatibility. Thus, they are widely used in different industry branches, including medicine, aerospace, and marine engineering. Recently, β -Ti alloys have gained particular interest from scientists due to their attractive properties, which are the result of their microstructure. β -Ti alloys could be subjected to heat treatment, involving annealing under solution-treated conditions and followed by aging. This process increases the strength of the β -Ti alloys due to dispersion strengthening arising from the partial $\beta \to \alpha$ transformation preceded by the secretion of the ω phase, which is a key factor responsible for the strengthening of these alloys.

In this work, the microstructure and properties of additively manufactured near- β Ti-5553 titanium alloy were systematically researched. Three cylindrical samples were simultaneously fabricated in the same process using Laser Engineered Net Shaping (LENS) method. Due to the 26 seconds of the interlayer time interval being reached for each sample. The prepared specimens were post-processed with heat treatment at 300°C, 700°C, and 750°C under a vacuum of 10^{-2} mbar for 1 hour. The manufacturing process with 26 seconds of interlayer delay enabled the evolution of a unique microstructure, which led to a beneficial combination of yield strength (1198 MPa) and strain-to-failure (16%). Heat treatment at 300 and 700°C significantly decreased the samples' ductility. However, annealing at 750°C caused grain growth in the α -phase, significantly reducing the material's strength and hardness while increasing elongation to 13%. Finally, it was found that the application of the LENS process enabled the manufacture of high-strength Ti-5553 alloy with satisfactory ductility without additional heat treatment processes.

Phase evolution and challenges in phase characterization of heat-treated additively manufactured 18Ni300 maraging steel.

N. Rońda¹, D. Zasada¹, <u>J. Dworecka-Wójcik^{1a}</u> and M. Polański¹

a e-mail: julita.dworecka@wat.edu.pl

¹ Institute of Materials Science and Engineering, Faculty of Advanced Technologies and Chemistry, Military University of Technology, Warsaw, Poland

Keywords: X-ray diffraction, EBSD, maraging steel

"MARtensite AGING" – the origin of the name *maraging* steel – reflects the key microstructural transformations responsible for the outstanding properties of these materials. Maraging steels derive their high strength and good ductility from a martensitic matrix that is precipitation-hardened through aging heat treatments. In addition to their excellent mechanical properties, these steels offer good performance over a broad temperature range. Also, their excellent weldability and high material cost (significant Ni, Mo, Co contents) makes additive manufacturing economically attractive in their case.

In this work, maraging steel samples were fabricated using the LENS® (Laser Engineering Net Shaping) technique. In this process, metal powder is fed through nozzles and melted by a high-power laser, allowing for the layer-by-layer fabrication of complex components. However, the repeated thermal cycling inherent in this process can strongly influence the microstructure, and phase composition especially through local reheating of previously deposited layers.

The produced samples were subjected to three distinct heat treatment routes: (a) aging only, (b) solution treatment followed by aging, and (c) double solution treatment followed by aging. Multiple aging conditions were explored, with variations in both temperature and duration. The resulting phase compositions were analyzed using X-ray diffraction (XRD) and Electron Backscatter Diffraction (EBSD).

Our study revealed significant differences in the amount of reverted austenite depending on the applied heat treatment. The as-built samples already contained a small fraction of reversed austenite, attributed to microsegregation of elements such as Ni, Mo, and Ti. Increased aging temperature and duration led to a higher fraction of reverted austenite.

Importantly, this work highlights the challenges associated with phase identification in additively manufactured maraging steels. Differences between volume-averaged techniques like XRD and local techniques such as EBSD, along with the effects of crystallographic texture, chemical segregation, and local heterogeneity, can lead to divergent interpretations of phase content and distribution. This work will focus on these methodological issues and their implications for interpreting microstructural evolution in AM maraging steels.

Evaluation of microstructure, crystal orientation and creep resistance in nickel-based single crystal turbine blades

<u>K. Gancarczyk</u>^{1a}, A. Gradzik¹, B. Kościelniak¹, M. Poręba¹, R. Albrecht²

^a kamilgancarczyk@prz.edu.pl

The paper presents the results of microstructure, crystal perfection analysis and creep resistance performed for single-crystal (SX) turbine blades used in aircraft engine high-pressure section. CMSX-4 and CMSX-4® Plus nickel-based superalloys turbine blades were manufactured in the Bridgman-Stockbarger process with the withdrawal rate varying between 1 and 5 mm/min [1,2]. The heat treatment of single crystals consisted of solution annealing and double aging. Microstructure analyses of single crystals were performed using light and scanning and electron microscopy. The degree of porosity of turbine blades and the morphology of the phase components of their microstructure were determined. The full crystal orientation of the blade castings was also determined. Primary orientation α angle, which is the value between the [001] crystallographic direction and the axis of the blade, β angle, defined as the rotation of the [001] direction around the direction of casting withdrawal rate from the furnace, and γ angle - the deviation of the projection line of the [010] direction vector from the adopted reference axis, were defined. Measurements of the angle values characterizing the crystal orientation of the blades were made using the Ω-scan method and OD-EFG1 X-ray diffractometer. In addition to structural analysis, creep tests were performed in order to verify the assessment of the perfection of the crystal structure of SX blade castings. The obtained test results of the creep test showed a difference in the mechanical properties of the CMSX-4 and CMSX-4® Plus superalloys for variable conditions of the Bridgman-Stockbarger process.

- [1] Sun, H.; Ma, D.; Zhao, Y.; Wei, J.; Gong, X.; Sun, Z. Dendrite Structure Refinement and Mechanical Property Improvement of a Single-Crystal Superalloy. Metals 2025, 15, 295.
- [2] Reed, R.C. The Superalloys: Fundamentals and Applications; Cambridge University Press: Cambridge, UK, 2008; pp. 1–216.

¹ Department of Materials Science, Faculty of Mechanical Engineering and Aeronautics, Rzeszow University of Technology, Powstańców Warszawy 12, 35-959, Rzeszów, Poland

² Institute of Materials Engineering, University of Silesia, 75 Pułku Piechoty 1A, Chorzów, 41-500, Poland

The analysis of the martensite tetragonality in steels using EBSD

K. Glowka^{1,2a}, G. Cios¹, A. Winkelmann¹ and P. Bała¹

^a glowka@agh.edu.pl, karsten.glowka@us.edu.pl

Keywords: Martensite Tetragonality, EBSD, Pattern Matching Indexing

Steel is one of the most widely used materials across various industries and everyday applications. The variations in carbon content contribute to forming different microstructures such as ferrite, austenite, pearlite, cementite and ledeburite. Moreover, thermal and mechanical treatments are commonly applied to tailor the steel's properties [1].

A notable example of such processing is the formation of martensite, which occurs when steel is rapidly cooled from the austenitization temperature. This rapid quenching results in a structural transformation that introduces tetragonality. This tetragonality arises from a change in the crystal structure from body-centered cubic (*BCC*) to body-centered tetragonal (*BCT*), caused by distortions in the lattice due to interstitial carbon atoms and the resulting change in the c/a lattice parameter. A linear relationship between carbon content and the c/a ratio has been reported, showing that increasing carbon concentration leads to a higher c/a ratio [2]. However, there is ongoing debate regarding the minimum carbon content required to induce tetragonality, the causes behind unusually high or low tetragonality in steels and how this property varies spatially within the material.

The spatial resolution of XRD is insufficient to capture local variations in tetragonality, especially when the c/a ratio is low due to peak overlapping with α -Fe reflections. It is expected that the presence of tetragonality can be inferred from XRD patterns when the {200} reflection splits into (200)/(020) and (002) peaks [3]. Due to that, an effective technique for evaluating local tetragonality is Electron Backscatter Diffraction (EBSD). This technique makes it feasible to investigate local tetragonality, offering a spatial resolution of approximately 100 nm [4]. Collected Kikuchi patterns and pattern matching indexing method could help collect phase composition maps and visualize regions with different c/a ratios and their distribution (Figure 1).

¹ Academic Centre for Materials and Nanotechnology, AGH University of Krakow, al. A. Mickiewicza 30, 30-059 Krakow, Poland

² Institute of Materials Engineering, University of Silesia in Katowice, 75 Pułku Piechoty 1a, 41500, Chorzów, Poland

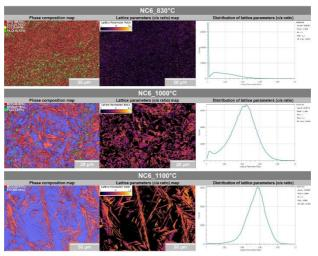


Figure 1. Phase composition maps, lattice parameters (c/a) distribution maps and distribution of the lattice parameters for NC6 steel after different austenitization temperatures for 30 minutes

To conclude, the martensite tetragonality in steels remains a complex scientific issue and a subject of ongoing research and discussion. Investigating this phenomenon requires analytical techniques with high spatial resolution. Due to that, conventional X-ray diffraction (XRD) struggles to detect tetragonality when the c/a ratio is low [3]. In contrast, electron backscatter diffraction (EBSD) offers a superior alternative, providing spatial resolution down to approximately 100 nm [4]. By analyzing Kikuchi patterns and performing detailed indexing, EBSD enables the precise examination of the local tetragonality of martensite in steels [5].

Acknowledgments: This work was supported by the Polish National Science Centre (NCN), grant number 2020/37/B/ST5/03669. The obtained results have been developed with the use of equipment financed from the funds of "Excellence Initiative - Research University" program at the AGH University of Krakow.

- [1] P. Uranga and J. María Rodríguez-Ibabe, Metals, Volume: 10 (2020), p. 1–4.
- [2] L. S. Kremnev, Tech. Phys., Volume: 58 (2013), p. 1288–1290.
- [3] T. Tanaka, N. Maruyama, N. Nakamura, and A. J. Wilkinson, Acta Mater., Volume: 195 (2020), p. 728–738.
- [4] G. Nolze, A. Winkelmann, G. Cios, and T. Tokarski, Mater. Charact., Volume: 175 (2021), p. 1–12.
- [5] G. Cios, A. Winkelmann, G. Nolze, T. Tokarski, Ł. Rychłowski, L. Dan, P. Bała, Ultramicroscopy, Volume: 253 (2023), p. 1–11.

Template – assisted synthesis of nanostructured polypyrrole powder

S. Golba^{1a}, J. Jurek-Suliga¹, I. Matuła¹, Z. Szaniewska¹

a sylwia.golba@us.edu.pl

¹ Institute of Materials Engineering, Silesian University in Katowice, 75 Pulku Piechoty 1A Street, 41-500 Chorzow, Poland

Keywords: polypyrrole, template synthesis, specific surface area

Electroactive polypyrrole is widely used in diverse directions with application ability strongly dependent on the morphology of the material [1,2]. In the current work we studied such materials derived by chemical oxidative polymerisation based on the template methodology with methyl orange (MO) as a structure guiding agent. We focused on the concentration of the dye to trace its templating ability.

Surface morphology of material dependent firmly on the amount of the supplied dye (Fig. 1 a,b) – increasing content of the dye provoked a decrease in the diameter of the forming tubes accompanied by a mutual increase in their number. The organization induced by the presence of MO was also reflected in surface active area of powders as determined by BET analysis (Fig. 1 c). The value of surface-active area increased markedly (5.8 times) from 12.58 m2/g for unmodified polymer to 74.00 m2/g for polymer synthesised in the highest concentration of modifier.

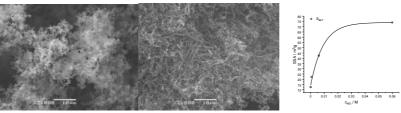


Figure 1. SEM images of pPy synthesised in a) the absence b) the presence of organic modificator, c) dependence of surface-active area of nanostructured polypyrrole with concentration of added dye

- K. Namsheer and Ch. Sekhar Rout, RSC Adv. 11 (2021), 5659
 Z. Huang, X. Li, Ch. Pan, P. Si, P. Huang and J. Zhou, Materials Chemistry and Physics 279 (2022) 125775

Effect of tungsten carbide addition on phase composition and wear resistance of Inconel 738LC nickel-based alloy layer deposited by laser cladding

A. Gradzik^{1a}, B. Kościelniak¹ and K. Gancarczyk¹

a andrzej gradzik@prz.edu.pl

¹ Department of Materials Science, Faculty of Mechanical Engineering and Aeronautics, Rzeszow University of Technology, Powstańców Warszawy 12, 35-959, Rzeszów. Poland

Keywords: phase composition, Inconel 738LC, laser cladding

Turbine blades of aircraft engines operate in harsh ambient conditions including high-temperature oxidizing gases stream, significant centrifugal forces and dynamic loads caused by high pressure gas flow, vibrations and solid particles. Consequently, they are susceptible to creep, corrosion, wear, erosion, and thermal fatigue. Furthermore, the contact surfaces of the blade shrouds are susceptible to abrasive wear and fretting. This can cause blade damage, requiring either their regeneration or replacement.

Nickel superalloys are known for their excellent high-temperature mechanical properties. Nevertheless, they exhibit low wear resistance under friction conditions. Therefore, a protective layer with higher abrasion resistance compared to the substrate material is applied to the contact surfaces of the blade shrouds. These layers are typically made from cobalt superalloys (Co-Cr-W-C-Stellites) and nickel superalloys (Ni-Cr-B-Si - Tribaloy) using welding and cladding processes. Conventional electric welding processes, as well as modern plasma and laser cladding processes, are employed for their production [1,2]

Laser cladding belongs to a group of modern processes for creating protective layers on gas turbine blade shrouds. It enables the exceptionally precise creation of small-sized layers – characteristic of blade shroud contact surfaces (< 1 cm²). It also allows for controlling the thermal energy input and, consequently, the melted volume of the substrate and filler material during the layer deposition process [3,4]

The wear resistance of the surfaced layer can be increased by introducing carbides, such as WC, W₂C, Cr₃C₂, and TiC, into the filler material used in the cladding process. Powder laser cladding also allows for precise control of the filler material's chemical composition, achieving desired properties of the manufactured layer that are beneficial for its projected application [5,6]

This study aimed to develop an Inconel 738LC laser cladded layer with tungsten carbide additions for increased wear resistance. Nickel superalloy powder Ni-16Cr-5.2Co-4.3Al-3Ta-2W-0.1Hf-0.1C (Ni-1278) with a chemical composition similar to Inconel 738LC was used in this research. Tungsten carbide (WC+W₂C) was added as an addition, up to 50 wt.%, to the powder mixture. A TRUMPF TruDisk 1000 disk laser, a TruLaser Cell 3008 workstation, and a GTV PF2/1 powder feeder were used in the research. The process was conducted using a laser head with powder feeding through three nozzles.

The laser cladding process parameters established were as follows: laser power -366 W, beam diameter -1.24 mm, surfacing speed -500 mm/min, and powder flow rate $91 \div 103$ mg/s.

The surfaced layers were analyzed for phase composition (XRD, EBSD), microstructure morphology (LM, SEM/EDS), hardness, and wear resistance (ball-on-disk test according to ASTM G99).

It was found that the Ni-1278-(WC+W₂C) protective layers have a dendritic structure composed of a solid solution – γ phase being a matrix for MC, M₂C, and M₆C type carbides, as well as WC and W₂C carbides introduced into the deposited powder.

The hardness of the layer and its wear resistance under raises with increasing (WC+W₂C) content in the cladded layer material. Hardness values of 270 HV10 for the Ni-1278 layer and 484 HV10 and 692 HV10 for the Ni-1278-30(WC+W₂C) and Ni-1278-50(WC+W₂C) layers, respectively, were obtained. Similarly, the surfaced layers showed up to 14 times greater wear resistance compared to the Inconel 738LC superalloy substrate material.

- [1] Reed C.R.: The superalloys: Fundamentals and applications. Cambridge University Press, Cambridge 2006.
- [2] Sims C. T.: A history of superalloy metallurgy for superalloy metallurgist. Superalloys, The Mineral Metals and Materials Society, (1984) 399-419.
- [3] Sexton L., Lavin S., Byrne G., Kennedy A.: Laser cladding of aerospace materials. Journal of Materials Processing Technology, 122 (2002) 1, 63÷68.
- [4] Egbewande A.T., Buckson R.A., Ojo O.A.: Analysis of laser beam weldability of Inconel 738 superalloy. Materials Characterization, 61 (2010) 5, 569-574.
- [5] Sun G. F., Liu C.S., Song L.J. Mazumder J.: Microstructure and Wear Behavior of Laser-Aided Direct Metal Deposited Co-285 and Co-285+WC Coatings. Metallurgical and Materials Transactions A, 41 (2010) 6, 1592-1603.
- [6] Toyserkani E., Khajepour A., Corbin S.: Laser cladding. CRC Press, Boca Raton 2005

Analysis of the influence of compositional changes in $Co_{1-x}Ni_xSi_2$ single crystals on key material properties

W. Gurdziel^{1a}, G. Dercz¹, Z. Wokulski¹

a wojciech.gurdziel@us.edu.pl

¹ University of Silesia in Katowice, Faculty of Science and Technology, Institute of Materials Engineering, Poland

Keywords: metal silicides, materials characterisations, crystal growth

This study presents the results of experimental investigations into the influence of chemical composition (x = 0.10, 0.25, 0.50) and growth method on the key material properties of $Co_{1-x}Ni_xSi_2$ solid solution single crystals. Due to their unique structural features, transition metal disilicides, particularly $CoSi_2$ and $NiSi_2$, represent a promising class of materials for modern micro- and nanoelectronics and thermoelectric applications [1, 2]. The main objective of this work was to examine how controlled changes in chemical composition and applied crystallisation techniques affect the microhardness, electrical resistivity, Seebeck coefficient, and specific heat of these materials.

Co_{1-x}Ni_xSi₂ single crystals were grown from the melt using both the Bridgman and Czochralski methods. Within the scope of the comprehensive experimental investigations conducted on the obtained single crystals, measurements included, among others, Vickers microhardness (µHV), analysis of temperaturedependent electrical resistivity (p) in the range of 4.2-300 K, Seebeck coefficient (S) in the range of 14-300 K, and specific heat (Cp/R) in the range of 2-300 K. During the investigations, it was found that the microhardness of the single crystals increases significantly with increasing nickel content (x). Additionally, samples grown via the Czochralski method consistently exhibited approximately 10% higher microhardness values and better electrical conductivity than those obtained by the Bridgman method. This is attributed to the greater compositional homogeneity, superior cooling control, and lower concentration of structural defects in the single crystals produced by this method [3, 4]. Electrical resistivity analysis revealed the lowest resistance values at a composition close to $x \approx 0.4$. This result suggests optimal conduction band filling with a moderate nickel content in the tested samples, indicating an improvement in electron transport efficiency within the material. Analogous dependencies, related to changes in electronic structure as a function of composition, have been confirmed in recent studies concerning silicon- and nickel-based compounds [5]. For the Seebeck coefficient, minimal values were observed in the $x \approx 0.4$ –0.6 range, indicating a thermally stable composition of the studied material, particularly valuable in applications requiring operation under varying temperature conditions. Regarding specific heat, a linear increase in its value with increasing x was found, which can be explained by the rise in the electronic density of states – analogous trends are observed in typically metallic silicides [6].

The results confirm that compositions with $x \approx 0.4$ –0.6 provide the most favourable combination of key material parameters: high microhardness, low resistivity, moderate Seebeck coefficient, and elevated specific heat. This combination makes $\text{Co}_{1 \text{--} x} \text{Ni}_x \text{Si}_2$ single crystals promising candidates for applications in microelectronics, thermoelectric structures, and systems requiring high mechanical performance and thermal stability. In future research, we plan to extend the analysis to include the impact of cyclic temperature changes, detailed control of lattice defects, and further optimising directional crystallisation conditions for these promising materials.

- [1] L. J. Chen, "Metal silicides: An integral part of microelectronics", ResearchGate, (2005).
- [2] S. P. Murarka, "Silicides for VLSI applications", Academic Press, London, (1983).
- [3] T. Berry, N. Ng, T. McQueen, "Single Crystal Growth Tricks and Treats", *arXiv*, (2022).
- [4] Pillaca Quispe, M. Single crystal growth and structural characterisation of intermetallic phases for thermoelectric applications (Doctoral dissertation, Ludwig-Maximilians-Universität München) (2020).
- [5] J. Kim et al. Potential of NiOx/Nickel Silicide/n+ Poly-Si Contact for Perovskite/TOPCon Tandem Solar Cells. *Energies*, *15*(3), 870 (2022).
- [6] S. Wang, Y. Pan, Y Wu, Y Lin., Insight into the electronic and thermodynamic properties of NbSi2 from first-principles calculations. RSC Advances, 8(72), 41539-41548, (2018).

The influence of structure morphology on the functional properties of selected self-adhesive hydrogels used in the treatment of thermal burns

<u>J.Jurek-Suliga^{1a}</u>, M. Wroniecka¹ and I. Matuła¹

^Ajustyna.jurek-suliga@us.edu.pl

11nstitute of Materials Science, Faculty of Science and Technology, University of Silesia, 41-500 Chorzów, 75 Pulku Piechoty 1a

Keywords: hydrogel dressings, polymers, thermal burns

Hydrogel dressings are made on the basis of hydrogels – hydrophilic polymers with the ability to swell in water. Constructed from cross-linked chains of homopolymers or copolymers, they create a three-dimensional structure. Due to their exceptional water absorption, they are often referred to as superabsorbents [1].

The effectiveness of hydrogel dressings in wound management is strongly influenced by their microstructure and morphology. These structural features determine the functional properties of the dressings, including their ability to maintain optimal moisture, absorb wound exudates, and provide mechanical comfort to the patient. Furthermore, the morphology of the hydrogel matrix plays a crucial role in facilitating the wound healing process by supporting tissue regeneration and reducing the risk of infection. As a result, hydrogel dressings with tailored structural characteristics are particularly effective in the treatment of various types of wounds, such as burns, pressure sores, chronic wounds, and ulcers.

These dressings were subjected to various tests, such as thermal analysis DSC, infrared spectroscopy FTIR and electron microscopy SEM. Their behavior in an acidic environment was also tested, and their water absorption capacity was assessed. The results of the tests showed significant differences in the structure and properties of individual dressings, which affects their different applications in medicine, e.g. in the treatment of burns, ulcers or chronic wounds.

^[1] Wichterle, O.; Lim, D. Hydrophhilic gels for biomedical use. Nature 1960, 3, 117-118.

Structural analysis and corrosion resistance of zinc coatings on DC01 steel depending on the thickness of the deposited layer

M. Karolus^{1a}, S. Lesz², A. Zarychta², A. Drygała², J. Kubisztal¹, K. Gołombek³, J. Wyrwał⁴, B. Grzegorczyk², M. Bodio²

a malgorzata.karolus@us.edu.pl

Keywords: zinc coating, corrosion resistance, XRD analysis, SEM method

The article presents the results of structural analysis and corrosion resistance of zinc coatings on DC01 steel depending on the thickness of the deposited layer obtained at different current density (1.7 and 2.5 A/dm²) and the galvanizing time. Coating thickness was determined using a thickness gauge and a scanning electron microscope (SEM).

The microstructure of the obtained zinc coatings was examined using a SUPRA 35 scanning electron microscope (SEM) (Carl Zeiss, Jena, Germany) equipped with an UltraDry EDS detector (Thermo Scientific, Waltham, USA).

XRD measurements were performed in Grazing Incident X-ray Diffraction Geometry (GIXRD) using a PANalytical Empyrean diffractometer equipped with a copper anode X-ray tube, a PIXcel detector and a 5-axis sample stage. Phase identification of obtained diffraction patterns for tested incident angles (0.25; 0.5; 1.0; 1.5; 2.0) was performed using the PANalytical HighScore Plus software integrated with the ICDD PDF5+ 2025 crystallographic database. Structural analysis, including refinement of lattice parameters of the main phase, crystallite size, and lattice strain determination, was conducted using the Rietveld method [1] and Williamson-Hall theory [2] implemented in the HighScore Plus software.

¹ University of Silesia, Institute of Materials Engineering, 1A, 75 Pułku Piechoty Street, Chorzów 41-500. Poland.

² Silesian University of Technology, Faculty of Mechanical Engineering, 18a Konarskiego Street, 44-100 Gliwice, Poland,

³ Silesian University of Technology, Materials Research Laboratory, Silesian University of Technology, 18a Konarskiego St, 44-100 Gliwice, Poland,

⁴ Silesian University of Technology, Faculty of Automatic Control, Electronics and Computer Science, Poland

- [1] L.B. McCusker, R.B. Von Dreele, D.E. Cox, D. Loue, P. Scardi, Rietveld refinement guidelines, J Appl Crystallogr 32 (1999) 36–50.
- [2] G.K. Williamson, W.H. Hall, X-ray line broadening from filed aluminium and wolfram, Acta Metallurgica 1 (1953) 22–31.

Multiscale analysis of defect structures in single-crystalline CMSX-4 superalloys

S. Kołodziej^{1a}, R. Paszkowski¹, M. Pawlyta^{2,3}, B. Chrząszcz¹

^a slawomir.kolodziej@us.edu.pl

Keywords: nickel-based superalloy; X-ray topography; positron annihilation lifetime spectroscopy; transmission electron microscopy; defects;

An analysis of defects creation in the vicinity of the selector-root connection plane in single-crystalline turbine blades made of CMSX-4 Ni-base superalloy was performed using several experimental methods. A coupling of scanning electron microscopy and X-ray diffraction topography allowed the visualization of dendritic arrays and surface defects in the root part of the blades. As a result, contrast inversions and areas where internal stresses occur were observed. The defects on a microscopic scale were characterized using positron annihilation lifetime spectroscopy and transmission electron microscopy. The registered positron lifetimes, above 0.5 ns, beyond the range characteristic for defects generally reported in metals and their alloys suggest the presence extremely large void type defects. Herein, we have identified large defects, ca. 2-5 nm in diameter, formed due to the contraction of fluid metal, captured in interdendritic regions during the liquid-to-solid transition. This work is a precursor to the almost untouched area of the discussion of lifetimes characteristic for positron bound states, called positronium (>0.5 ns) in relation to the morphology of void-type defects in single-crystalline superalloys.

¹ Institute of Materials Engineering, University of Silesia in Katowice, 1A 75 Pułku Piechoty St., 41-500 Chorzów, Poland

² Materials Research Laboratory, Faculty of Mechanical Engineering, Silesian University of Technology, Konarskiego 18 A, 44-100 Gliwice, Poland

³ Electron Microscopy Facility, School of Chemistry, University of St Andrews, St Andrews KY16 9AJ, UK

Utilisation of porous AAO structure for tribological application

J. Korzekwa^{1a}, M. Bara¹, M. Niedźwiedź¹, G. Dercz¹

a joanna.korzekwa@us.edu.pl

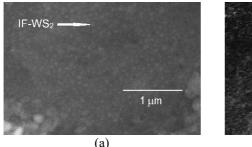
¹ Institute of Materials Engineering, Faculty of Science and Technology, University of Silesia in Katowice, 75 Pułku Piechoty 1a, 41-500 Chorzów, Poland

Keywords: AAO coatings, IF-WS2, SEM/EDS, XRD

The structure and properties of anodic aluminium oxide (AAO) coatings on aluminium alloys have long been known, as has their formation in various electrolytes. Hard oxide layers improve hardness, strength, and corrosion resistance. The mechanical and tribological performance of AAO depends on surface condition, porosity, and thickness, which are influenced by anodising parameters such as voltage, temperature, and electrolyte composition. Porosity also serves as a lubricant reservoir, enabling self-lubricating systems that reduce friction and wear [1,2].

The presented research focuses on tribological pairs: AAO and AAO-modified fullerene-like tungsten disulfide (IF-WS₂) sliding against 1.14401 steel or ZrO₂ ceramic.

Figure 1 shows the SEM images of AAO coating with embedded IF-WS₂ and the wear track of AAO/IF-WS₂ coating after friction with 1.4401 steel.



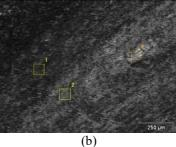


Fig. 1. SEM images of (a) AAO with embedded IF-WS₂, (b) wear track of AAO/IF-WS₂ coating.

Figure 2a shows the example of EDS analysis of area no. 1 from Fig. 1b. One can conclude that besides the Al from the aluminium alloy, the peaks from IF-WS₂ and wear debris from 1.1441 steel were observed. The sample diffraction

pattern shown in Figure 2b clearly indicates that the analysed wear products in powder form are multiphase. Reflections corresponding to the aluminium phase and its oxide, iron oxidation products originating from the steel ball, and the presence of the WS₂ compound were identified.

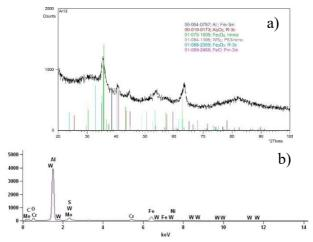


Fig. 2. (a) EDS analysis of area no.1 from Fig. 1b; (b) XRD analysis of wear debris after friction of AAO/IF-WS₂ with 1.14401 steel.

SEM/EDS and XRD studies provide crucial information about the structure and microstructure of coatings, enabling the identification of wear phases and mechanisms. Their use allows for a better understanding of the relationship between coating structure and its tribological properties. This is crucial for further material optimisation when using AAO structures in low-friction applications.

Acknowledgment: The project was co-financed by the European Union within the program "The European Funds for Śląsk (Silesia) 2021-2027"

- [1] G. S. Lee, J. H. Choi, Y. C. Choi, S. D. Bu, and Y. Z. Lee, "Tribological effects of pores on an anodised Al alloy surface as a lubricant reservoir," Curr. Appl. Phys., vol. 11, no. 5 SUPPL., pp. S182–S186, 2011, doi: 10.1016/j.cap.2011.03.057.
- [2] M. Maejima, K. Saruwatari, and M. Takaya, "Friction behaviour of anodic oxide film on aluminum impregnated with molybdenum sulfide compounds," Surf. Coatings Technol., vol. 132, no. 2–3, pp. 105–110, 2000, doi: 10.1016/S0257-8972(00)00849-5.

Microstructure and oxidation resistance of DMV 617 mod superalloy in a steam environment at 750 °C

B. Kościelniak^{1a}, I. Bednarczyk², M. Sozańśka², A. Gradzik¹, K. Gancarczyk¹, J. Nawrocki¹, M. Góral¹

a b.koscielnia@prz.edu.pl

Keywords: nickel-based superalloy, microstructure characterisation, resistance to steam oxidation.

The electric power industry is a vital sector for every country, as it plays a crucial role in ensuring energy security and driving economic development. Therefore, it is essential to enhance the technical and economic performance of boilers in power plants, with a particular focus on improving their efficiency. To achieve this, it is important to use alloys that exhibit microstructural stability, high creep resistance and excellent corrosion resistance in aggressive and high-temperature environments for critical components of advanced boilers [1]. One of the dedicated alloys suitable for boiler pressure elements is the DMV 617 mod. This alloy is known for its excellent mechanical properties at elevated temperatures, as well as its resistance to corrosion in aggressive environments [2].

In this paper, the microstructural changes and oxidation resistance in steam environments at a temperature of 750°C for DMV 617 mod alloy were characterised. The isothermal oxidation test was conducted at 750°C in a steam atmosphere under atmospheric pressure for various durations: 100, 250, 500, 1000, and 2000 hours. After oxidation, microstructure observations and chemical phase analysis were conducted using scanning electron microscopes as well as scanning transmission electron microscopes. Phase identification was carried out using electron diffraction in a transmission electron microscope. A quantitative assessment of microstructural components was conducted using computer image analysis.

The results indicated that heating the alloy to 750° C resulted in changes to the microstructure of the tested superalloy. Specifically, this heating process affected the size of the γ ' phase precipitates and intensified the precipitation of carbides (Fig. 1). Additionally, three distinct types of $M_{23}C_6$ carbides were observed within the alloy matrix. These carbides exhibited variations in both

¹ Department of Materials Science, Faculty of Mechanical Engineering and Aeronautics, Rzeszow University of Technology, Powstańców Warszawy 12, 35-959 Rzeszów, Poland

² Department of Materials Technologies, Faculty of Materials Engineering, Silesian University of Technology, Akademicka 2A, 44-100 Gliwice, Poland

morphology and arrangement, which were attributed to the addition of boron to the alloy's chemical composition.

The study of oxidation products in the presence of steam revealed the formation of a fine-crystalline Cr_2O_3 oxide layer on the surface of the superalloy (Fig. 2a). Additionally, TiO_2 crystallites were formed at the boundary between the Cr_2O_3 layer and the steam. The presence of α -Al $_2O_3$ oxides at the boundary between the Cr_2O_3 layer and the superalloy substrate was also observed. Furthermore, an internal oxidation zone developed within the superalloy, where α -Al $_2O_3$ crystallites acted as internal oxides (Fig.2b). The Kirkendall phenomenon was noted as well, particularly with the extension of the oxidation time.

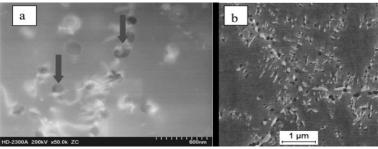


Fig.1. Microstructure of DMV 617 mod: a) γ' phase precipitates (arrows) and b) $M_{23}C_6$ carbides

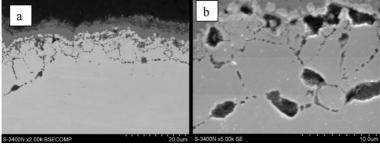


Fig.2. Oxidation products resulting from corrosion in a steam environment include: a) a Cr_2O^3 oxide layer on the surface and b) an internal oxidation zone.

- [1] B. Tramošljika, P. Blecich, I. Bonefačić, V. Glažar, Sustainability 13 (2021), p. 801
- [2] Bednarczyk, K. Rodak, A. Hernas, V. Vodárek, Engineering Proceedings 64 (2024), p. 12.

Artificial Intelligence to Power the Future of Materials Science and Engineering

L. Kozielski^{1a}

a lucjan.kozielski@us.edu.pl

¹ Institute of Materials Engineering, Faculty of Science and Technology, University of Silesia in Katowice, 75 Pulku Piechoty 1a, 41-500 Chorzów, Poland

Keywords: artificial intelligence, machine learning, properties predictions

In recent decades, the use of artificial intelligence (AI) techniques in the field of materials science has received significant attention owing to their excellent ability to analyse a vast amount of data and reveal correlations between several complex interrelated phenomena.

ML and AI technologies already impact our every-day lives. However, as practitioners of the physical sciences, we may ask what has changed, or why should a scientist be concerned now with ML and AI technologies for Properties of Solids? Aren't these technologies simply sophisticated curve fits or "black box" tools? Is there any physics there?

Less sceptically and more objectively, one might also ask what are the important achievements from these tools, and how are those achievements related to familiar physics? Finally, how can one best apply the newest advances in ML and AI to improve Properties of Solids analysis results?

Speculating still further, why are there no emerging AI-based engineering design systems that recognize component features, attributes, or intended performance to make recommendations about directions for final design, manufacturing processes, and materials selections or developments? Such systems are possible over the next 20 years. Indeed, many authors suggest that machine learning is likely to be one of the most transformative technologies of the 21st century and therefore cannot be neglected in any long-range development of Statical and Dynamical Properties of Solids practices.

The presentation is intended to serve as a selective introduction to ML and AI methods and applications, as well as to give perspective on their use in the Properties of Solids Prediction.

Acknowledgements: Special acknowledgement for the investigation financial support for GreenMat Programme "GreenMat - Development of the University of Silesia in Katowice in the field of new material technologies towards the green transformation of the region".

Dendritic structure and chemical composition in the cooling bores area of single-crystalline turbine blades

J. Krawczyk^{1a} and M. Soczówka¹

a jacek.krawczyk@us.edu.pl

¹ Institute of Materials Engineering, Faculty of Science and Technology, University of Silesia in Katowice, 1a 75 Pułku Piechoty St. 41-500 Chorzów, Poland

Keywords: superalloy, turbine blade, chemical composition

Turbine engines in the aerospace industry are among the most complex machines. Engine components, such as turbine blades, operate at extremely high temperatures to meet increasing standards of efficiency and economy. To prevent overheating, the blades are internally cooled by air that circulates through complex internal channels or bores. However, these channels or bores' complex shape and arrangement cause various defects to be raised during directional crystallization, including chemical inhomogeneity.

Today, turbine blades are most often produced of cobalt- or nickel-based superalloys. Superalloys are characterized by high mechanical strength, phase stability, resistance to oxidation, corrosion, and creep at high temperatures. The condition for these properties is a low concentration of defects, and homogeneity of the dendritic microstructure and chemical composition.

The studied cored model single-crystal turbine blades made of the CMSX-4[®] superalloy were produced by directional crystallization using the Bridgman technique. The withdrawal rate was 3 mm/min. The assumed, preferred crystal orientation was [001]-type direction, parallel to the blade withdrawal direction and the main vertical blade axis along which the primary dendrite arms have grown.

The chemical microanalysis was performed by scanning electron microscopy using the energy dispersive spectroscopy technique (SEM-EDS). The percentage atomic content of the chemical elements was analyzed in the areas near the cooling bores on several transverse and longitudinal sections of the blades. The quantitative distribution of chemical elements on section surfaces near the cooling bores was determined. Changes in the chemical composition were determined concerning the location of the analyzed blade fragment. The dendritic structure SEM observations were also performed, and a possible relation between changes in the morphology of the dendrite set and changes in the chemical composition in the area of the cooling bores was suggested.

High-entropy powder (Mn, Fe, Co, Ni, Cu)₃O₄ in a porous Ni matrix as an oxygen evolution electrocatalyst

J. Kubisztal^{1a}

a julian.kubisztal@us.edu.pl

¹ University of Silesia in Katowice, Institute of Materials Engineering, 75 Pułku Piechoty 1A, Chorzów, 41-500, Poland

Keywords: high-entropy oxide, porous electrode, oxygen evolution reaction

Efficient and durable oxygen evolution reaction (OER) electrocatalysts are essential for renewable energy conversion devices based on water electrolysis. In this work, a porous nickel substrate was modified by depositing onto its surface a high-entropy powder (Mn, Fe, Co, Ni, Cu)₃O₄ (HEO), synthesized by co-precipitation. The chemical composition and crystal structure of the HEO powder were characterized by EDS and XRD, while the surface morphology and elemental distribution at the Ni/HEO interface were examined by SEM/EDS. Electrochemical characterization comprised three-electrode measurements in 1 M KOH (LSV, CV, EIS) and full-cell assessment in a two-electrode setup.

XRD analysis showed that HEO crystallizes in a spinel structure with an average crystallite size of 69(4) nm. SEM/EDS confirmed a homogeneous morphology and a uniform distribution of Mn, Fe, Co, Ni, and Cu across the Ni/HEO composite surface. The Ni/HEO composite exhibits a lower overpotential than bare Ni at a given current density. The lower Tafel slope indicates faster OER kinetics. Furthermore, the specific charge-transfer resistance (specific $R_{\rm ct}$) of Ni/HEO is approximately 70% lower than that of Ni at an overpotential of 340 mV. The double-layer capacitance ($C_{\rm dl}$) is approximately 35% higher for Ni/HEO, indicating a larger number of active sites than for Ni. In the two-electrode setup, an electrolyzer with a Ni/HEO anode and a Ni cathode achieved a lower cell voltage (\sim 1.54 V at 10 mA cm $^{-2}$) than the Ni|Ni configuration (\sim 1.58 V) and remained stable for 24 h.

These results demonstrate that combining porous Ni with a high-entropy spinel powder (Mn, Fe, Co, Ni, Cu) $_3$ O4 substantially enhances OER kinetics and improves long-term stability. The large electrochemically active surface area (inferred from the higher $C_{\rm dl}$) and the reduced specific $R_{\rm ct}$ are key contributors to the enhanced catalytic performance of the Ni/HEO composite.

Intragranular and intergranular contributions to charge transport and temperature sensitivity of Mn-Ni-Fe spinel oxide

M. Kubisztal^{1a}

a marian.kubisztal@us.edu.pl

¹ Institute of Materials Engineering, University of Silesia in Katowice, ul. 75 Pułku Piechoty 1A, 41-500 Chorzów.

Keywords: temperature sensor, electrical conductivity, spinel structure

This study focuses on designing novel semiconducting materials for potential temperature sensor applications [1, 2]. The chemical co-precipitation technique, followed by sintering of cold-pressed powders, was used to obtain a single-phase oxide with a spinel structure containing Mn, Ni, and Fe. Electron microscope images reveal that the synthesized compound is partially densified and exhibits a characteristic granular microstructure formed during the sintering process. The AC and DC electrical responses of the synthesized material were investigated using impedance spectroscopy and electrical equivalent circuit analysis (testing signal range: $10~{\rm Hz}-1~{\rm MHz}$, temperature range: $300~{\rm K}-400~{\rm K}$). Complex impedance plots of the examined compound show two distinct arcs, attributed to grain interior and grain boundary effects. A detailed analysis of these arcs reveals that the charge hopping process in the intragranular and intergranular regions follows Mott's nearest-neighbor hopping model. The temperature coefficient of resistance (TCR) for the compound ranges from -2.9%/K to -5.2%/K.

- [1] Feteira, J. Am. Ceram. Soc. 92[5] (2009), p. 967.
- [2] T. Dinh, H.P. Phan, A. Qamar, P. Woodfield, N.T. Nguyen and D.V. Dao, J. Microelectromechanical Syst. 26 (2017), p. 966.

Comparative analysis of structural properties of zirconia powder reflected in its XRD spectra

S. Kulesza^{1a}, M. Bramowicz¹

a slawomir.kulesza@uwm.edu.pl

¹ Wydział Nauk Technicznych, Uniwersytet Warmińsko-Mazurski w Olsztynie ul. Oczapowskiego 11, 10-719 Olsztyn, Poland

Keywords: grain-size distribution, crystalline structure, zirconia powder

Zirconia (ZrO2) is a multipurpose material with many applications due to its unique properties including (but not limited to): high hardness, wear resistance, and thermal stability [1-2]. Crystalline zirconia is a polymorph that takes one of three possible forms: monoclinic (M), which is stable from room temperature up to 1170 °C, tetragonal (T), which becomes stable from 1170 to 2370 °C, and cubic (C), which is favorable above 2370 °C [3-5]. The applications of zirconia range from structural ceramics to dental materials to thermal barrier coatings, and many others [6-8], but the quality of obtained solids strongly depend on the initial structure of the processed material.

In this work three different approaches have been used to determine various crystalline properties of zirconia powders reflected in their XRD spectra, e.g.: crystal size, lattice strains, and relative phase content. These parameters were determined using classical Scherrer method and its extension proposed by Williamson and Hall together with Pielaszek method introduced for multidisperse materials. On the other hand, the relative phase contents were determined using the Rietveld refinement method with the help of VESTA application software [9]. Obtained results demonstrate the limits of reliability of each method in terms of granular, multiphase materials.

- [1] Arellano Moncayo, A.M.; Peñate, L.; Arregui, M.; Giner-Tarrida, L.; Cedeño, R. State of the Art of Different Zirconia Materials and Their Indications According to Evidence-Based Clinical Performance: A Narrative Review. Dent. J. 2023, 11, 18. https://doi.org/10.3390/dj11010018
- [2] Lagunov, V.L.; Ali, B.; Walsh, L.J.; Cameron, A.B.; Litvinyuk, I.V.; Rybachuk, M.; George, R. Properties of Zirconia, Lithium Disilicate Glass Ceramics, and VITA ENAMIC® Hybrid Ceramic Dental Materials Following Ultra-Short Femtosecond (30 fs) Laser Irradiation. Appl. Sci. 2024, 14, 7641. https://doi.org/10.3390/app14177641
- [3] Yu Hui, Yu Zhao, Sumei Zhao, Lijian Gu, Xizhi Fan, Ling Zhu, Binglin Zou, Ying Wang, Xueqiang Cao, Fluorescence of Eu3+ as a probe of phase transformation of zirconia, Journal of Alloys and Compound, 2013, 573(5):177-181

- [4] Bokhimi X., Morales A., Novaro O., Portilla M., Lo T., Tzompantzi F. et al. Tetragonal Nanophase Stabilization in Nondoped Sol–Gel Zirconia Prepared with Different Hydrolysis Catalysts, J Solid state chemistry, 1998, 135:28-35
- [5] Sayılkan F., Asilturk M., Burunkaya E., Arpac E., Hydrothermal synthesis and characterization of nanocrystalline ZrO2 and surface modification with 2acetoacetoxyethyl methacrylate, J Sol-Gel Science and Technology, 2009, 51:182-189
- [6] Zafer E., Reactions in hydroxylapatite–zirconia composites, Ceramics International, 2007, 33: 987-991
- [7] Kim H.W., Noh Y.J., Koh Y.H., Kim H.E., Kim H.M., Effect of CaF2 on densification and properties of hydroxyapatite–zirconia composites for biomedical applications, Biomaterials, 2002, 23: 4113-4121
- [8] Chevalier J., What future for zirconia as a biomaterial?, Biomaterials, 2006, 27:535-543
- [9] K. Momma and F. Izumi, "VESTA 3 for three-dimensional visualization of crystal, volumetric and morphology data," J. Appl. Crystallogr., 44, 1272-1276 (2011)

Synthesis of biocompatible metal-metal composite with variable size of reinforcing particles

<u>I. Laszko^{1a}</u>, I. Matuła¹, A. Barylski¹, W.Michalik¹ and G. Dercz^{1b}

^a ilaszko@us.edu.pl, ^b grzegorz.dercz@us.edu.pl

¹ University of Silesia in Katowice, Institute of Materials Engineering, 75 Pułku Piechoty Street 1A, 41-500 Chorzów, Poland

Keywords: composite, biomaterial, MMC

The increasing number of elderly patients has intensified the demand for advanced biomaterials in orthopaedic and dental treatments, driving the search for innovative solutions. Titanium alloys, particularly Ti6Al4V, are widely applied owing to their strength, corrosion resistance, and biocompatibility, accounting for over 50% of medical titanium use, compared to 20–30% for commercially pure Ti [1,2]. A promising strategy is the development of biocompatible composites combining Ti6Al4V with pure titanium to balance mechanical performance, economic viability and biological safety.

Titanium-based metal-metal composites were fabricated via powder metallurgy, using pure titanium as the matrix and Ti6Al4V particles as reinforcement. Different particle sizes (~45 μm and ~450 μm) and volume fractions (20 wt.% and 40 wt.%) were used to investigate their effect on the microstructure and properties.

Metal-metal composites consisting of Ti6Al4V particles embedded in a Ti matrix were successfully fabricated using powder metallurgy. Microstructural analysis (OM) revealed a non-uniform particle distribution with agglomeration, particularly for larger particles (450 μm). Increasing reinforcement content was found to promote porosity. The Ti6Al4V particles exhibited a lamellar structure with a hardness gradient, higher in the cores and lower near the particle-matrix interface. The EDS analysis confirmed interdiffusion processes and the formation of diffusion-type bonds, indicating effective particle-matrix bonding but also the presence of local chemical and mechanical heterogeneities. Phase analysis confirmed that the composites have a biphasic nature, consisting of α -titanium and β -titanium.

Acknowledgment: This work was supported by the Polish National Science Centre, Poland (Polish: Narodowe Centrum Nauki, abbr. NCN) under the research project OPUS-27 no. UMO-2024/53/B/ST11/00431

- [1] M. Najafizdaeh, et al., Journal of Alloys and Compounds Communications 3 (2024), p. 100019
- [2] N. Koju, S. Niraula and B. Fotovvati, Metals 12 (2022), p. 687

Micro-arc oxidation of plastically deformed titanium for future dental implants: effect of Ag nanoparticles on microstructure and properties

<u>Ł. Maj¹a</u>, F. Muhaffel², A. Jarzębska¹, A. Trelka¹, D. Toboła³, G. Cempura⁴, K. Brudecki⁵, M. Bieda¹ and H. Cimenoglu²

a l.maj@imim.pl

Keywords: titanium; micro-arc oxidation; Ag nanoparticles

Micro-arc oxidation (MAO) technique gained significant popularity in terms of surface modification of so-called "valve" metals such as titanium and its alloys aimed at improving surface hardness, wear resistance, corrosion resistance, bioactivity, antibacterial performance etc. Among many advantages of the MAO method, its versatility should be emphasized, which allows to incorporate various elements into the coating microstructure, e.g. in the form of nanoparticles, improving functional properties, such as antibacterial performance [1]. In this way, popular Ag nanoparticles are considered as the most efficient in interaction with DNA of bacteria cell securing antimicrobial protection of future medical implants [2]. It should be noted that the effect of Ag-NPs on the microstructure and functional properties of the MAO coatings remains barely investigated.

In this work, the effect of Ag-NPs concentration on microstructure and properties of MAO coatings deposited on plastically deformed titanium was studied. Titanium grade 4, subjected to multi-pass hydrostatic extrusion, was used as a substrate. The MAO coatings were deposited with the use of bipolar pulsed power supply with suspended Ag nanoparticles. The surface topography and microstructure of the coatings were investigated with scanning and transmission electron microscopes, respectively. Release of Ag ions was determined with ICP-MS spectrometer for a total time of 7 days. The adhesion of the coatings to the substrate as well as their tribological performance were assessed with scratch and reciprocal wear tests, respectively.

¹ Institute of Metallurgy and Materials Science, Polish Academy of Sciences, Krakow, Poland

² Istanbul Technical University, Istanbul, Turkey

³ Lukasiewicz Research Network – Krakow Institute of Technology, Krakow, Poland

⁴ AGH University of Krakow, Krakow, Poland

⁵ Institute of Nuclear Physics, Polish Academy of Sciences, Krakow, Poland

The plan-view observations of surface topography with SEM method and cross-sectional study with TEM microscope coupled with EDS chemical analysis allowed to prove that the Ag nanoparticles are uniformly dispersed on the upper surface of the coating as well as incorporated in the areas close to the inherent porosity. Results of the reciprocal wear testing indicate a positive role of Ag-NPs in reducing the coefficient of friction as well as the wear rate. The scratch test proved that addition of Ag-NPs allowed to delay the cracking of the MAO coatings under the action of indenter, represented by L_{C1} parameter.

Acknowledgments: This research was financially supported by the National Centre for Research and Development of Poland, grant number LIDER13/0175/2022

- [1] Fattah-alhosseini, M. Molaei, N. Attarzadeh, K. Babaei, F. Attarzadeh, Ceramics International 46 (2020) p. 20587-607.
- [2] X. He, X. Zhang, X. Wang, L. Qin, Coatings 7(3) (2017) p. 45

The gradient titanium-based materials for potential medical applications produced by modified powder metallurgy method

I. Matuła^{1a}, G. Dercz¹

a izabela.matula@us.edu.pl

¹ Institute of Materials Engineering, University of Silesia in Katowice, 75 Pułku Piechoty Street 1 A, 41-500 Chorzów, Poland;

Keywords: titanium-based material, porosity, powder metallurgy

Titanium-based materials are widely used in medicine due to their excellent biocompatibility, but remain far from being ideal implant materials. One of the key limitations is the mismatch of Young's modulus between metallic implants and natural bone. This difference induces stress at the bone–implant interface, often leading to tissue damage, premature implant failure, and the need for early reimplantation.

A promising strategy to overcome this issue is the design of functionally graded materials (FGMs) with controlled porosity. Gradient structures allow for a smooth transition in chemical composition, microstructure, and mechanical properties, thus improving implant integration and long-term performance.

In this study, porous gradient titanium-based materials were fabricated by powder metallurgy method. The production method resulted in interconnected pore networks with dimensions suitable for osseointegration, which are highly promising for bone and dental implants.

Additionally, process innovation was introduced through a minor addition of tin (3 wt.%) as a process control agent. This modification improved nanocrystallization of titanium phases, refined particles, and enhanced homogenization by reducing cold-welding and agglomeration during mechanical alloying. In parallel, the effects of silver and copper additions were also investigated, providing further insights into how different alloying elements influence the microstructure and processing behavior of titanium-based materials.

Microscopic observations confirmed the formation of strong inter-particle bonds, while preliminary mechanical tests revealed a gradual change of properties across the samples, consistent with the gradient design. These results demonstrate that the proposed processing route provides an effective way to engineer porous, functionally graded titanium-based materials with significant potential for next-generation biomedical implants.

Acknowledgment: Conference participation was supported by the GreenMat project, co-funded by the European Union under the program "European Funds for Silesia 2021–2027".

Structure, martensitic transformation, and properties of Ni-Co-Mn-In-Fe-Cr magnetic shape memory alloys

E. Matyja^{1a}, K.Prusik¹, M. Zubko¹, R. Santamarta², J. Torrens-Serra², M. Kubisztal¹, and G. Dercz¹

a edyta.matyja@edu.edu.pl

¹ University of Silesia in Katowice, Institute of Materials Engineering, Faculty of Science and Technology, 75 Pulku Piechoty 1a, Chorzów, 41 500, Poland
 ² Departament de Física, Universitat de les Illes Balears, Cra. de Valldemossa km 7.5, Palma de Mallorca, 07122, Spain

Keywords: magnetic shape memory alloys, Ni-Co-Mn-In alloy, martensitic transformation, gamma particles

In recent years, NiMn-based Heusler alloys have great interest due to their potential as magnetic shape memory alloys (MSMAs) in magnetic actuator applications and magnetic cooling systems [1]. To overcome the brittleness problem and enhance the mechanical and functional properties of Ni-Mn-In-based alloys, some modifications, such as alloying, microstructural control, and processing techniques, are used. Although the impact of Fe and Cr additions on ternary Ni-Mn-In alloys has been studied, their common effect on quaternary Ni-Co-Mn-In alloys remains unknown. In off-stoichiometric Ni-Mn-In alloys, martensitic transformation (MT) temperatures strongly depend on the electron concentration ratio (e/a). Based on the theoretical considerations, the alloy compositions have been designed to obtain MT near room temperature.

In this work, a series of $Ni_{47}Co_3Mn_{36.5-2x}In_{13.5}Fe_xCr_x$ (x = 0, 0.5, 1, 1.5 at.% %) polycrystalline alloys were produced by the arc melting technique and thermal treatment at 900°C for 24 h with quenching.

The phase composition determined by X-ray diffraction (XRD) and scanning electron microscopy (SEM) with EDS and EBSD revealed that all samples exhibited the austenite/martensite phases with the fine-grained γ particles. The morphology of the γ phase changed from equiaxed to needle-like shape between samples with x = 0.5 and x = 1. The temperature range of martensitic transformation, which is driven by the temperature and magnetic field, significantly decreased with an increase in Fe and Cr at.%. The microhardness slightly increased (about 17 %) in the alloy doped with 1.5% at. Fe and Cr in comparison to the quaternary alloy.

Acknowledgment: Conference participation was supported by the GreenMat project, co-funded by the European Union under the program "European Funds for Silesia 2021–2027".

[1] J. Liu, T. Gottschall, K.P. Skokov, J.D. Moore, O. Gutfleisch, Giant magnetocaloric effect driven by structural transitions, Nat. Mater. 11 (2012) 1–7.

Design and fabrication of biocompatible metal-metal composite with β titanium alloy as reinforcing fraction

W. Michalik^{1a}, I. Matuła¹, A. Barylski¹, I. Laszko1 and G. Dercz^{1b}

^a wmichalik3@us.edu.pl, ^b grzegorz.dercz@us.edu.pl

¹ University of Silesia in Katowice, Institute of Materials Engineering, 75 Pułku Piechoty Street 1A, 41-500 Chorzów, Poland

Keywords: composites, biomaterials, Ti-Mo

The continuous development and aging population are driving the ongoing increase in interest in engineering materials that can be successfully applied in medicine. This growing demand highlights the need for multifunctional solutions, which makes composite materials particularly attractive, as their properties can be tailored through the selection and combination of constituent phases [1]. Metal matrix composites (MMC) based on titanium exhibit huge potential in medicine, especially due to their unique properties including high biocompatibility, relatively low Young's modulus, paramagnetic properties and corrosion resistance [2].

This study focuses on evaluating the effect of biocompatible molybdenum on the properties of titanium matrix composites. The six compositions of MMC composites were developed from initial powders of Ti and Ti16Mo. Powder and sintered samples were subjected to imaging using optical microscopy (OM), scanning electron microscopy (SEM) and phase analysis by X-ray diffraction (XRD) analysis. Preliminary mechanical properties were evaluated.

Composite materials were successfully fabricated using powder metallurgy. Phase analysis confirmed the coexistence of α - and β -Ti, with increasing molybdenum content promoting β -Ti formation and transition zones enriched in this phase. The addition of TiMo altered grain morphology and led to lamellar structures at α/β interfaces, characteristic of diffusion processes. Mechanical testing demonstrated that the titanium matrix exhibited the highest average values of Vickers hardness, instrumental hardness, and elastic modulus.

Acknowledgment: This work was supported by the Polish National Science Centre, Poland (Polish: Narodowe Centrum Nauki, abbr. NCN) under the research project OPUS-27 no. UMO-2024/53/B/ST11/00431

- [1] Dobrzański L. A., Warszawa, 2002, s. 28,46.
- [2] Karakurt E. M., Cetin Y., Incesu A., Demirtas H., Kaya M., Yildizhan Y., Tosun M., Huang Y. Materials 2023, 16, 4240. DOI: https://doi.org/10.3390/ma16124240

The effect of withdrawal rate on crystal structure perfection and microstructure of single crystal castings made from high Ni content alloy

J. Nawrocki^{1a}, K. Gancarczyk¹, A. Gradzik¹ and B. Kościelniak¹

a jaceknaw@prz.edu.pl

¹ Department of Materials Science, Faculty of Mechanical Engineering and Aeronautics, Rzeszow University of Technology, Powstancow Warszawy 12, 35-959, Rzeszów. Poland

Keywords: nickel base alloy; single crystal; crystal structure perfection

Castings of high-pressure turbine aircraft engines operate in particularly difficult conditions of dynamic impact of oxidizing gases at high temperature. Hence, the material from which they are made must be resistant to creep, high-temperature corrosion and thermal fatigue. Such a material is commonly used as nickel superalloys with a single-crystal structure [1]. Creep behaviour of a single crystal is determined by its structure perfection and microstructure [2]. The technological process based on the Bridgman-Stockbarger method is the most commonly used in industry for manufacturing nickel-based superalloy singlecrystal castings. [3]. Under industrial conditions crystallization process takes a value in the range from 1 to 5 mm/min [4]. There are several generations of nickel superalloys differing in their chemical composition [5]. In most of them, the base nickel content ranges from 66,3 wt.% (SRR99 alloy) to 70,5 wt.% (SC16 alloy). The higher nickel content, the fewer alloying additions and thus the specific density of the material is lower, which is desirable due to lower engine operating costs. The paper attempts to characterize single-crystal castings made of an alloy with a higher nickel content – 73,1 wt.%. Three SX casting processes were conducted at withdrawal rates of 2, 3 and 4 mm/min. Casting were examined by primary dendrite arm spacing (PDAS) measurement, microporosity measurement and evaluated crystal perfection. PDAS was measured using a Nikon EPIPHOT 300 metallographic microscope equipped with a digital camera and NIS-Elements-AR image analysis software. Porosity was determined from unetched metallographic microsections. Micrographs of pores were captured using a Leica DMI3000M light microscope at 50x magnification. Ten images per each casting from different areas of the sample surface (1.4 mm²) were analysed. The relative volume of pores, chord of pore and anisotropy factor were calculated using Leica Application Suite v3.7 software. Crystal structure perfection was evaluated by measuring the changes in three angles: the primary orientation angle (αz), which represents the angle between the [001] crystallographic direction and the blade axis "z"; the rotation angle (βz), which describes the rotation of the [001] direction around the casting direction and the third orientation angle (γz), which measures the deviation of the [010] direction from the reference axis. The crystal orientation measurements were taken using the Ω -scan method and an OD-EFG1 X-ray diffractometer [23]. A copper lamp was used (CuK α = 0,154nm), a round collimator with a diameter of 0.8 mm. The voltage applied to the lamp was 40kV, the current 30mA. Crystallographic orientation was confirmed by another technique EBSD.

It was found that the increasing of withdrawal rates above 3 mm/min to cause lower values of angle αz and γz . Lattice parameter is similar for all castings. It was determined that microporosity is characterized by one-sided statistical distribution. Lowest value of relative volume of pores is observed for withdrawal rates 4 mm/min. Mean chord and anisotropy factor is similar for all castings.

Acknowledgement: This work is a part of the Project: 101103504-EDF-2021-ENERENV-D-2. The program is funded by the European Union. Views and opinions expressed are however those of the author(s) only and do not necessarily reflect those of the European Union. Neither the European Union nor the granting authority can be held responsible for them.

- [1] Reed, R.C. The Superalloys, Fundamentals and Applications, (Cambridge University Press: Cambridge, UK) (2006).
- [2] Szeliga, D., Gancarczyk, K., Ziaja, W. The Control of Solidification of Ni-Based Superalloy Single-Crystal Blade by Mould Design Modification using Inner Radiation Baffle. Adv. Eng. Mater. 20 (2018), 1700973.
- [3] Dai, H.J.; Dong, H.B.; D'Souza, N.; Gebelin, J.-C.; Reed, R.C.; Dong, H. Grain Selection in Spiral Selectors During Investment Casting of Single-Crystal Components: Part II. Numerical Modeling. Met. Mater. Trans. A 42 (2011), 3439– 3446.
- [4] J. Jaroszewicz, H. Matysiak, J. Michalski, K. Matuszewski, K. Kubiak, K. J. Kurzydłowski, Characterization of single-crystal dendrite structure and porosity in nickel-based superalloys using x-ray micro-computed tomography, Advanced Materials Research, 278 (2011) 66-71.
- [5] J.R.Davis, ASM Speciality Handbook. Nickel Cobalt and their Alloys. (ASM International: Material Park, OH, USA) (2000).

Polyvinylpyrrolidone with diverse topologies as effective polymer matrices for tuning desired properties of liquid crystalline drugs

L. Orszulak^{1a}, R. Bernat², T. Lamrani³, K. Jurkiewicz³, M. Tarnacka³, D. Żakowiecki⁴, E. Kamińska⁵, K. Kamiński³

a luiza.orszulak@us.edu.pl

Keywords: itraconazole, polyvinylpyrrolidone, binary mixtures

Active pharmaceutical ingredients (APIs) with liquid-crystalline structures represent a particularly intriguing class of compounds due to their dual character, exhibiting features of both liquids and solids. Unfortunately, most of them belong to the class of compounds that are poorly soluble in water. Consequently, researchers continuously seek methods for effectively modulating their molecular order, thereby enabling the fine-tuning of physicochemical properties as required. One of the approaches to improving the performance of active substances is the formation of amorphous mixtures with various excipients. In this context, polymeric materials are frequently employed, among which polyvinylpyrrolidone (PVP) — a non-toxic and biocompatible polymer widely used in the pharmaceutical industry — plays a particularly important role. However, current studies address only the influence of the molecular weight (M_n) of commercially available PVP on drug bioavailability, while crucial aspects such as dispersity (D), topology, and polymer microstructure remain almost entirely overlooked in the literature.

To address this compelling research gap, the present study aimed to investigate the influence of PVP architecture on the molecular order of a model active substance – itraconazole (ITZ) – and its solubility. Synthetic routes were developed to obtain PVP homopolymers with distinct topologies and precisely controlled macromolecular parameters (M_n , D). Subsequently, the innovative linear (linPVP) and star-shaped (starPVP) polymers were employed to prepare

¹ Institute of Chemistry, Faculty of Science and Technology, University of Silesia in Katowice, Poland

² Institute of Materials Engineering, Faculty of Science and Technology, University of Silesia in Katowice, Poland

³ Institute of Physics, Faculty of Science and Technology, University of Silesia in Katowice, Poland

⁴ Chemische Fabrik Budenheim KG, Germany

⁵ Department of Pharmacognosy and Phytochemistry, Faculty of Pharmaceutical Sciences in Sosnowiec, Medical University of Silesia in Katowice, Poland

binary mixtures with ITZ, which were further characterized using various techniques, including differential scanning calorimetry, X-ray diffraction, and broadband dielectric spectroscopy. Interestingly, even at the stage of mixture preparation, a remarkable trend was observed: *star*PVP exhibited superior miscibility with the API compared to *lin*PVP. Calorimetric studies revealed that even a small fraction of the polymer matrix effectively suppressed the liquid-crystalline order of ITZ. Notably, only *star*PVP macromolecules demonstrated the ability to completely disrupt mesophases and produce a fully amorphous material. Structural and dielectric analyses confirmed the thermal findings, while long-term diffraction studies verified the highest stability of the ITZ–*star*PVP system and the absence of any tendency to rebuild the liquid-crystalline structure. Furthermore, solubility experiments demonstrated a significant enhancement in API solubility across all binary systems compared to the pure drug, with the most pronounced effect observed for ITZ–*star*PVP mixtures.

Overall, this study highlights that by carefully selecting an appropriate polymeric matrix and its concentration, it is possible to readily modulate the molecular order of liquid-crystalline drugs and thereby fine-tune their properties according to the rapeutic requirements.

Acknowledgements: The research was financed by the Ministry of Education and Science within the "Pearls of Science" Grant (No. PN/01/0078/2022).

The influence of the thermomechanical processing on the microstructure and grain boundary character distribution of Zn0.1Cu alloy

D. Orzeł^{1a}, J. Kawałko¹, P. Bała^{1,2}

a danorzel@agh.edu.pl

Keywords: zinc alloys, microstructure, grain boundaries

Zinc is considered as a promising bioresorbable material for medical applications, such as cardiovascular stents, bone implants, etc. However, the implementation of this metal faced problems with its poor mechanical properties and its tendency to creep under constat load. Current research focuses on the preparation of specific zinc alloys, followed by their plastic deformation under selected thermomechanical procedures. Most investigations are concentrated mainly on the macro-scale mechanical and corrosive properties [1].

The presented study aims to modify the microstructure through thermomechanical processing and to analyse the obtained grain boundaries. Observations conducted using electron microscopy and the EBSD mapping technique allow for identifying relationships between processing procedures and the microstructure, texture, and grain boundary character distributions. The research evaluated the state of the microstructure, its homogeneity, and texture after channel die compression at various temperatures in Zn0.1Cu (%at.) alloy, what provided information about the behaviour of low-alloyed zinc during compression at specific temperature. With increasing compressing temperature, an increase in average grain size, the disappearance of bimodal grain size distribution, and the development of a sharp (0001) fiber texture were observed. Moreover, the application of an additional secondary compressing at cryogenic temperature led to the significantly increased fraction of twin boundaries. The data obtained confirm the possibility of controlling the resulting microstructure and generating grain boundaries of a specific type in low-alloyed zinc by selecting the temperature of the deformation process.

Acknowledgements: This work was supported by the Polish National Science Centre under grant number: UMO-2021/43/D/ST8/03183.

¹ Academic Centre for Materials and Nanotechnology, AGH University of Krakow, Al. A. Mickiewicza 30, 30-059, Krakow, Poland

² Faculty of Metals Engineering and Industrial Computer Science, AGH University of Krakow, Al. A. Mickiewicza 30, 30-059, Krakow, Poland

[1]] H. Kabir *et al.*, 'Recent research and progress of biodegradable zinc alloys and composites for biomedical applications: Biomechanical and biocorrosion perspectives', Bioactive Materials, vol. 6, no. 3, pp. 836–879, Mar. 2021, doi: 10.1016/j.bioactmat.2020.09.013

Crystal structure of a new hybrid compound based on an iodido-plumbate(II) anionic motif

M. Oualid

walid.mokhnache@gmail.com

University of Tunis El Manar

Keywords: Crystal structure; Organic-inorganic hybrid; Iodoplumbate (II); Hexamethylenetetramine; Hybrid compound; Vibrational studies; Photoluminescence; Optical properties.

A new organic—inorganic hybrid material of formula 2[(CH₃)C₆N₄H₁₂]⁺[Pb₂I₆]²-compound was obtained by slow evaporation at room temperature of a solution containing lead iodide and (NH₃)C₆N₄H₁₂ in a 1:2 molar ratio. Single crystal diffraction was carried out at 298 K and 100 K. The same P2₁/m monoclinic space group has been found for both temperatures. No structural difference has been noted apart from a typical increase of the cell parameters with temperature. The supramolecular structure cohesion is ensured by weak hydrogen bonding C–H···I interactions. The photoluminescence investigations reveal two distinct emission bands. The room-temperature infrared and Raman spectra are recorded. The theoretical infrared spectrum, crystal morphology and molecular orbital transition are calculated and discussed.

Influence of plastic deformation method on the microstructure and mechanical properties of Duplex stainless steel

R. Paszkowski^a, I. Matuła, K. Kowalczyk-Skoczylas and K. Aniołek

a robert.paszkowski@us.edu.pl

¹ University of Silesia in Katowice, Institute of Materials Engineering, 75 Pułku Piechoty Str., 1 A, 41-500 Chorzów, Poland

Keywords: duplex stainless steel, plastic deformation, microstructural characterization

Duplex stainless steels are commonly used in the chemical and petrochemical sectors due to their excellent strength, corrosion resistance, and advantageous mechanical properties. This research explored the structural and mechanical properties of duplex stainless steel 1.4462 for two types of rod-like specimens undergoing various plastic deformation methods: hot rolling and cold drawing.

The tested material was thoroughly analysed by X-ray diffraction, optical and scanning electron microscopy. Additionally, Vickers microhardness tests were performed.

XRD analysis showed significant changes in the locations of the primary diffraction peaks for the cold-drawn samples in relation to the hot-rolled samples. This suggests a distortion of the unit cell caused by plastic deformation and the accumulation of residual stress during cold working. Optical microscopy revealed a typical banded microstructure typical of duplex steels, featuring alternating regions of austenite and ferrite. SEM investigations supported these observations and were complemented by EDS point and line analyses, confirming a homogeneous distribution of key alloying elements (Fe, Cr, Ni, Mo) with no significant segregation.

Hardness tests revealed a significant gradient from the surface to the core of the rods. In hot-rolled specimens, Vickers hardness varied from 320 HV at the periphery to 265 HV at the centre. In comparison, the cold-drawn rods showed greater hardness measurements, ranging from 370 HV at the edge to 340 HV at the centre.

In conclusion, the plastic deformation method significantly affects the microstructure and mechanical behaviour of duplex steel 1.4462, with cold drawing causing greater lattice distortion and hardness than hot rolling. These insights may aid optimization of processing methods for duplex steels in demanding applications.

Acknowledgment: Conference participation was supported by the GreenMat project, co-funded by the European Union under the program "European Funds for Silesia 2021–2027

Structural investigation of Mg₆Pd_{1-x}Pt_x alloys for hydrogen storage applications

M. Pęska^{1a}, A. Dębski², S. Terlicka², W. Gierlotka³, A. Sypień², W. Gasior², M. Polański¹

a magda.peska@wat.edu.pl

Keywords: hydrogen storage, magnesium based alloys

This study presents results on the synthesis and structural characterization of $Mg_6Pd_{1-x}Pt_x$ -type intermetallic compounds prepared by mechanical synthesis. This study aims to investigate whether palladium in Mg-based hydrogen storage alloys can be partially or fully replaced by platinum, and how such substitution affects their structure and ability to absorb hydrogen.

Alloys with varying Pt content (x = 0.25, 0.5, 0.75, 1.0) were synthesized and investigated using X-ray diffraction (XRD) methods both before and after hydrogenation. The discussion focuses on the changes of crystallographic phases during hydrogen absorption and the significance of replacing Pd atoms with Pt atoms. The hydrogen absorption capacity was tested using a Sieverts apparatus, while the amount of desorbed hydrogen and the hydride decomposition temperature were assessed using DSC-TGA analysis.

¹ Military University of Technology, Warsaw, Poland

² Institute of Metallurgy and Materials Science, Polish Academy of Sciences, Cracov, Poland

³ National Dong Hwa University, Department of Materials Science and Engineering Department, Hualien, Taiwan

Characterization of refractory concrete with high silicon carbide (SiC) content

K. Rogalewska^{1a}, K. Dudek¹, A. Gerle¹, R. Kusiorowski¹, J. Podwórny¹, A. Śliwa¹

^a karolina.rogalewska@icimb.lukasiewicz.gov.pl

¹ Lukasiewicz Research Network – Institute of Ceramics and Building Materials, Center of Refractory Materials, Poland

Keywords: refractory concrete, phase composition, silicon carbide (SiC)

Concretes are composed of cement and aggregates, which provide the required mechanical strength and essential service properties. In refractory concretes, the aggregates are typically high-temperature resistant materials such as corundum, silicon carbide, grogs, and ceramic scrap. The addition of SiC significantly improves the stability of cementitious mixtures under extreme thermal conditions. Compared with conventional oxide ceramics, SiC based castables exhibit high strength, excellent thermal shock resistance, good abrasion resistance, and enhanced stability against oxidation and other forms of corrosion [1].

SiC structure can be described as a sequence of repeating bilayers of silicon and carbon atoms. Each bilayer consists of a two-dimensional, hexagonal close-packed arrangement of carbon atoms with silicon atoms positioned above them. Differences in the stacking order of these bilayers lead to polytypism. Common crystallographic polytypes include 2H-SiC, 4H-SiC, and 6H-SiC, while less common ones are 15R-SiC and 21R-SiC. Each carbon atom is surrounded by four silicon atoms, and vice versa, forming a tetrahedral coordination. Strong covalent Si–C bonds, with an energy of about 4.6 eV, are responsible for the material's exceptional hardness and refractoriness. [2].

This paper presents the results of investigations on low-cement concrete BN SC 80 containing 80% silicon carbide. The sample was fired at 1350 °C in an air atmosphere, with a 5-hour hold at the nominal temperature, followed by furnace cooling. Phase composition was analysed by X-ray diffraction (XRD) using copper lamp. The microstructure was examined using scanning electron microscopy (SEM) coupled with Energy-dispersive X-ray spectroscopy (EDS). Additionally, chemical composition was determined by X-ray fluorescence (XRF) analysis, and thermal properties were studied using differential thermal analysis (DTA) and thermogravimetric analysis (TG). Basic physical and

mechanical properties, such as porosity, bulk density, and gas permeability, were also measured.

XRD analysis revealed the presence of the main cementitious phases as well as silica phases, including cristobalite and feldspars. Mullite (3Al₂O₃·2SiO₂) was also identified. Trace amounts of gehlenite and grossite were detected. Silicon carbide was primarily present in the form of hexagonal polytypes 4H and 6H. Chemical analysis confirmed the composition declared by the producers. Physical and mechanical tests showed different than expected values for porosity but low gas permeability. Thermal analyses (DTA/TG) did not reveal significant phase transformations or weight changes within the tested temperature range.

- [1] Montgomery R., Heat-resisting and refractory concretes, Advanced Concrete Technology, Elsevier, t. 4, Oxford, 2003, s. 1–13.
- [2] Ruys A. J., Silicon Carbide Ceramics: Structure, Properties and Manufacturing, w: Advanced Ceramic Materials, Elsevier, Amsterdam, 2023.

The influence of thermal history on the phase composition and mechanical properties of parts additively manufactured by Wire Arc Additive Manufacturing

<u>I. Mierzejewska^{1, 2a}, N. Rońda^{1b}</u>, D. Siemiaszko¹, D. Klobčar³, D. Bračun³, M. Polański¹

^aizabela.mierzejewska@student.wat.edu.pl, ^b natalia.ronda@wat.edu.pl

Keywords: additive manufacturing, thermal history, phase composition

Additive manufacturing enables the production of complex components in a layer-by-layer manner with high material efficiency. One prominent technique, Wire Arc Additive Manufacturing (WAAM), employs an electric arc to melt metal wire, allowing the rapid fabrication of large-scale components [1]. However, the repeated thermal cycling inherent to the WAAM process, caused by the deposition of successive layers, strongly influences the microstructure and mechanical behavior of the final material [2, 3].

This study investigates the challenges associated with monitoring thermal history during WAAM and its influence on the phase composition and mechanical properties of two alloys: 18Ni-300 maraging steel and AlMg5 aluminum alloy. Thermal history was recorded in situ using an infrared (IR) camera. Phase composition was examined using high-resolution synchrotron radiation XRD and Electron Backscatter Diffraction (EBSD), with the former enabling detailed phase analysis of bulk material as a function of distance from the substrate. Mechanical properties were assessed via tensile testing and microhardness measurements.

The results revealed that the 18Ni-300 maraging steel exhibited a variable amount of reverted austenite along the build height, attributed to the effects of thermal cycling and interactions with the substrate. In contrast, the AlMg5 alloy demonstrated a uniform phase composition throughout the structure. Microhardness measurements for the maraging steel ranged from 350 to 450 HV, indicating sensitivity to thermal gradients, whereas the AlMg5 alloy showed a consistent microhardness of approximately 80 HV, independent of

¹ Military University of Technology, Institute of Materials Science and Engineering, Warsaw, Poland

² Institute of Fundamental Technological Research Polish Academy of Sciences, Warsaw, Poland

³ University of Ljubljana, Faculty of Mechanical Engineering, Ljubljana, Slovenia

build height. Tensile tests confirmed mechanical anisotropy in the maraging steel, with both strength and ductility dependent on the testing direction.

- [1] Y. Zhang et al., Journal of Materials Engineering and Performance 27(2017), p. 1-13.
- [2] H. Chae et al., Journal of Alloys and Compounds 857 (2021), p. 157555.
- [3] X. Wang and K. Chou, Additive Manufacturing 18 (2017), p. 1-14.

Analysis of martensite tetragonality in medium-carbon steels using EBSD mapping

P. Salwa^{1a}, G. Cios¹, Aimo Winkelmann¹, Piotr Bała¹

a salwap@agh.edu.pl

¹ Academic Centre for Materials and Nanotechnology, AGH University of Kraków, al. A. Mickiewicza 30, 30-059 Krakow, Poland

Keywords: tetragonality, martensitic steel, EBSD

Demand for the development of steels of high strength requires intrinsic knowledge on the microstructure and chemical composition and their changes throughout alloys during fabrication or additional treatment of the alloy. One of the more discussed phenomena occurring in steels with C>0.7 wt.% that undergo additional heat treatment is martensite tertagonality -c/a, which in high carbon steels is linearly dependent on the carbon content [1]. However in steels with lower carbon content results are varying and highly reliant on quality of acquired XRD diffraction pattern and following Rietveld analysis method of bulk material. Additionally this most common method of analysing crystal structure does not accommodate for spatial and/or local variation in tetragonality [2].

One of the possible analysis techniques is Electron BackScatter Diffraction method (EBSD), which enables to resolve variable local variation of the lattice parameters with spatial resolution in tens of nanometres scale. Thus using EBSD mapping techniques, changes in martensite tetragonality can be observed in singular grains [3].

In present study samples of commercially available, medium-carbon steels (C content of 0.3 to 0.6 wt.%) undergone quenching at temperatures in their respective dual-phase (ferrite α , and austenite γ) ranges and then quenched in water. After sample preparation changes in martensite tetragonality were analysed using EBSD and Transmission Kikuchi Diffraction mapping techniques. Obtained data confirms not only different c/a tetragonality ratios throughout samples volume but also in individual martensite grains.

- [1] T Tanaka, N Maruyama, N Nakamura, A. J. Wilkinson, Tetragonality of Fe-C martensite a pattern matching electron backscatter diffraction analysis compared to X-ray diffraction, Acta Materialia, vol 195 (2020), p. 728-738
- [2] S. Uehara, S. Kajiwara, T. Kikuchi, Origin of Abnormally Large Tetragonality of Martensite in High Carbon Iron Alloys Containing Aluminum, Materials Transactions, JIM, vol 33 (1992), p. 220-228

[3] G. Nolze, A. Winkelmann, G. Cios, T. Tokarski, Tetragonality mapping of martensite in a high-carbon steel by EBSD, Materials Characterization, vol 175 (2021), 111040

Texture of FeAl sintered samples prepared using the pressure-assisted induction sintering (PAIS) method

D. Siemiaszko^{1a}, E. Wesołowska¹

^a dariusz.siemiaszko@wat.edu.pl

¹ Faculty of Advanced Technologies and Chemistry, Military University of Technology, Kaliskiego 2, 00-908 Warsaw, Poland

Keywords: intermetallic, sintering, texture.

Fe-Al alloys based on the intermetallic phases Fe₃Al and FeAl are among the most extensively studied materials in recent years. This interest arises from their unique functional properties, such as excellent resistance to oxidation, carburization, and sulfidation, high wear resistance, and relatively low cost compared to corrosion-resistant steels. Unfortunately, these alloys also have significant drawbacks that limit their use as structural materials. The most critical issues are their low ductility and susceptibility to brittle fracture at room temperature, primarily due to the presence of long-range order.

The considerable difference in melting points between iron and aluminum, along with their mutual reactivity and high oxygen affinity, poses challenges during conventional manufacturing methods such as melting and casting. This typically results in coarse-grained structures, which further reduce ductility. Powder metallurgy offers a solution to this problem. However, due to the occurrence of SHS (Self-propagating High-temperature Synthesis) reactions in the Fe-Al system, advanced sintering techniques such as PAIS (Pressure-Assisted Induction Sintering) are required. In this method, compressive stress is applied during sintering to prevent porosity formation during the SHS reaction. The presence of compressive stresses may lead to texture formation in the final component, and texture is directly related to the degree of long-range ordering, which in turn affects the mechanical properties.

This study presents the results of research conducted on Fe40Al compacts obtained by PAIS induction sintering. The sintered samples were soaked at 1080°C for periods ranging from 5 to 100 hours. X-ray diffraction analyses were then performed in two variants: with sample rotation (as a reference state) and without rotation (angle variation from -90° to +90° relative to the compression direction). Based on the obtained diffractograms, both the degree of long-range ordering and texture were determined.

Structural characterization of anodic oxide nanotube layers for potential biomedical applications

A. Stróż^{1a}, G. Dercz¹, B. Terlecki¹, D. Stróż¹

a agnieszka.stroz@us.edu.pl

¹ University of Silesia, Institute of Materials Engineering, Chorzów, Poland

Keywords: anodic oxide nanotubes, crystallographic analysis, biomedical applications

Due to its high biocompatibility, titanium is one of the most commonly used materials in implantology, capable of functioning in the body for up to 25 years [1]. The growing interest in titanium as a biomedical material requires the development of effective surface modification methods that reduce the risk of adverse biological reactions, such as inflammation [1,2].

In this study, anodic oxidation was used to produce titanium oxide (TiO₂) nanotubes on the surface of titanium, with particular emphasis on anodizing voltages of 15 and 20 V at a time of 30 minutes. The studies showed that nanotubes were clearly formed at these voltage values, and their diameter increased with increasing voltage. Anodization at 20 V in an electrolyte containing 0.8% HF resulted in nanotubes with the best quality and surface homogeneity.

Physicochemical characterization using SEM, EDS, and GIXD methods confirmed the self-organizing, nanotubular nature of the obtained oxide layers. The results indicate that controlled selection of anodizing parameters, especially voltage, is crucial for the production of functional TiO₂ nanostructures with potential biomedical applications.

Acknowledgment: Conference participation was supported by the GreenMat project, co-funded by the European Union under the program "European Funds for Silesia 2021–2027

- [1] A., Cipriano, C., Miller, Liu, H.. J. Biomed. Nanotechnol. 2014, 10, 2977–3003.
- [2] S. Sobieszczyk, Adv. Mater. Sci. 2009, 9, 25–41.

Synthesis and structure analysis of ZnMgEr P-type quasicrystal

R. Strzałka^{1a}, I. Bugański¹, J. Wolny¹, J. Kusz², and N. Fujita³

a strzalka@fis.agh.edu.pl

Keywords: aperiodic crystal, icosahedral quasicrystal, synthesis, structure analysis

In this presentation we report a synthesis and structure refinement of the new samples ZnMgEr in P-type Bergman type icosahedral quasicrystal family. The synthesis was performed using a self-flux method obtaining single crystal grains of millimeter-size. Selected samples were measured by the single crystal X-ray diffraction resulting in approx. 2500 peaks (|F| < u(|F|)). The final structure model was refined against the diffraction data with lowest R-factor of 14%. The number of parameters was less than 350. Compared to previously studied structure of Zn₇₀Mg₂₀Tm₁₀ [1] the structure model was significantly constrained (with much lower number of free parameters) due to low quality of diffraction data. The future work will be focused on improving the quality of the measurement result and finer structure model allowing for detailed analysis of the influence on the potential physical properties, like magnetism.

Acknowledgements: The work was supported by the Polish National Science Centre under grant no. 2022/47/I/ST3/00340.

[1] Bugański, J. Wolny and H. Takakura, Acta Cryst. A 76 (2020) 180-196.

¹ AGH University of Krakow, Faculty of Physics and Applied Computer Science, Krakow, Poland

² University of Silesia, Faculty of Science and Technology, Katowice, Poland

³ Tohoku University, Institute of Multidisciplinary Research for Advanced Materials, Sendai, Japan

Doping influence on structural ferroelectric phase transitions and electrical features of barium calcium titanate

A. Z. Szeremeta¹, J. Macutkevic², M. Zubko^{3,4}, S. Miga³, Š. Svirskas², I. Gruszka¹, J. Koperski¹, J. Banys², A. Molak¹

¹August Chełkowski Institute of Physics, University of Silesia in Katowice, ul. 75 Pułku Piechoty 1, 41-500 Chorzów, Poland.

²Institute of Applied Electrodynamics and Telecommunications, Faculty of Physics, Vilnius University, Saulėtekio av. 3, LT-10257 Vilnius, Lithuania.

³Institute of Materials Engineering, University of Silesia in Katowice, ul. 75 Pułku Piechoty I, 41-500 Chorzów, Poland.

⁴Department of Physics, Faculty of Science, University of Hradec Králové, Hradec Králové, Czech Republic.

The BaTiO₃ is a classic ferroelectric perovskite-type material investigated in literature for over 75 years. This compound has many applications because of its dielectric, ferroelectric, and piezoelectric features [1].

Our work focuses on ferroelectric features of (Ba_{0.83}Ca_{0.17})TiO₃ (BCT) and shows the differences in electrical properties of these ceramics sintered by the solid-state reaction method. The BCT ceramics exhibits a high magnitude of permittivity and increased sensitivity of ferroelectric-paraelectric phase transition on applied hydrostatic pressure, which is essential from an application point of view [2]. Moreover, we show the characterization of the structure and chemistry of a sintered BCT and ceramics doped with the same amount of Sr, Mn, Cr, and Mg ions using several techniques: X-ray diffraction, scanning electron microscopy, and electrical impedance measured over a wide temperature and frequency ranges. Based on the distribution of relaxation times estimated according to the Tikhonov regularization method, we show the occurrence of mixed order disorder and displacive components in the discontinuous phase transition. Local structural disorder corresponding with dipoles created by oxygen vacancies was confirmed. Introduced disorder enabled recognition of the relaxor features of dipolar-glass-like behavior in BCT doped by Mg ions ceramics [3].

Acknowledgment: Conference participation was supported by the GreenMat project, co-funded by the European Union under the program "European Funds for Silesia 2021–2027

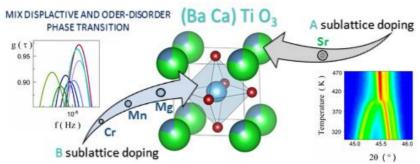


Figure 1. Schematic of a unit cell of doped BCT.

- [1] B. Jaffe, in Piezoelectric Ceramics, Academic Press, India, 1971.
- [2] A. Molak, A. Winiarski, A. Z. Szeremeta, D. K. Mahato, J. Macutkeviĉ, I. Gruszka,
- [3] S. Miga, J. Koperski, E. Palaimiene, S. Pawlus, Journal of Alloys and Compounds 856, 2021.
- [4] A. Z. Szeremeta, J. Macutkevič, M. Zubko, S. Miga, Š. Svirskas, I. Gruszka, J. Koperski, J. Banys, A. Molak, Journal of the European Ceramic Society 43, 2023.

Bioactive composite coatings of natural polymers with ZnO and Ag particles on titanium alloys obtained by electrophoretic deposition

M. Szklarska^{1a}, K. Waloch¹, G. Dercz¹, S. Golba¹, M. Zubko¹

a magdalena.sklarska@us.edu.pl

¹ Institute of Materials Engineering, Faculty of Science and Technology, University of Silesia in Katowice. Poland

Keywords: EPD, Ti15Mo, biomaterial

Surface modification of titanium alloys is essential for improving implant integration and reducing the risk of infection. Natural polymer-based coatings enriched with bioactive particles are promising candidates, as they combine biocompatibility with additional functional properties. In this study, electrophoretic deposition (EPD) was employed to obtain composite coatings on Ti15Mo alloy using chitosan and hyaluronic acid as polymer matrices. ZnO nanoparticles were introduced to enhance bioactivity and osteoblast adhesion, while Ag particles were incorporated for their strong antibacterial effect.

Composite coatings were deposited from colloidal suspensions containing chitosan or sodium hyaluronate with different particle concentrations. The influence of deposition voltage and time on coating formation was investigated. Structural and morphological characterization was carried out using XRD, SEM/EDS, and FTIR.

Both ZnO and Ag particles were successfully embedded into polymer matrices, forming continuous and adherent coatings. Increasing deposition parameters improved coating thickness, but excessive nanoparticle content caused cracking and reduced adhesion. ZnO addition accelerated the EPD process and promoted uniform distribution within the chitosan matrix. Ag incorporation provided homogeneous coatings with significant antibacterial potential.

Electrophoretic deposition is an effective method for producing multifunctional composite coatings on Ti15Mo alloy. ZnO-based coatings enhance bioactivity and deposition efficiency, while Ag-containing layers introduce antibacterial properties. These findings highlight the potential of natural polymer–nanoparticle systems as surface modifications for titanium implants.

Acknowledgment: Conference participation was supported by the GreenMat project, co-funded by the European Union under the program "European Funds for Silesia 2021–2027

Mechanism of plastic deformation in new designed TWIP High Manganese Steels

B. Terlecki^{1a}, Z. Gronostajski^{2,6}, M. Kostka³, M. Tkocz³, S. Bożek¹ K. Kowalczyk⁵ R. Chulist⁴, K. Jasiak² A. Królicka^{2,6} and M.B. Jabłońska^{1b}

bartosz.terlecki@imn.lukasiewicz.gov.pl
magdalena.jablonska@imn.lukasiewicz.gov.pl

Keywords: high-manganese TWIP steel, dynamic deformation, twinning

Twinning-induced plasticity (TWIP) steels are high-manganese alloys that exhibit a combination of high strength and exceptional ductility, a phenomenon attributed to the concurrent action of deformation twinning and dislocation slip [1, 3]. In new designed steel Fe–21Mn–2.5Al–0.4C (wt.%), the addition of aluminium-elevated stacking-fault energy in the crystal lattice (γ -fcc) has been shown to promote the formation of deformation twins and suppress the $\gamma \to \epsilon$ phase trans formation-induced martensite [2, 5]. The present study investigates the correlation between twinning vs. dislocation glide, strain rate, and the actual temperature rise resulting from plastic work during tensile deformation

Quasi-static tests ($\varepsilon \approx 10^{-3} - 10^{-1} \, s^{-1}$) and high-strain rate tests (up to 750 s⁻¹) were performed. Digital Image Correlation was used to capture strain localisation, and fast IR thermography was employed to track temperature evolution. At elevated rates, the process approaches adiabatic conditions, and neck temperatures of approximately 250°C were observed at fracture, consistent with prior determinations for this alloy class [6, 7]. The mechanism of plastic deformation is that increasing the strain rate initially raises the yield stress (positive rate sensitivity).

However, progressive adiabatic heating leads to a reduction in work-hardening at larger strains for slow strains rate (thermal softening). From the other side

Lukasiewicz Research Network – Institute of Non-Ferrous Metals, Gliwice, Poland

² Wrocław University of Science and Technology, Mechanical Engineering Faculty, Wrocław, Poland

³ Silesian University of Technology, Katowice, Poland

⁴ AGH University of Krakow, Faculty of Metals Engineering and Industrial Computer Science, Kraków, Poland

⁵ University of Silesia, Faculty of Science and Technology, Katowice, Poland

⁶ Centre of Materials Science and Metal Forming, Wrocław University of Science and Technology, Wrocław, Poland

quasi adiabatic heating can be observe during deformation with high strain rates in specimens microareas.

In terms of microstructure, low deformation rate detected by EBSD technics, produces a high number of primary and secondary twins. By contrast, at high strain rates, twins become finer and less numerous, and shear bands appear at approximately 45° to the tensile axis. This is indicative of an increased contribution of dislocation glide deformation mechanism [4, 9, 10]. EBSD/IPF-texture analysis supports a shift from twin-related (115)/(100) components towards a stronger (111) fibre associated with slip as the rate (and temperature) rises, with only a modest drop in twin volume fraction at the highest rate examined.

In summary, strain-rate strengthening coexists with thermally softening; the coupled action of rate and deformation temperature governs the twinning/slip balance in Fe–21Mn–2.5Al–0.4C. This phenomenon play a crucial role in the designing of crash-relevant components where impact-rate performance is critical [3,8].

Work carried out within the framework of the project UMO-2019/35/B/ST8/02184 "Effect of the heat generated during deformation at high strain rates on the structure and properties of high manganese steels with twinning as the dominant deformation mechanism" and UMO-2023/51/B/ST11/01607 "The influence of complex strain path on the microstructure, deformation mechanisms and mechanical properties of TWIP steel" financed by the NCN.

- S. Allain, J.P. Chateau, O. Bouaziz, S. Migot, N. Guelton, Mater. Sci. Eng. A 387–389 (2004) 158–162.
- [2] S. Curtze, V.T. Kuokkala, Acta Mater. 58 (2010) 5129-5141.
- [3] B.C. De Cooman, Y. Estrin, S.K. Kim, Acta Mater. 142 (2018) 283–362.
- [4] X. Feng, X. Liu, S. Bai, Y. Tang, Y. Ye, J. Mater. Res. Technol. 26 (2023) 639–653.
- [5] S.W. Hwang, J.H. Ji, K.T. Park, Mater. Sci. Eng. A 528 (2011) 7267–7275.
- [6] M.B. Jabłońska, K. Jasiak, K. Kowalczyk, M. Skwarski, K. Rodak, Z. Gronostajski, Int. J. Mater. Form. 16 (2023).
- [7] K. Jasiak, Z. Gronostajski, M.B. Jabłońska, J. Mater. Res. Technol. 28 (2024) 856– 864.
- [8] L.E. Murr, M.A. Meyers, C.-S. Niou, Y.J. Chen, S. Pappu, C. Kennedy, Acta Mater. 45 (1997) 157–175.
- [9] K.M. Rahman, V.A. Vorontsov, D. Dye, Mater. Sci. Eng. A 589 (2014) 252–261.
- [10] Y.F. Shen, N. Jia, R.D.K. Misra, L. Zuo, Acta Mater. 103 (2016) 229-242.

Integrated experimental stereological quantification and critical methodological review of the γ' phase in single-crystal nickel-based superalloys

B. Terlecki^{1,2 a}, and K. Gancarczyk³

^a bartosz.terlecki@imn.lukasiewicz.gov.pl

Keywords: Superalloys, Stereology, Scanning Electron Microscopy

The intermetallic γ' compound, Ni₃ (Al, Ti, Ta), is the foremost source of precipitation hardening in singlecrystal nickelbase superalloys cast for turbineblade applications. The precipitate's morphology, volumetric share, and particle size—number statistics exert decisive control over mechanical response, most conspicuously creep deformation and thermomechanical fatigue life. This contribution delivers a critical synthesis of the influence exerted by γ' stereological descriptors on macroscopic performance, benchmarking the measurement practices prevalent in the contemporary literature against the canonical prescriptions of ASTM E562 and ISO 9042.

Procedural disparities are dissected, with particular attention to the integration of advanced characterisation platforms: fieldemission scanning electron microscopy, (scanning) transmission electron microscopy, sitespecific focusedionbeam milling, and atomprobe tomography.

A complementary experimental programme interrogates γ' topology in singlecrystal CMSX4 and CMSX6 as a function of withdrawal velocity during directional solidification (V_t = 1 and 3 [mm/min^{-t}]). Classical stereology, implemented via optical and scanning electron microscopy, quantifies precipitate statistics. Accelerated withdrawal induces systematic refinement of γ' precipitates and promotes enhanced γ/γ' interfacial coherence, trends that accord quantitatively with thermodynamic–kinetic phasefield simulations.

The suite of quantitative metrics—particle dimension and aspect ratio, volumetric fraction $(V_{\nu}),$ surfacespecific number density $(N_A),$ γ/γ' interfacial perimeter length $(P_L),$ and rafting index—corroborates the exceptional microstructural stability exhibited by CMSXtype alloys under the extreme thermalmechanical exigencies encountered in aeroengine service.

¹ Lukasiewicz Research Network – Institute of Non-Ferrous Metals

² University of Silesia in Katowice– Institute of Materials Engineering

³ Rzeszów University of Technology-the faculty of Mechanical Engineering and Aeronautics

- [1] J.Q. Wu, Z. Yu and H. Zhou, Nature 586 (2020), pp. 250254.
- [2] M. Giraud, C. Guedou and G. Cailletaud, Acta Materialia 60 (2012), pp. 58735884.
- [3] Szczotok, M. Seibert and M. Krupiński, Materials Characterization 60 (2009), pp. 12381244.
- [4] M. Dubiel and A. Czyrska Filemonowicz, Journal of Microscopy 237 (2010), pp. 145153.
- [5] M. Ali, K. Sultan and A. Khan, Materials Science and Engineering A 791 (2020), Art. 139316.
- [6] Y. Liu, L. Zhao and X. Li, Journal of Materials Science & Technology 140 (2023), pp. 7688.
- [7] Y. Zhang, H. Li and X. Jiang, Journal of Alloys, and Compounds 919 (2023), Art. 169711.
- [8] Ł. Rakoczy, D. Sitnicka and J. Świątnicki, Journal of Thermal Analysis and Calorimetry 141 (2020), pp. 34113423.
- [9] P. Panwisawas, R.C. Reed and A. Mottura, Acta Materialia 126 (2017), pp. 251263.
- [10] ASTM International, "ASTM E56219: Standard Test Method for Determining Volume Fraction by Systematic Manual Point Count", ASTM, West Conshohocken, PA, USA (2019).
- [11] International Organization for Standardization, "ISO 9042:2003 Metallic Materials Micrographic Determination of Apparent Grain Size", ISO, Geneva, Switzerland (2003).

Translational symmetry - a way to efficient EBSD diffraction pattern analysis

K. Wójciak^{1a}, T. Tokarski¹, G. Cios¹, A. Winkelmann¹ and G. Nolze^{2,3}

a kwojciak@agh.edu.pl

³ TU Bergakademie, Freiberg, Germany

Keywords: Electron Backscatter Diffraction, Kikuchi patterns, translation symmetry

Electron backscatter diffraction (EBSD) imaging is inherently complex due to the internal origin of the signal within the sample, resulting in intricate Kikuchi patterns composed of superimposed effects from multiple diffraction planes. Despite this complexity, each Kikuchi band can be interpreted as a projection of a specific lattice plane, characterized in three-dimensional space [1]. Modern EBSD systems are capable of detecting over 100 distinct Kikuchi bands within a single diffraction pattern. The spatial relationship between the Kikuchi band centers and the projection center (PC) allows for the precise reconstruction of the 3D orientation of corresponding crystallographic planes [2].

Each lattice plane can be described by a unit normal vector representing a direction in reciprocal space. The corresponding band width provides information about the lattice spacing, thereby determining the magnitude of the reciprocal vector. By extracting this information across multiple bands, a cloud of reciprocal space vectors can be generated, enabling reconstruction of the Bravais lattice [3]. In a naive approach, treating each band independently introduces $n \times 3$ parameters (two for orientation, one for magnitude) where n is the number of bands, resulting in significant computational complexity and necessitating advanced optimization techniques.

To address this challenge, we propose a novel approach that exploits the translational symmetry inherent to crystalline materials, reducing the degrees of freedom from hundreds to just nine, the number required to define the Bravais lattice [4]. This dramatically simplifies the computational demands and increases robustness. Our method named Crystallographic Analysis of Lattice Metric (CALM), contrasts with conventional commercial solutions, which often rely on Hough/Radon transforms or pattern matching algorithms, by leveraging a geometrically driven framework that interrelates reciprocal space vectors through symmetry constraints.

¹ AGH – University of Science and Technology, Academic Center for Materials and Nanotechnology, Krakow, Poland

² Federal Institute for Materials Research and Testing (BAM), Berlin, Germany

We present the theoretical foundation and algorithmic implementation of CALM method, followed by an analysis of its sensitivity to Kikuchi band detection accuracy and projection center optimization. Several case studies illustrate the practical advantages of the proposed technique and highlight pathways for further development in high-precision crystallographic orientation determination.

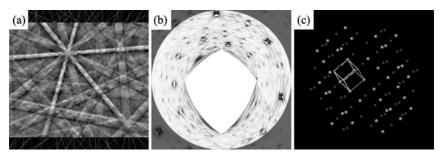


Fig.1. Key stapes of the CALM analysis: a) experimental pattern with marked traces of crystallographic planes b) Funk transformation c) reciprocal lattice with the unit cell for the experimental pattern

Acknowledgements: This work was supported by Polish Nation Science Centre grant no. 2020/37/B/ST5/ 03669

- [1] C. Maurice and R. Fortunier, J. Microsc. **230** (2008), p. 520-529.
- [2] Winkelmann, G. Nolze., G. Cios., et al., Materials, 13 (2020)
- [3] L. Li, M. Han (2015). J. Appl. Cryst. 48, p. 107–115.
- [4] G. Nolze, T. Tokarski, Ł. Rychłowski Ł, et al., J. Appl. Crystall., 54 (2021), p. 1012-1022

Magnetic properties of Fe-Nb-B-RE melt spun ribbons

A. Chrobak¹, <u>G. Ziółkowski^{1a}</u>, Ondrej Zivotsky², Piotr Pawlik³, Marcin Fijałkowski⁴, Joanna Klimontko⁴

a grzegorz.ziolkowski@us.edu.pl

Keywords: melt-spinning technique; magnetic properties of Fe-Nb-B-RE

The presented work refers to the magnetic anisotropy properties of Fe-Nb-B-RE (RE = Tb, Nd, Tb/Y) amorphous alloys. The samples (i.e. $(Fe_{80}Nb_6B_{14})_{1-x}RE_x$, 0.04 < x < 0.12) were prepared by a typical melt-spinning technique. The occurrence of the amorphous state was confirmed by XRD and thermomagnetic measurements. Some selected magnetic properties and domain structure were determined from hysteresis loops (measured at different temperatures) and Kerr effect (MOKE) observations.

The Fe-Nb-B family of amorphous alloys is widely known as an excellent soft magnetic material (e.g. the so-called NANOPERM type of alloys) with extremely low power losses and coercivity [1]. Despite the lack of crystal structure such alloys reveal ferromagnetic ordering of Fe magnetic moments. On the other hand, some rare earth elements can introduce magnetic anisotropy into many Fe-RE structurally ordered compounds as a consequence of strong spin-orbit coupling [2,3]. It is interesting to see whether the RE alloying additions can cause magnetic anisotropy in the case of amorphous Fe-based magnets and how they influence the magnetic structure as well as the interactions between magnetic atoms.

It was shown that the applied RE additions has an effect on magnetic properties such as coercivity, the Curie temperature and domain structure. Surprisingly, the small addition of localized magnetism, introduced by the RE elements, significantly changed the magnetic exchange interactions between the Fe atoms, which is widely discussed based on the numerical analysis utilizing the mean field theory (MFT) approach.

¹ Institute of Materials Engineering, University of Silesia in Katowice, 75 Pułku Piechoty 1A, 41-500 Chorzów, Poland

²Department of Physics, VŠB-Technical University of Ostrava, 17 listopadu 15/2172, 708 33 Ostra-va-Poruba, Czech

³Institute of Physics, Częstochowa University of Technology, Al. Armii Krajowej 19, 42-200 Częstochowa, Poland

⁴Institute of Physics, University of Silesia in Katowice, 75 Pułku Piechoty 1A, 41-500 Chorzów, Poland

Acknowledgment: Conference participation was supported by the GreenMat project, co-funded by the European Union under the program "European Funds for Silesia 2021–2027

- [1] Chrobak, G. Haneczok, D. Chrobak, Ł. Madej, G. Chełkowska, M. Kulpa, Studies of the relaxed amorphous phase in the Fe80Nb6B14 alloy. J. Magn. Magn. Mater. 2008, 320, 770-773.
- [2] Chrobak, G. Ziółkowski, K. Granek, D. Chrobak, Disorder-based cluster Monte Carlo algorithm and its application in simulations of magnetization processes. Comput. Phys. Commun. 2019, 238, 157–164.
- [3] Chrobak, G. Ziolkowski, N. Randrianantoandro, J. Klimontko, D. Chrobak, K. Prusik, J. Rak, Ultra-high coercivity of (Fe86-xNbxB14)0.88Tb0.12 bulk nanocrystalline magnets. Acta Materialia 2015, 98, 318-326.

Microstructure of LaNiTiYSi: a La-containing High-Entropy Alloy

M. Zubko^{1,a}, K. Balin², P. Świec¹

a maciej.zubko@us.edu.pl

Keywords: high-entropy alloys, La alloys, X-ray diffraction, mirostructure

High-entropy alloys (HEAs) are a new class of metallic materials which, unlike traditional alloys, are not based on a single main element but consist of several components in comparable proportions. Due to their high configurational entropy, they exhibit unusual properties such as stability at high temperatures, wear resistance, and the ability to form simple solid phases (fcc, bcc) despite their multicomponent nature. For this reason, HEAs are currently an intensive area of research in materials engineering.

This presentation shows the results of microstructural characterization of the LaNiTiYSi alloy, which contains the rare earth element lanthanum. Due to its large atomic radius, the addition of lanthanum can significantly affect phase stability, segregation phenomena, and microstructure morphology.

The alloy was obtained by arc melting. The crystal structure and phase composition were analysed using X-ray diffraction (XRD). Microstructural observations were performed using scanning electron microscopy (SEM) with energy dispersive spectroscopy (EDS) detector. Particular attention was paid to the presence of secondary phases and local segregation phenomena associated with the presence of lanthanum. The results of the research indicate that the LaNiTiYSi alloy exhibits a multiphase structure, and lanthanum plays an important role in stabilizing specific phases and modifying grain morphology. The data obtained expand our knowledge of the influence of rare earth elements on the microstructure of highly dispersed alloys and may serve as a basis for designing new materials with improved properties.

Acknowledgment: This research was funded in part by the National Science Centre (Poland), grant number: Miniatura 8 No. 2024/08/X/ST11/01471.

Conference participation was supported by the GreenMat project, co-funded by the European Union under the program "European Funds for Silesia 2021–2027

¹ Institute of Materials Engineering, University of Silesia, 75 Pułku Piechoty 1A, Chorzów, 41-500, Poland

² Institute of Physics, University of Silesia, 75 Pułku Piechoty 1A, Chorzów, , Poland

A wide microstructure characterization of refractory powder materials for LPBF method

A.Czech^{1a}, A.Wrona¹, M.Lis¹, M. Kot² and Ł. Major³

a anna.czech@imn.lukasiewicz.gov.pl

Keywords: refractory metal powders, microstructural characterization (SEM, TEM, EDS), plasma spheroidization

Due to their unique properties, such as high-temperature strength, tungsten (W) and molybdenum (Mo) are attracting increasing attention, particularly for applications in demanding environments [1-3]. The high strength and low ductility of body-centered cubic (BCC) metals, including W and Mo, result from the non-planar core of screw dislocations [3, 4]. Among the elements that form solid solutions with tungsten and molybdenum, rhenium (Re) stands out as a key alloying addition. It increases the recrystallization temperature by substituting solvent atoms in the crystal structure. While the cubic structure remains unchanged, the lattice parameter of the unit cell varies with solute content. Since the discovery of the "rhenium effect", rhenium has been recognized for its ability to improve the low-temperature ductility of Group VIA metals with BCC crystal structures [3–8]. From a microstructural perspective, several theories attempt to explain the benefits of rhenium addition, although the exact mechanism remains unclear. Alloying aims to enhance ductility by improving dislocation mobility, eliminating interstitial impurities, refining the microstructure, or increasing the recrystallization temperature [2, 4, 9–11]. Extensive research supports the advantages of rhenium alloying. This approach, pioneered in the 1950s by G. Geach and colleagues, is known as solution softening. It reduces Peierls stress and introduces additional slip planes, such as {112}, thereby enhancing ductility [2, 12]. Proposed explanations for these effects include the transformation of the non-planar dislocation core to a planar core, which promotes solid solution softening, the formation of twin boundaries that enhance material deformation, and the electron concentration effect, which reduces oxygen content at grain boundaries and lowers Peierls stress [2, 13].

¹ Łukasiewicz Research Network- Institute of Non-Ferrous Metals, 44-100 Gliwice, Poland

AGH University of Krakow, Faculty of Mechanical Engineering and Robotics,
 Department of Machine Design and Maintenance, 30-059 Cracow, Poland
 Institute of Metallurgy and Materials Science, Polish Academy of Sciences, 30-059 Cracow, Poland

This study aims to characterize W-Re and Mo-Re powders using various advanced techniques. A microstructural analysis was conducted, employing scanning electron microscopy (SEM), transmission electron microscopy (TEM), energy-dispersive spectroscopy (EDS), and nanohardness testing. This multitechnique approach provided a thorough understanding of the microstructural evolution and elemental distribution within the powders.

References

- [1] Y.J. Hwang, Y. Kim, S.H. Park, S.Ch. Park, K.A. Lee, Wear and Corrosion Properties of Pure Mo Coating Layer Manufactured by Atmospheric Plasma Spray Process, Arch. Metall. Mater. 69,1, 81-85 (2024)
- [2] Ren, C., Fang, Z. Z., Koopman, M., Butler, B., Paramore, J., & Middlemas, S. (2018). Methods for improving ductility of tungsten-A review. International Journal of Refractory Metals and Hard Materials, 75, 170-183
- [3] H. Xu et al, Mechanical and microstructural responses in molybdenum-rhenium alloys under hot compressions, Journal of Materials Research and Technology 30, 3877-3885 (2024)
- [4] Miao, S., Xie, Z. M., Yang, X. D., Liu, R., Gao, R., Zhang, T., ... & Lian, Y. Y. (2016). Effect of hot rolling and annealing on the mechanical properties and thermal conductivity of W-0.5 wt.% TaC alloys. International Journal of Refractory Metals and Hard Materials, 56, 8-17
- [5] P. Jéhanno, M. Böning, H. Kestler, M. Heilmaier, H. Saagem, M. Krüger, Molybdenum alloys for high temperature applications in air, Powder Metallurgy 51.2, 99-102 (2008)
- [6] K.J. Leonard, J.T. Busby, S.J. Zinkle, Microstructural and mechanical property changes with aging of Mo-41Re and Mo-47.5 Re alloys, Journal of nuclear materials 366.3, 369-387 (2007)
- [7] J.L Garin, R. L. Mannheim, Manufacturing of Mo-25 Re and Mo-50 Re alloys by means of powder sintering at medium temperatures, Material and manufacturing process, 13.5, 731-747 (1998)
- [8] C.C Eckley et al, Evaluating Molybdenum-Rhenium Alloys Through Additive Manufacturing, JOM 75.6, 1928-1940 (2023)
- [9] Li, H., Wurster, S., Motz, C., Romaner, L., Ambrosch-Draxl, C., & Pippan, R. (2012). Dislocation-core symmetry and slip planes in tungsten alloys: Ab initio calculations and microcantilever bending experiments. Acta materialia, 60(2), 748-758
- [10] Kharchenko, V. K., & Bukhanovskii, V. V. (2012). High-temperature strength of refractory metals, alloys and composite materials based on them. Part 1. tungsten, its alloys, and composites. Strength of Materials, 44, 512-517
- [11] Leonhardt, T. (2009). Properties of tungsten-rhenium and tungsten-rhenium with hafnium carbide. Jom, 61(7), 68-71.
- [12] Eckley, C. C., Kemnitz, R. A., Fassio, C. P., Hartsfield, C. R., & Leonhardt, T. A. (2021). Selective laser melting of tungsten-rhenium alloys. Jom, 73, 3439-3450
- [13] Cheng, G. M., Xu, W. Z., Jian, W. W., Yuan, H., Tsai, M. H., Zhu, Y. T., ... & Millett, P. C. (2013). Dislocations with edge components in nanocrystalline bcc Mo. Journal of Materials Research, 28, 1820-1826.

CAC 2025 XXV Conference on Applied Crystallography

